Supporting information

Visible-light-mediated semi-heterogeneous black TiO_2/nickel dual catalytic C (sp2)-P bond formation toward arylphosphonates

Mehdi Koohgard[†], Haniehsadat Karimitabar[†], and Mona Hosseini-Sarvari[*,†]
[†]*Department of Chemistry, Shiraz University, Shiraz 7194684795, I.R. Iran.*

**Correspondence to: Mona Hosseini-Sarvari; E-mail: Hossaini@shirazu.ac.ir*

Contents

1. Experimental information

General Information. TiO_2 (the mixture of anatase and rutile, specific surface area: 5۰-51 m^2g^{-1}) was purchased from a local supplier. Starting materials were purchased from commercial suppliers and used without further purification. All the solvents (HPLC grade) were dried and purified according to standard methods. The phase evolution of the catalyst was characterized by X-ray diffraction technique using Bruker D8-advance X-ray diffractometer with Cu Ka (λ = 1.54178 Å) radiation. The distribution and morphology of the product were analyzed by JEOL, JSM-7610F Fe-SEM. UV–vis diffuse reflectance spectrum was performed with a Shimadzu UV-2450 spectrophotometer. Brunauer–Emmett–Teller (BET) surface area, pore volume, and Barret–Joyner–Halenda (BJH) pore size distribution on the basis of nitrogen adsorption–desorption isotherms were determined with a Micromeritics ASSP 2020 equipment. Melting points were measured on a Buchi 510 apparatus in open capillary tubes and were uncorrected. ^{1}H NMR, ^{13}C NMR, and ^{31}P NMR spectra were recorded in $CDCl_3$, unless otherwise noted, using residual solvent peaks as an internal standard or Me_4Si, ^{31}P NMR spectra were referenced to external H_3PO_4 (0 ppm), Bruker Advance DPX FT 300 MHz and Bruker Ultrashield 400 MHz spectrometry (multiplicity: s = singlet, d = doublet, t = triplet, dd = doublet of doublets, m = multiplet), coupling constants (J): in Hertz (Hz)). FT-IR spectra were obtained by a Shimadzu FT-IR 8300 spectrophotometer. The reactions were monitored by thin layer chromatography (TLC): silica gel PolyGram SIL G/UV 254 plates and visualized by UV lamp at 254 nm. The products purified by hand-made column chromatography: short columns of SiO_2 60 (230–400 mesh) in glass columns (0.5 –1.0 cm).

Experimental

Preparation of black TiO_2 photocatalyst.

Black TiO_2 NPs were prepared according to a reported procedure[1]. Briefly, 2.0 g of TiO_2 NPs powder (anatase and rutile) were mixed with 0.75 g of $NaBH_4$ and the obtaining mixture was ground for 40 min at room temperature. Next, this mixture was placed into a porcelain boat, and transferred in a tubular furnace. The porcelain boat was heated from room temperature to 350 ^{0}C (10 ^{0}C/min) then held for 60 min under an Ar atmosphere. The reaction was allowed to cool down to room temperature; the colored TiO_2 was washed with deionized water (three times) and ethanol (three times) and dried at 75 ^{0}C on the vacuum oven.

Typical procedure for C-P bond formation.

4-Iodotoluene (109 mg, 0.5 mmol), diphenylphosphine oxide (120 mg, 0.6 mmol), black TiO_2 NPs (3.0 mg), $NiCl_2$·glyme (10.9 mg, 10 mol %), dtbbpy (13.4 mg, 10 mol %), CS_2CO_3 (163 mg, 1.0 equiv.) were placed in the vessel, equipped with a stir bar then capped with a septum and parafilm, and 3.0 mL of dried MeCN was injected into the vessel. The vessel was then degassed

with Ar for 10 minutes and the reaction mixture was sonicated for 5-10 min. Afterward, the mixture was stirred, under Ar, at room temperature under 15 W white LED for 24h. After completion, the reaction mixture was centrifuged to separate the catalyst, then, the solvent was removed by vacuum and the crude was diluted with ethylacetate or dichloromethane (15 ml), washed with brine (2× 10 ml) then the organic phase was dried over $MgSO_4$, filtered, and the solvent was removed under redued pressure. The residue was purified by flash chromatography on silica gel (eluent: hexane/dichloromethane (6:1~1:1)) to afford the desired product **3a** in 91% yield.

The box used for the reactions

Figure S1. The box containing 15 W blue LED lamp (λ > 410 nm) and the reaction setup up under sunlight.

2. Synthesis and characterization of black TiO_2

Black TiO_2 NPs was prepared by applying a feasible method based on the treatment of a grinded mixture of TiO_2 (p25) and $NaBH_4$ in a tubular furnace heated under an inert atmosphere. The resulting black TiO_2 NPs was washed, dried and characterized *via* Fourier-transform infrared spectroscopy (FT-IR), X-ray diffraction energy (XRD), Scanning electron microscope (SEM), and diffuse reflectance ultraviolet-visible spectrophotometry (UV–Vis). As depicted in Figure S2a, both white and black TiO_2 exhibited similar transmittance patterns in FT-IR. The broad band appeared in the spectrum at the 500 to 900 cm^{-1} was ascribed to the stretching peaks of Ti-O-Ti

bonds. Moreover, O–H stretching (bridging O–H groups) and bending vibration of absorbed water (H-O-H bonds) appeared at 3426 cm^{-1}, 2922 cm^{-1}, 2852 cm^{-1}, and 1634 cm^{-1}, respectively[2]. However, the intensity of the water absorbed peaks have been reduced in black TiO_2 rather than white TiO_2. This change probably raised from the incorporation of hydrogen into the TiO_2 which generated oxygen vacancy and partly passivate the number of oxygen dangling bonds. The XRD was applied to characterize the crystalline phase change of TiO_2 nanocrystals before and after treatment with $NaBH_4$ (Figure S2b). The diffraction peaks at 2θ values of 25.6° and 27.7° were ascribed to the diffractions of (101) and (110) planes for anatase and rutile structures, respectively [3]. According to the maximum diffraction peaks (black TiO_2) in Figure 1b and using Scherrer's equation ($D=K\lambda/\beta\cos\theta$), where D is the crystallite size, K is Scherrer constant usually taken as 0.9 in this case, λ is the wavelength of the X-ray radiation (0.15418 nm for Cu Kα), and β is the full width at half maximum (FWHM) of the diffraction peaks measured at 2θ, the average sizes of black TiO_2 crystal for anatase and rutile (101 and 110) are estimated ~24.8 nm and ~53.9 nm, respectively (25.7 nm and 55.6 nm for white TiO_2). These values exhibited there is no significant change in particle size of black TiO_2 after treatment with $NaBH_4$. However, some peaks of black TiO_2 showed slightly broadening, which are probably in connection with oxygen vacancies resulted from disorder-induced lattice strains. Moreover, two new peaks appeared (shown with * in the spectrum of black TiO_2). It can be assumed a new crystalline phase was probably formed due to the mixture of reduced TiO_2 species such as Ti_9O_{17}, Ti_8O_{15}, and Ti_3O_5[1].

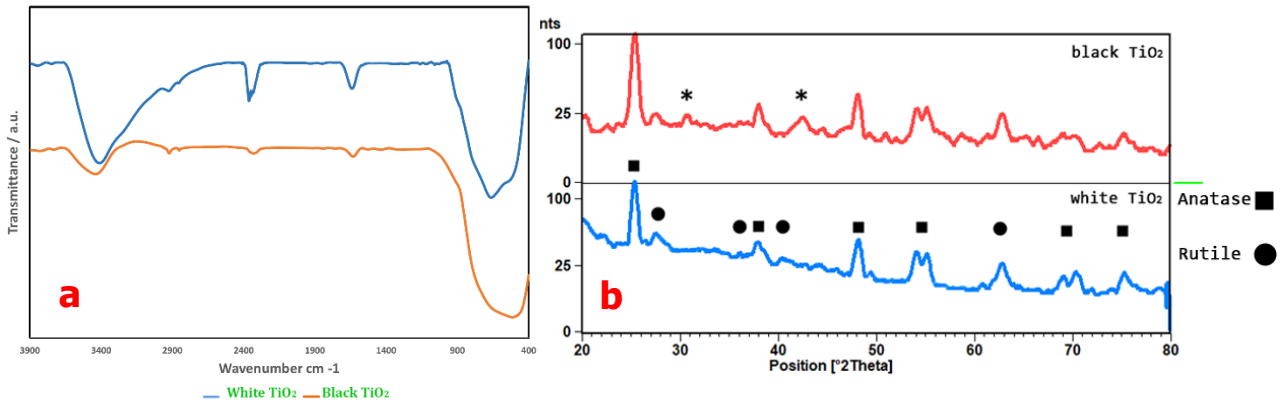

Figure S2. FT-IR spectra of white and black TiO_2 (a), The XRD patterns of white and black TiO_2 (b).

While the diffuse reflectance UV-Vis spectrum (UV-DRS) of white TiO_2 showed absorption band lower than 400 nm (charge transfer from O 2p valence band to Ti 3d conduction band[4]), black TiO_2 revealed a broad absorption, starting at 400 nm to 900 nm, along with significant improvement in the visible light absorption rather than white TiO_2 (Figure S3a). Moreover, the band gap of black TiO_2 was calculated by using Tauc's equation and found to be about 2.6 eV

which band-gap narrowing of 0.6 eV was observed in comparison with white TiO_2. According to the SEM image, after hydrogen doping in black TiO_2, there is no significant change in the morphology of the black TiO_2 NP rather than before treatment with $NaBH_4$. Also, it could be surveyed by the N_2 adsorption experiment. The BET analysis revealed that specific surface areas of black TiO_2 and white TiO_2 are 5۰٫۵ m^2g^{-1} and 50 m^2g^{-1}, respectively. Notably, energy dispersive X-ray (EDX) analysis revealed about 1.9 % of Na impurity in TiO_2 after treatment with $NaBH_4$ (Figure S3d and S3e).

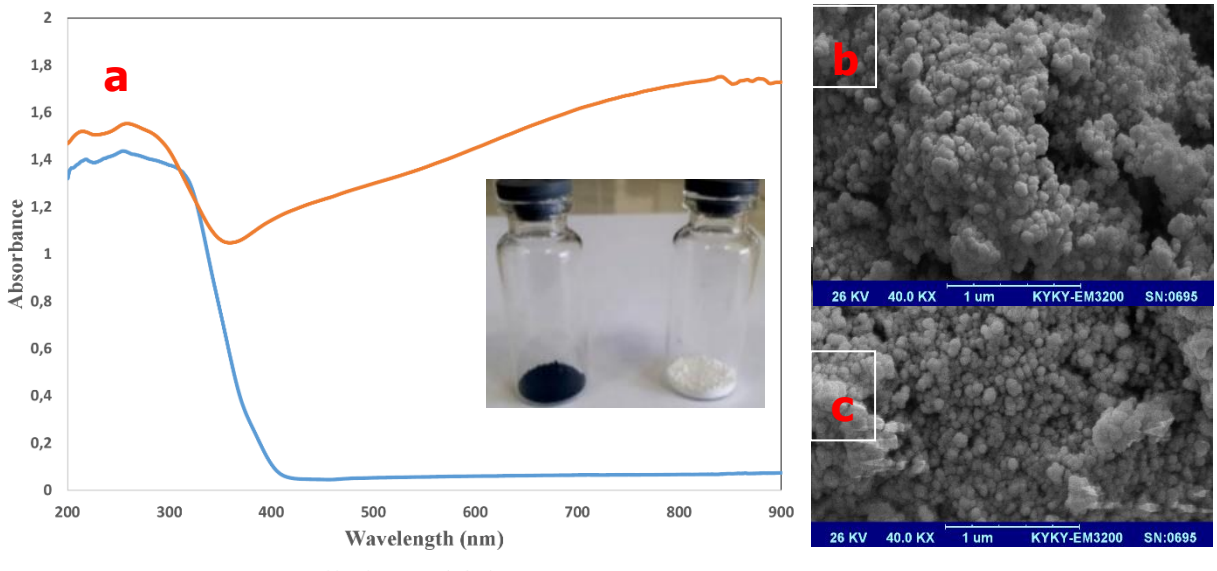

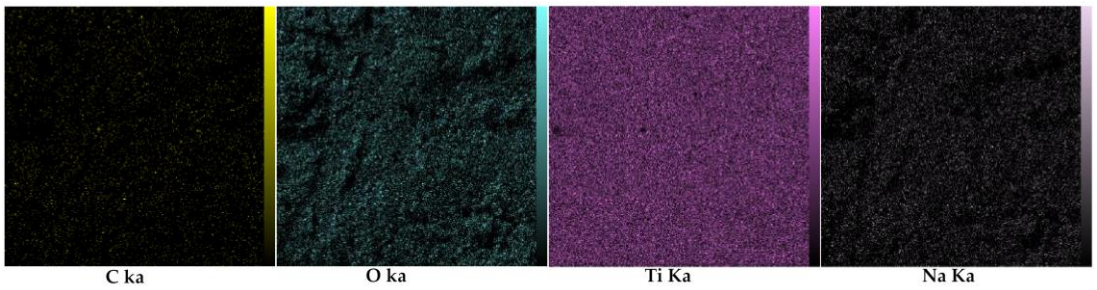

d

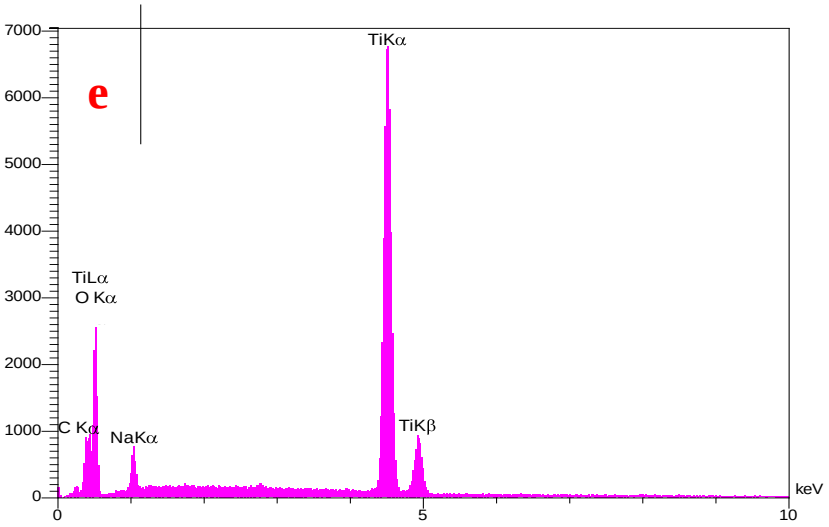

Figure S3. UV-Vis spectra of white and black TiO_2 (a), SEM of black TiO_2 (b) and white TiO_2 (c), mapping (d) and EDX (e) of black TiO_2.

Calculation of band Gap

The optical band gap of the semiconductors can be calculated by using the absorption spectrum and the following equation to draw Tauc plot[5].

Eq.1: $(\alpha h\nu)^{1/n} = A(h\nu - Eg)$

h: Planck's constant, ν: frequency of vibration,
α: absorption (extinction) coefficient
Eg: band gap,
A: proportionality constant
n: the value of the exponent ***n*** denotes the nature of the transition

In this study, this method was applied to estimate the band gap energy value of black TiO_2 and white TiO_2 photocatalyst which obtained from UV–Vis spectra of the coresponding semiconductors[6]. Figure S4 depicts the plot of band-gap energy for black TiO_2 and white TiO_2, obtained by Tauc's equation (1) [7].

Eq.2: $[ahv]^{1/2} = A(hv-Eg)$

The calculated band-gap energy found to be 2.6 eV for black TiO_2 and 3.2 eV for white TiO_2 (anatase), respectively. Noticeably, by treatment of hydrogen with TiO_2, the band-gap of black TiO_2 was significantly reduced.

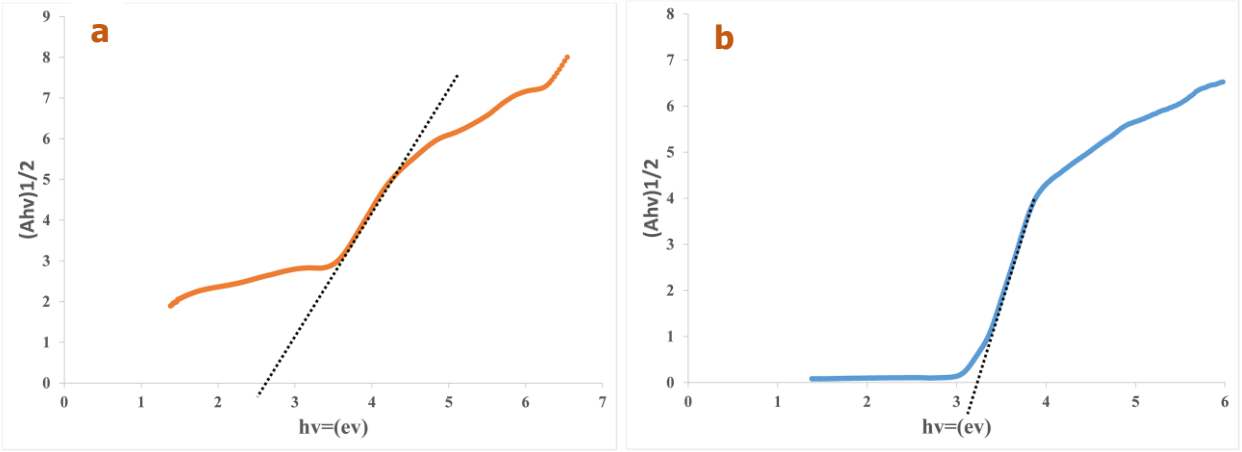

Figure S4. The plot for the band gap calculation of black TiO_2 NPs (a) and white TiO_2 NPs (b).

BET and BJH results

BJH desorption summary			BET
Surface Area	Pore Volume	Pore Diameter (d)	Surface Area
65.231 m^2/g	0.439 cm^3/g	34.268 nm	50.51 m^2/g

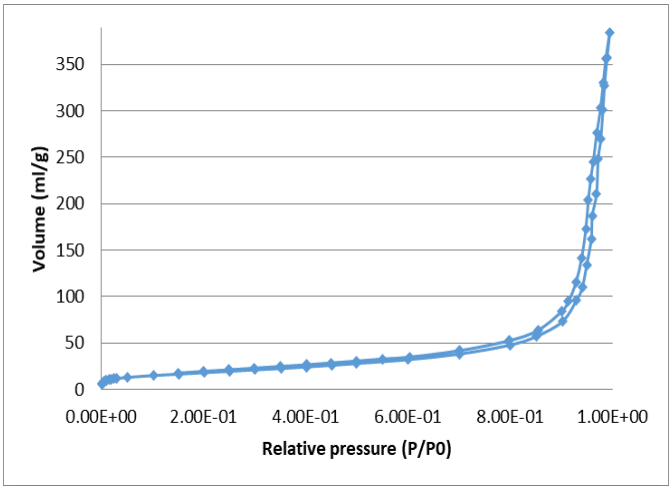

3. Sun light, gram-scale and reusability tests

When the model reaction was carried out under sunlight (the reaction vessel was sealed, evacuated and refilled with Ar gas for three times, followed by addition of degassed MeCN, in two consecutive sunny days at Shiraz University, Jul. 21, 22 2018, 29°59′ north latitude and 52°58′ east longitude, 1500 m above the sea level), 92 % of desired product was obtained with a shortened reaction time (Scheme S1a). The gram-scale reaction was further carried out and exhibited an acceptable efficiency after 30h (Scheme S1b). Recoverability and reusability are key factors of a heterogeneous catalyst, so, we tested the reusability of black TiO_2 in this photocatalytic process. The model reaction was conducted for five cycles and after each run, the mixture was centrifuged to remove black TiO_2; then, the photocatalyst was washed with EtOH and MeCN, dried in a vacuum oven and used in the subsequent run. The reusability test revealed the black TiO_2 maintained a high efficiency during five subsequent runs (Figure S6) and the product yield decreased only 12 % after the last run. This decrease would be rationalized by the loss of small amounts of black TiO_2 (about 0.5 mg after last run) during these consequent runs.

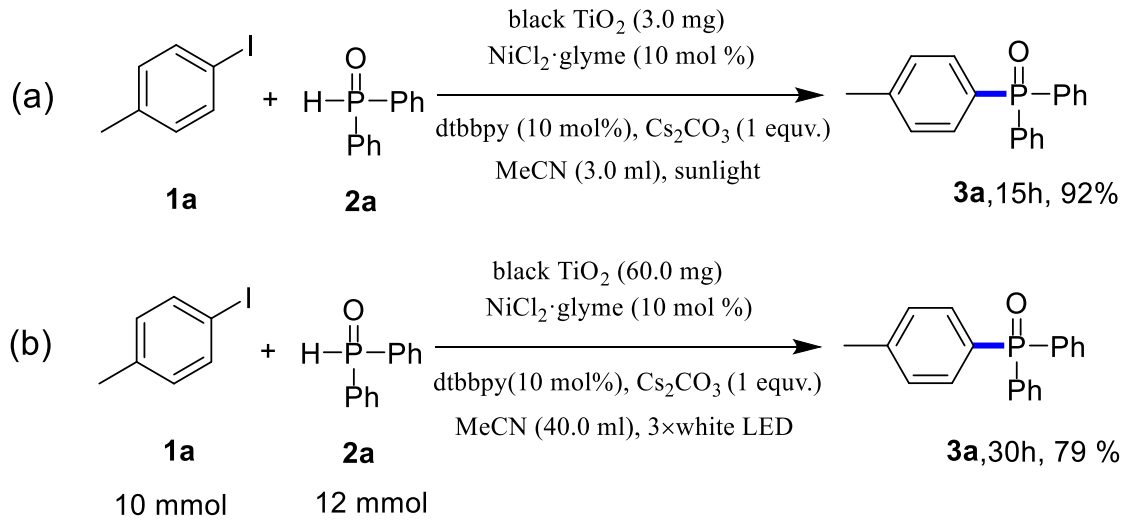

Scheme S1. Visible-light-mediated C-P formation under sunlight (a) and gram-scale reaction (b).

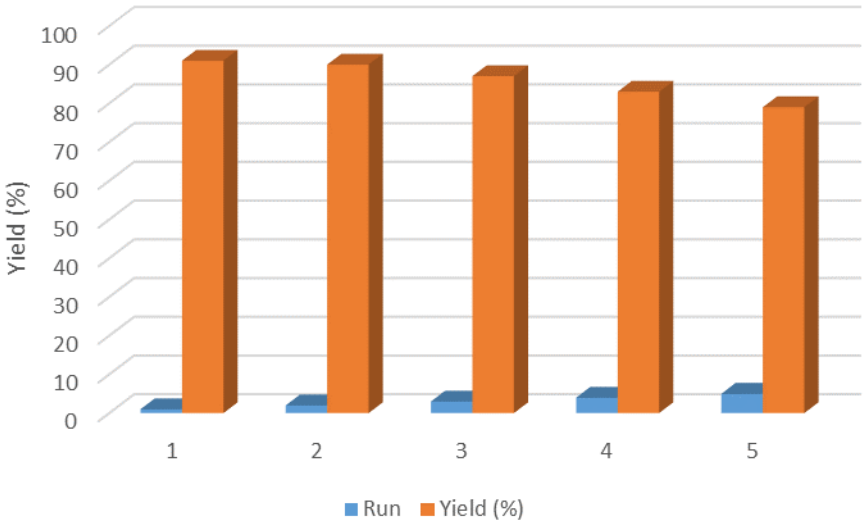

Figure S6. Reusability of black TiO_2 in semi heterogeneous dual catalytic C-P formation.

It was possible that a small amount of nickel could be deposited onto the surface of recovered black TiO_2 during cycles. So, after the last run, we surveyed nickel content by inductively coupled plasma (ICP) and atomic absorption spectroscopy. The result revealed 0.8 % of nickel on the surface of black TiO_2. However, when the recovered photocatalyst without nickel complex and ligand ($NiCl_2$.glyme and dtbbpy) was applied in the reaction, it resulted in only 11 % of the corresponding product (**3a**), upon ^{31}P NMR yield.

After the last run, the recovered photocatalyst was characterized *via* FT-IR, XRD, and UV–Vis. As expected, no apparent change was observed in XRD pattern and IR spectrum of recovered black TiO_2 owning to small crystallite size and low amount of nickel content onto the surface of the recovered photocatalyst[8]. As demonstrated in Figure S7, the FT-IR and UV–DRS analysis revealed no significant change in transmittance patterns and absorption of black TiO_2 before and after recovery. In addition, XRD patterns showed that the recovered photocatalyst has maintained the crystalline phase during experiments.

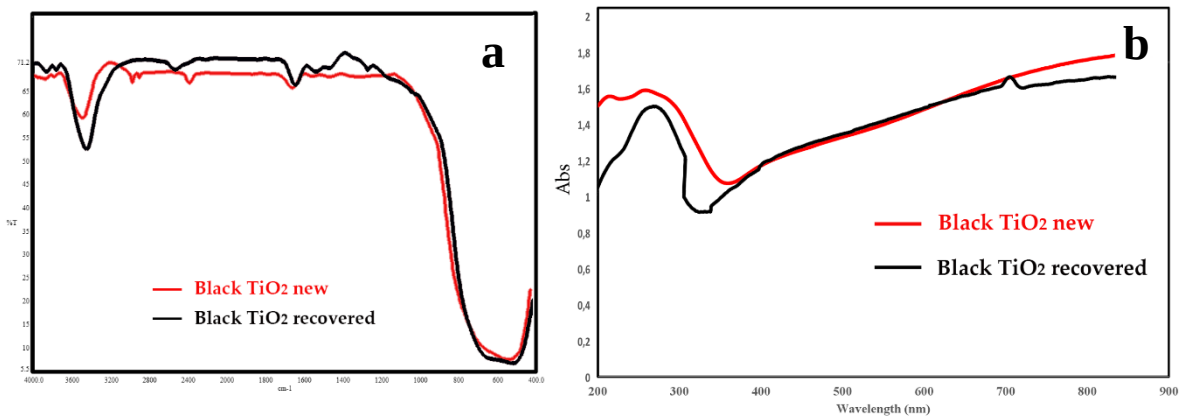

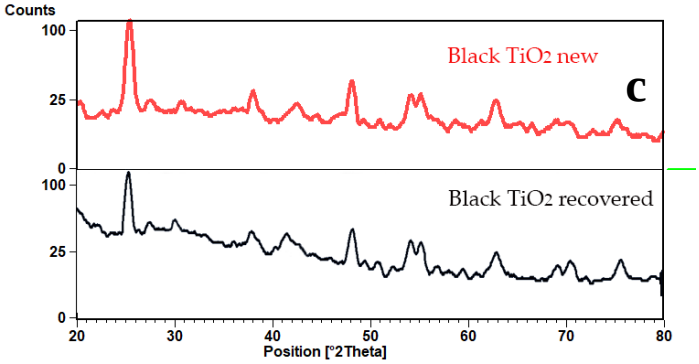

Figure S7. The characterization of the recovered photocatalyst, FT-IR (a), Uv-Vis (b) and XRD (c).

4. Control experiments

First, 2,2,6,6-Tetramethylpiperidinyl-1-oxy (TEMPO) as a common radical scavenger and 5,5-dimethyl-1-pyrroline-N-oxide (DMPO) as an electron-trapping agent for semiconductors[9] were separately employed under typical reaction condition which suppressed the generation of the corresponding product (**3a**). Then, two scavengers namely triethanolamine (TEA) and ethylenediaminetetraacetic acid (EDTA) were applied in this reaction condition to trap the photogenerated holes[9a, 10] of the photocatalyst which resulted in a sharp decrease of the product yield (Scheme S2). Next, an "On/off" LED irradiation experiment was performed under typical condition except for interval on/off light irritation after every 3h. Accordingly, the reaction progress merely occurred during the periods of light irradiation (Figure S8).

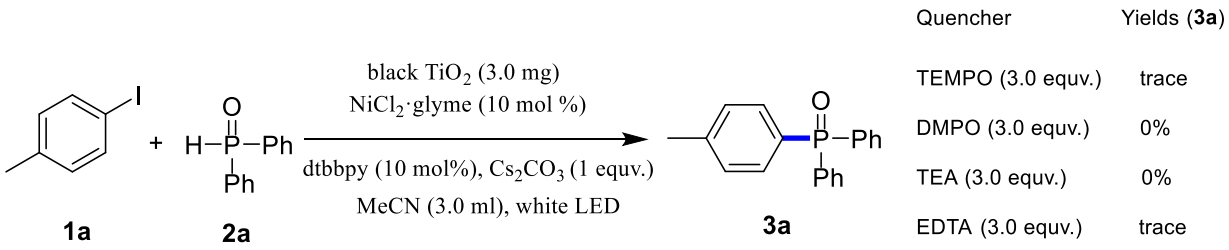

Scheme S2. Control experiment in the presence of quenchers.

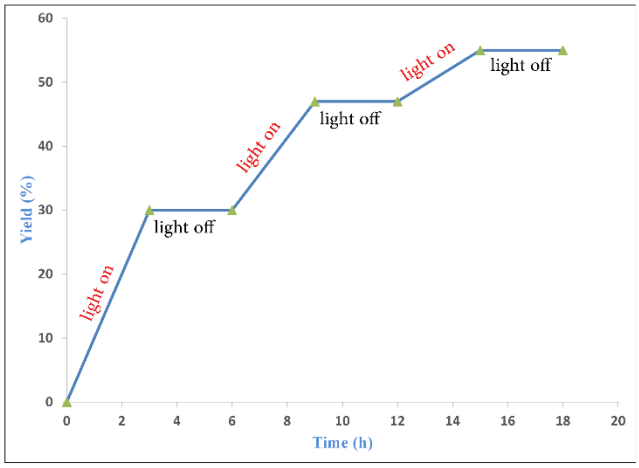

Figure S8. "On/off" LED irradiation experiment, ^{31}P NMR yields of **3a** using triethyl phosphate as an internal standard.

Moreover, the correlation of the black TiO_2 performance with light irradiation was investigated through wavelength and light intensity tests. As illustrated in Figure S9a, whereas in the wavelengths range of white, blue and green LED lamps (15 W) the product yields are nearly the same, in the range of red LED lamp (15 W) it exhibited a sharp decrease yield under typical condition. These results might be justified with the band gap of modified photocatalyst (2.6 eV). Similarly, the correspondence of the photocatalytic activity and intensity of the light source was surveyed. According to Figure S9b, by increasing the irritation intensity from 5w bulb-shaped white LED lamps to 15 W, the reaction progress showed gradual enhance in the product yields. Notably, all the LED lamps were used at an identical distance.

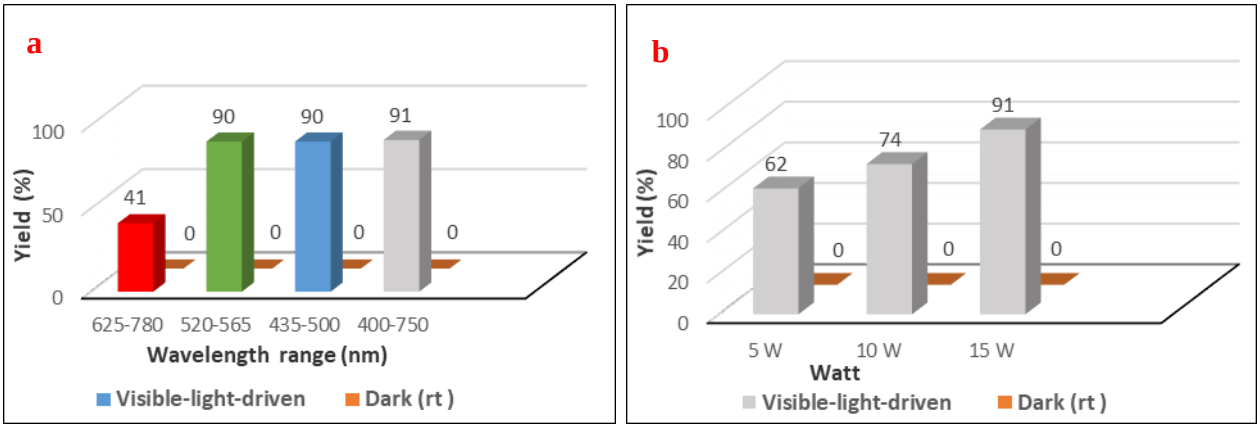

Figure S9. The dependence of the photocatalytic activity of black TiO_2 on the wavelength of the light irradiation (a) and the intensity of the light irradiation (b), isolated yield.

5. Characterization of compounds

diphenyl(p-tolyl)phosphine oxide (3a)[11]

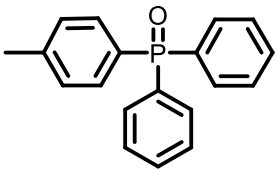

White solid, mp = 131-132 ºC (lit. 130.4-131.3 ºC). ^{1}H NMR (400 MHz, $CDCl_3$) δ 7.70 – 7.63 (m, 4H), 7.59 – 7.50 (m, 4H), 7.41-7.45 (m, 4H), 7.25 (dd, *J* = 8.1, 2.7 Hz, 2H), 2.38 (s, 3H). ^{13}C NMR (101 MHz, $CDCl_3$) δ 142.43 (d, *J* = 2.6 Hz), 132.22 (d, *J* = 104.1 Hz), 132.08 (d, *J* = 10.2 Hz), 132.05 (d, *J* = 9.8 Hz), 131.98 (d, *J* = 2.6 Hz), 130.74 (d, *J* = 106.7 Hz), 130.62 (d, *J* =12.6 Hz), 129.30 (d, *J* = 12.0 Hz), 128.33 (d, *J* = 11.9 Hz), 21.58. ^{31}P NMR (162 MHz, $CDCl_3$) δ 27.85.

(4-(tert-butyl)phenyl)diphenylphosphine oxide (3b)[12]

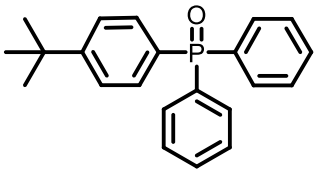

White solid; mp 131-132 °C (lit. 132-133 ºC). ^{1}H NMR (400 MHz, $CDCl_3$) δ 7.78 – 7.65 (m, 6H), 7.54 – 7.40 (m, 8H), 1.33 (s, 9H). ^{13}C NMR (101 MHz, $CDCl_3$) δ 153.92, 132.27 (d, *J* = 104.5 Hz), 132.25 (d, *J* = 9.7 Hz), 132.02(d, *J* = 10.3 Hz), 131.84 (d, *J* = 2.0 Hz), 128.46 (d, *J* = 107.2 Hz), 127.77 (d, *J* = 12.1 Hz), 125.70 (d, *J* = 12.5 Hz), 34.62, 31.17. ^{31}P NMR (162 MHz, $CDCl_3$) δ 28.26.

(4-methoxyphenyl)diphenylphosphine oxide (3c)[13]

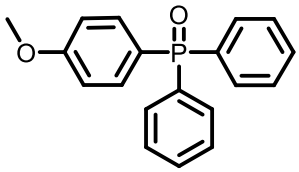

White solid , mp 113-115 °C (lit. 114.1-115.2 ºC). ^{1}H NMR (400 MHz, Chloroform-*d*) δ 7.66 (dd, *J* = 12.1, 7.7 Hz, 2H), 7.59 (dd, *J* = 11.4, 8.4 Hz, 1H), 7.51-7.54 (m, 1H), 7.41-7.46 (m, 2H), 6.95 (d, *J* = 8.1 Hz, 1H), 3.83 (s, 1H). ^{13}C NMR (101 MHz, $CDCl_3$) δ 162.50 (d, *J* = 2.8 Hz), 134.0 (d, *J* = 11.2 Hz), 133.46 (d, *J* = 104.4 Hz), 132.43 (d, *J* = 10.0 Hz), 131.99 (d, *J* = 2.7 Hz), 128.48 (d, *J* = 12.2 Hz), 123.36 (d, *J* = 110.3 Hz), 114.08 (d, *J* = 13.2 Hz), 55.34. ^{31}P NMR (162 MHz, $CDCl_3$) δ 28.97.

triphenylphosphine oxide (3d)[14]

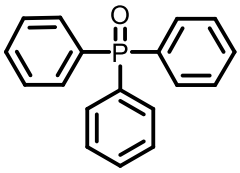

White solid, mp 155-157 °C (lit. 154.5-156.2 °C). ^{1}H NMR (300 MHz, Chloroform-*d*) δ 7.76 – 7.62 (m, 6H), 7.61 – 7.51 (m, 3H), 7.51 – 7.41 (m, 6H). ^{13}C NMR (75 MHz, Chloroform-*d*) δ 133.29 , 132.15 (d, J = 104.6 Hz) , 132.02 (d, J = 9.9 Hz) , 131.90 (d, J = 2.2 Hz), 128.53 (d, J = 12.1 Hz). ^{31}P NMR (122 MHz, $CDCl_3$) δ 28.98.

(4-fluorophenyl)diphenylphosphine oxide (3e)[14]

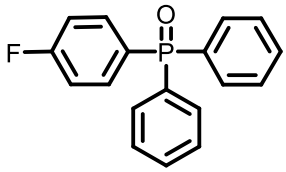

White solid, m.p.: 134-135 °C (lit. 133.6-135.5 °C). ^{1}H NMR (400 MHz, Chloroform-*d*) δ 7.62-7.68 (m, 6H), 7.50-7.54 (m, 2H), 7.41-7.46 (m, 4H), 7.10-7.14 (m, 2H). ^{13}C NMR (101 MHz, $CDCl_3$) δ 165.01 (dd, $J_{C\text{-}F}$ = 253.5, $J_{C\text{-}P}$ = 3.2 Hz), 134.55 (dd, $J_{C\text{-}P}$ = 11.1, $J_{C\text{-}F}$ = 8.8 Hz), 132.28 (d, $J_{C\text{-}P}$ = 104.8 Hz), 132.07 (d, $J_{C\text{-}P}$ = 3.03), 131.97 (d, $J_{C\text{-}P}$ = 10.1 Hz), 128.56 (dd, $J_{C\text{-}P}$ = 106.5, $J_{C\text{-}F}$ = 3.4 Hz), 115.86 (dd, $J_{C\text{-}F}$ = 21.4, $J_{C\text{-}P}$ = 13.2 Hz). ^{31}P NMR (162 MHz, $CDCl_3$) δ 28.27.

diphenyl(4-(trifluoromethyl)phenyl)phosphine oxide (3f)[15]

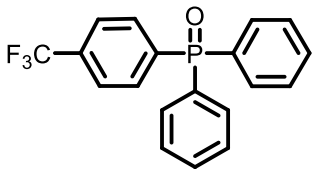

White solid, mp 88–90 °C (lit. 89-90 °C). ^{1}H NMR (400 MHz, $CDCl_3$) δ 7.80-7.85 (m, 2H), 7.75-7.62 (m, 6H), 7.54-7.60 (m, 2H), 7.46-7.50 (m, 4H). ^{13}C NMR (101 MHz, $CDCl_3$) δ 136.99 (d, $J_{C\text{-}P}$ = 99.3 Hz), 133.14-134.15 (m, $J_{C\text{-}P}$ and $J_{C\text{-}F}$), 132.55 (d, $J_{C\text{-}P}$ = 10.1 Hz), 132.39 (d, $J_{C\text{-}P}$ = 2.7 Hz), 132.01 (d, $J_{C\text{-}P}$ = 10.0 Hz), 130.71 (d, $J_{C\text{-}P}$ = 11.2 Hz), 128.71 (d, $J_{C\text{-}P}$ = 12.2 Hz), 125.39 (dq, $J_{C\text{-}P}$ = 12.1 Hz, $J_{C\text{-}F}$ = 3.5 Hz), 122.19. ^{31}P NMR (162 MHz, $CDCl_3$) δ 28.01.

methyl 4-(diphenylphosphoryl)benzoate (3g)[14]

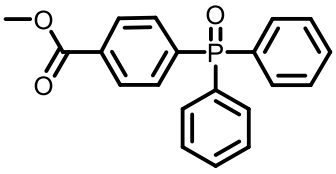

White solid. m.p 114-115 °C (lit. 113.4–114.5 °C). ^{1}H NMR (400 MHz, $CDCl_3$) δ 8.12 (dd, *J* = 8.3, 2.5 Hz, 2H), 7.86 – 7.74 (m, 2H), 7.65-7.70 (m, 4H), 7.56-7.60 (m, 2H), 7.46 – 7.51 (m, 4H), 3.95 (s, 3H). ^{13}C NMR (101 MHz, $CDCl_3$) δ 167.24, 137.07, 132.31, 132.23 133.2 (d, *J* = 2.7 Hz), 132.15 (d, *J* = 10.2 Hz), 131.27, 129.41 (d, *J* = 12.2 Hz) 128.65 (d, *J* = 12.2 Hz), 52.45. ^{31}P NMR (162 MHz, $CDCl_3$) δ 28.48.

(2-methoxyphenyl)diphenylphosphine oxide (3h)

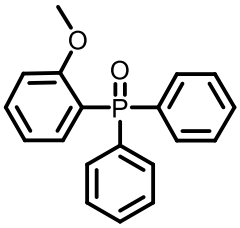

White solid. ^{1}H NMR (400 MHz, $CDCl_3$) δ 7.80 – 7.65 (m, 5H), 7.53 – 7.44 (m, 3H). 7.37-7.42 (m, 4H), 7.05 (td, *J* = 7.6, 2.0 Hz, 1H), 6.89 (dd, *J* = 8.3, 5.3 Hz, 1H), 3.52 (s, 3H). ^{13}C NMR (101 MHz, $CDCl_3$) δ 160.83 (d, *J* = 3.0 Hz), 134.87 (d, *J* = 7.0 Hz), 134.31 (d, *J* = 2.0 Hz), 133.70, 132.63, 131.76 (d, *J* = 10.1Hz), 131.44 (d, *J* = 3.0 Hz), 130.66 (d, *J* = 12.1 Hz), 128.90 (d, *J* = 12.1 Hz), 128.09 (d, *J* = 13.1 Hz), 121.94 (d, *J* = 12.1 Hz), 120.74, 119.71, 111.46 (d, *J* = 7.0 Hz), 55.24. ^{31}P NMR (162 MHz, $CDCl_3$) δ 27.39.

diphenyl(o-tolyl)phosphine oxide (3i)[12]

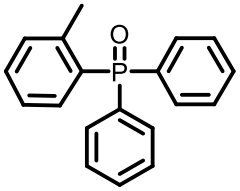

Light yellow solid. ^{1}H NMR (400 MHz, $CDCl_3$) δ 7.70 – 7.61 (m, 4H), 7.56 – 7.49 (m, 2H), 7.49 – 7.37 (m, 5H), 7.26 (dd, *J* = 7.7, 4.2 Hz, 1H), 7.11 (td, *J* = 7.6, 2.6 Hz, 1H), 7.03 (ddd, *J* = 13.8, 7.7, 1.5 Hz, 1H), 2.45 (s, 3H). ^{13}C NMR (101 MHz, $CDCl_3$) δ 143.25 (d, *J* = 8.1 Hz), 133.39 (d, *J* = 12.4 Hz), 132.79 (d, *J* = 104.5 Hz), 132.06 (d, *J* = 2.1 Hz), 131.88 (d, *J* = 10.1 Hz), 131.74 (d, *J* = 2.1 Hz), 130.82 (d, *J* = 104.3 Hz), 128.53 (d, *J* = 12.1 Hz),125.16 (d, *J* = 12.7 Hz), 21.67 (d, *J* = 4.4 Hz). ^{31}P NMR (122 MHz, $CDCl_3$) δ 31.62.

phenanthren-9-yldiphenylphosphine oxide (3j)

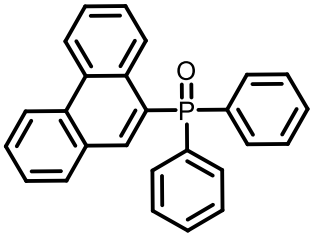

White solid. ^{1}H NMR (300 MHz, $CDCl_3$) δ 8.75 – 8.61 (m, 3H), 7.82 – 7.67 (m, 7H), 7.65 – 7.62 (m, 1H), 7.60 – 7.51 (m, 3H), 7.4٧,٤٩-٣ (m, 5H). ^{13}C NMR (75 MHz, $CDCl_3$) δ 136.86 (d, *J* = 11.3 Hz), 133.37, 132.16 (d, *J* = 9.7 Hz), 132.00 (d, *J* = 2.8 Hz), 130.97 (d, *J* = 8.5 Hz), 130.76 (d, *J* = 8.6 Hz), 130.05, 129.70 (d, *J* = 14.8 Hz), 129.14, 128.67 (d, *J* = 12.2 Hz), 127.20 (d, *J* = 4.2 Hz), 127.04, 123.05, 122.65. ^{31}P NMR (122 MHz, $CDCl_3$) δ 32.58.

naphthalen-2-yldiphenylphosphine oxide (3k)[14]

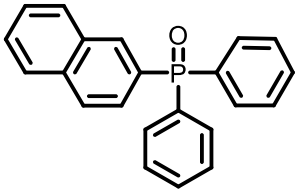

Light yellow oil. ^{1}H NMR (400 MHz, $CDCl_3$) δ 8.35 – 8.26 (m, 1H), 7.85-7.91 (m, 3H), 7.69-7.75 (m, 4H), 7.62-7.66 (m, 1H), 7.50 – 7.58 (m, 4H), 7.43-7.48 (m, 4H). ^{13}C NMR (101 MHz, $CDCl_3$) δ 134.71 (d, *J* = 2.5 Hz), 134.02 (d, *J* = 9.2 Hz), 133.06, 132.42 (d, *J* = 13.2 Hz), 132.14 (d, *J* = 10.0 Hz), 132.01 (d, *J* = 2.6 Hz), 131.38 (d, *J* = 10.2 Hz), 130.70 (d, *J* = 11.5 Hz), 130.07, 128.96, 128.56 (d, *J* = 12.1 Hz), 128.38, 128.27 (d, *J* = 2.3 Hz), 127.84, 126.97, 126.84 (d, *J* = 10.6 Hz). ^{31}P NMR (162 MHz, $CDCl_3$) δ 29.17.

naphthalen-1-yldiphenylphosphine oxide (3l)[11]

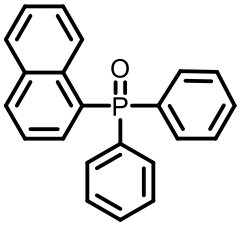

White solid, mp 183-184 ºC (lit. 184.8-185.7 ºC). ^{1}H NMR (400 MHz, $CDCl_3$) δ 8.63 (d, *J* = 8.4 Hz, 1H), 8.01 (d, *J* = 8.0 Hz, 1H), 7.88 (d, *J* = 8.1 Hz, 1H), 7.71 (dd, *J* = 12.1, 7.6 Hz, 4H), 7.50-7.55 (m, 2H), 7.42-7.48 (m, 2H), 7.47 – 7.37 (m, 4H), 7.40 – 7.27 (m, 2H). ^{13}C NMR (101 MHz, $CDCl_3$) δ 133.91 (d, *J* = 9.1 Hz), 133.71 (d, *J* = 6.2 Hz), 133.34 (d, *J* = 2.9 Hz), 132.76 (d, *J* = 104.4 Hz), 132.08 (d, *J* = 9.8 Hz), 131.95 (d, *J* = 2.8 Hz), 129.36, 128.81, 128.62 (d, *J* = 12.0 Hz), 128.35, 127.60 (d, *J* = 5.8 Hz), 126.94 (d, *J* = 84.5 Hz), 124.18 (d, *J* = 14.3 Hz). ^{31}P NMR (162 MHz, $CDCl_3$) δ 32.45.

diphenyl(pyridin-3-yl)phosphine oxide (3m)[14]

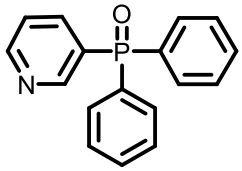

White solid, mp 124–126 °C (lit. 124.1–125.6 °C) . ^{1}H NMR (300 MHz, $CDCl_3$) δ 8.86 -8.60 (m, 2H), 8.02 (t, *J* = 9.8 Hz, 1H), 7.75 – 7.59 (m, 4H), 7.60 – 7.51 (m, 2H), 7.48 - 7.35 (m, 5H). ^{13}C NMR (75 MHz, $CDCl_3$) δ 152.58, 152.41, 148.73 (d, *J* = 86.2 Hz), 139.72 (d, *J* = 7.8 Hz), 132.41 (d, *J* = 2.8 Hz), 131.95 (d, *J* = 10.2 Hz), 130.71, 128.75 (d, *J* = 12.4 Hz), 123.45 (d, *J* = 8.9 Hz). ^{31}P NMR (122 MHz, $CDCl_3$) δ 26.49.

(1H-indol-5-yl)diphenylphosphine oxide (3n)[16]

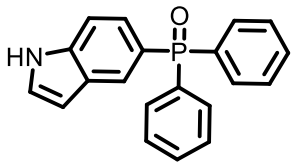

White solid. ^{1}H NMR (300 MHz, $CDCl_3$) δ 10.75 (s, 1H), 7.87 (dd, *J* = 13.4, 1.4 Hz, 1H), 7.77 – 7.67 (m, 4H), 7.57 – 7.48 (m, 2H), 7.48 – 7.39 (m, 5H), 7.35 – 7.28 (m, 1H), 7.19 (t, *J* = 2.8 Hz, 1H), 6.47 (t, *J* = 2.5 Hz, 1H). ^{13}C NMR (75 MHz, $CDCl_3$) δ 138.15, 133.34 (d, *J* = 103.9 Hz), 131.74 (d, *J* = 2.7 Hz), 128.44 (d, *J* = 12.1 Hz), 127.60 (d, *J* = 15.2 Hz), 126.52, 125.95 (d, *J* = 12.0 Hz), 124.24 (d, *J* = 11.9 Hz), 121.62, 120.15, 112.13 (d, *J* = 14.0 Hz), 102.52. ^{31}P NMR (122 MHz, $CDCl_3$) δ 32.65.

diphenyl(thiophen-2-yl)phosphine oxide (3o)[12]

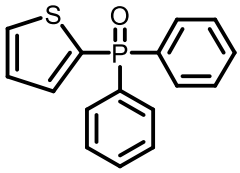

Pale yellow oil. ^{1}H NMR (300 MHz, $CDCl_3$) δ 7.76 – 7.62 (m, 5H), 7.57-7.52 (m, 2H), 7.48 – 7.38 (m, 5H), 7.18-7.15 (m, 1H). ^{13}C NMR (75 MHz, $CDCl_3$) δ 137.05 (d, *J* = 10.3 Hz) 134.57 (d, *J* = 112.0 Hz), 133.97 (d, *J* = 5.9 Hz), 133.59 (d, *J* =110.5 Hz), 132.61 (d, *J* = 2.6 Hz), 131.83 (d, *J* = 10.5 Hz), 128.99 (d, *J* = 12.5 Hz), 128.37 (d, *J* = 13.8 Hz). ^{31}P NMR (122 MHz, $CDCl_3$) δ 21.82.

phenyldi-p-tolylphosphine oxide (3p)[12]

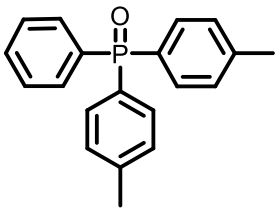

White solid. ^{1}H NMR (400 MHz, $CDCl_3$) δ 7.57-7.78 (m, 2H), 7.51-7.56 (m, 7H), 7.25-7.49 (m, 4H), 2.37 (s, 6H). ^{13}C NMR (101 MHz, $CDCl_3$) δ 142.6 (d, *J* = 2.7 Hz), 133.0 (d, *J*= 104.3 Hz), 132.3 (d, *J* = 10.3 Hz), 132.1 (d, *J* = 9.7 Hz), 131.6 (d, *J* = 2.8 Hz), 129.8 (d, *J* = 12.7 Hz), 129.1 (d, *J* = 105.7 Hz), 128.2 (d, *J* = 12.3 Hz), 21.4 (d, *J* = 1.1 Hz). ^{31}P NMR (162 MHz, $CDCl_3$) δ 28.20.

bis(4-methoxyphenyl)(phenyl)phosphine oxide (3s)[12]

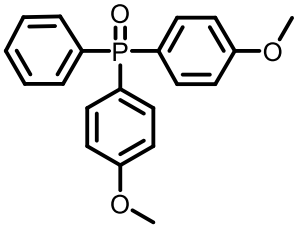

Light yellow oil. ^{1}H NMR (400 MHz, $CDCl_3$) δ 7.54-7.51 (m, 6H), 7.49-7.31 (m, 3H), 6.97-7.04 (m, 4H), 3.80 (s, 6H). ^{13}C NMR (101 MHz, $CDCl_3$) δ 161.91 (d, *J* = 2.5 Hz), 133.69 (d, *J* = 11.3 Hz), 132.25, 131.98 (d, *J* = 10.3 Hz), 131.84 (d, *J* = 2.3 Hz), 128.47 (d, *J* = 12.6 Hz), 124.20 (d, *J* = 110.4 Hz), 113.86 (d, *J* = 13.4 Hz), 55.35. ^{31}P NMR (162 MHz, $CDCl_3$) δ 28.16.

6. ^{1}H and ^{13}C, and ^{31}P NMR Spectra of Products.

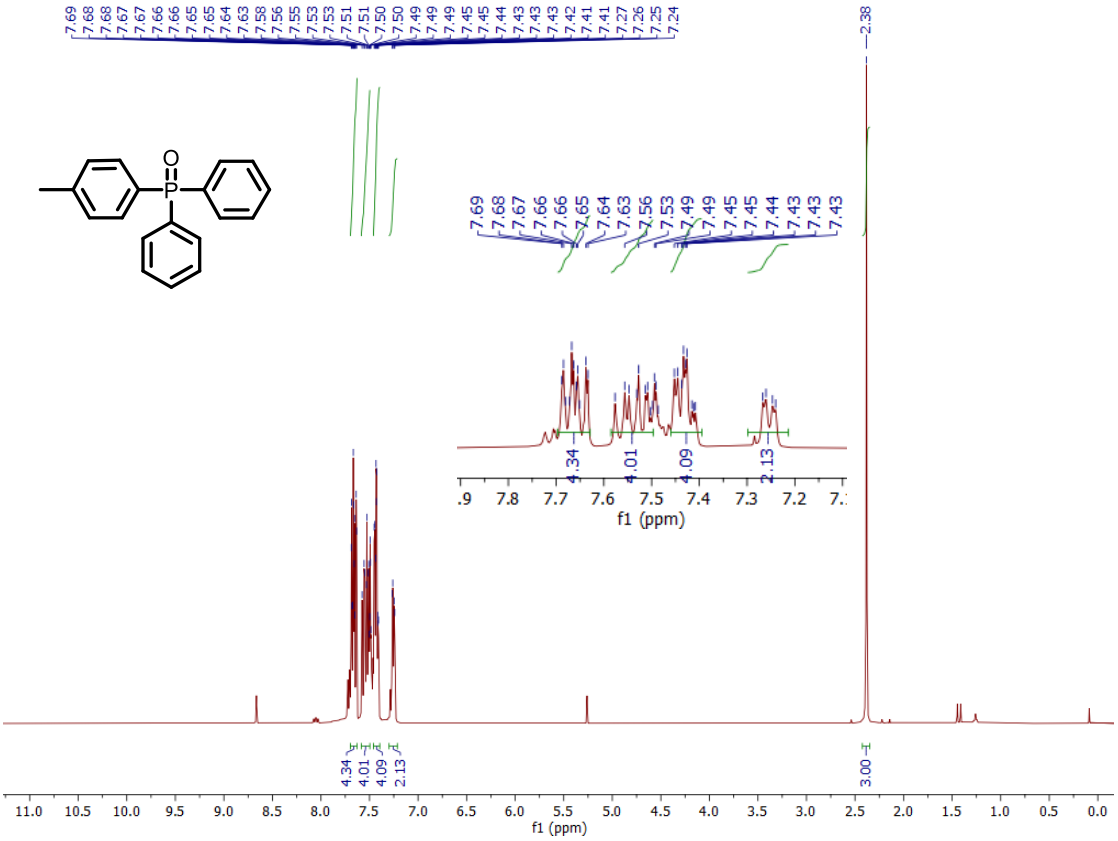

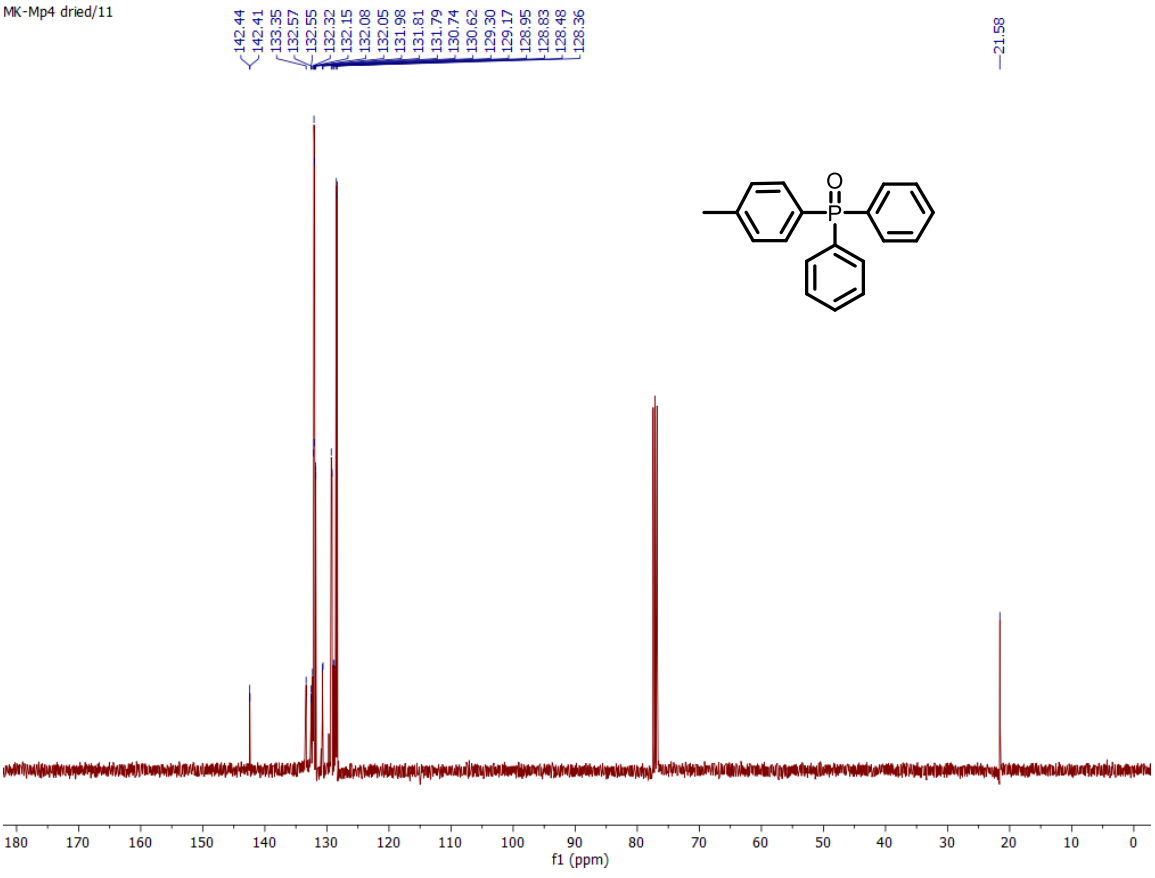

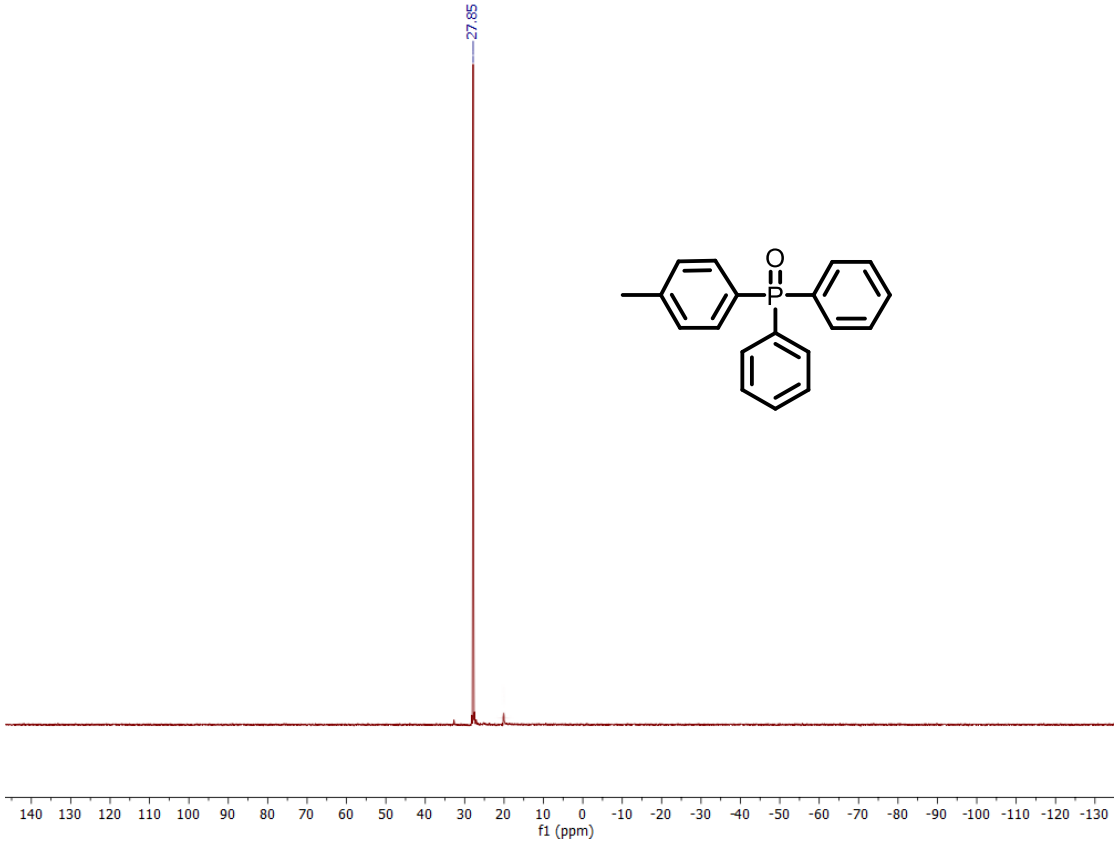
27.85
O
P
140 130 120 110 100 90 80 70 60 50 40 30 20 10 0 -10 -20 -30 -40 -50 -60 -70 -80 -90 -100 -110 -120 -130
f1 (ppm)

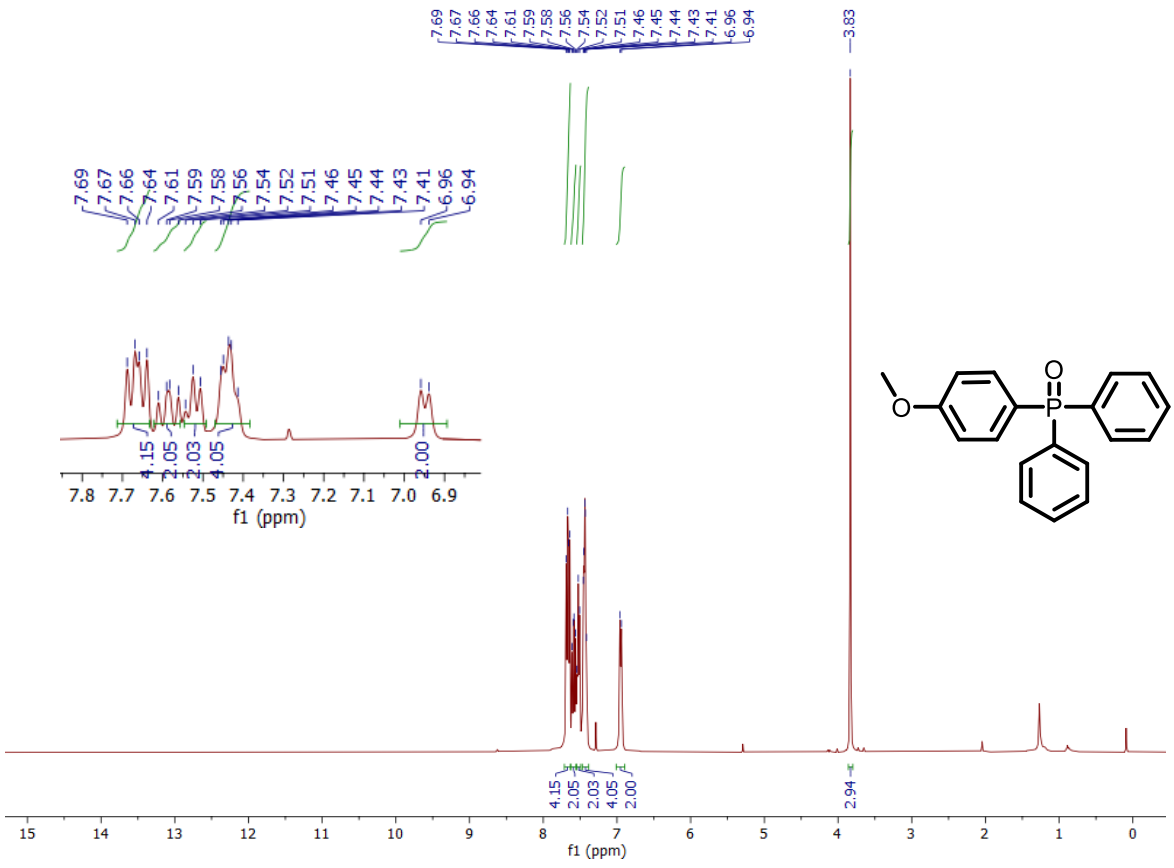
7.69
7.67
7.66
7.64
7.61
7.59
7.58
7.56
7.54
7.52
7.51
7.46
7.45
7.44
7.43
7.41
6.96
6.94
3.83
O
P
4.15
2.05
2.03
4.05
2.00
2.94
7.8 7.7 7.6 7.5 7.4 7.3 7.2 7.1 7.0 6.9
f1 (ppm)
15 14 13 12 11 10 9 8 7 6 5 4 3 2 1 0
f1 (ppm)

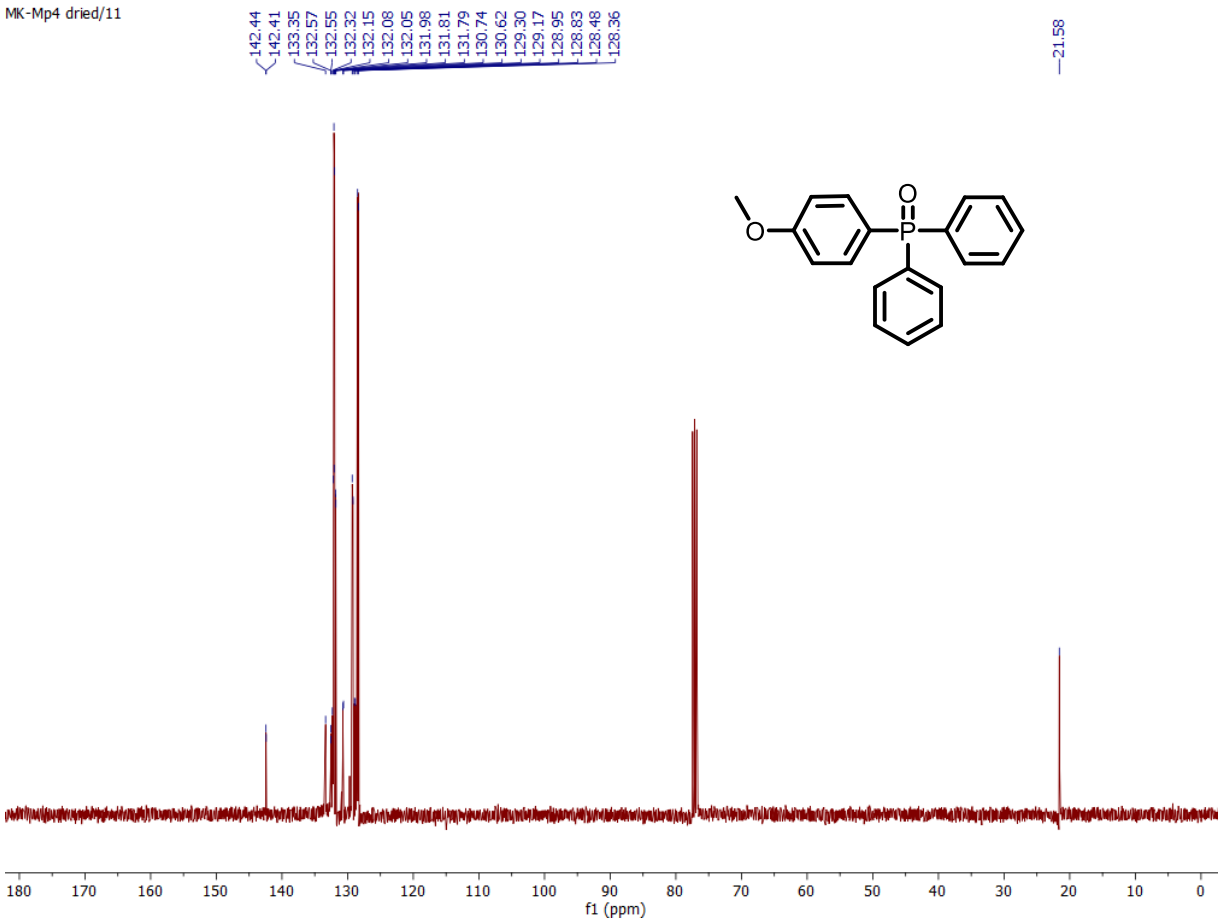
MK-Mp4 dried/11
142.44
142.41
133.35
132.57
132.55
132.32
132.15
132.08
132.05
131.98
131.81
131.79
130.74
130.62
129.30
129.17
128.95
128.83
128.48
128.36
21.58
O
O
P
180 170 160 150 140 130 120 110 100 90 80 70 60 50 40 30 20 10 0
f1 (ppm)

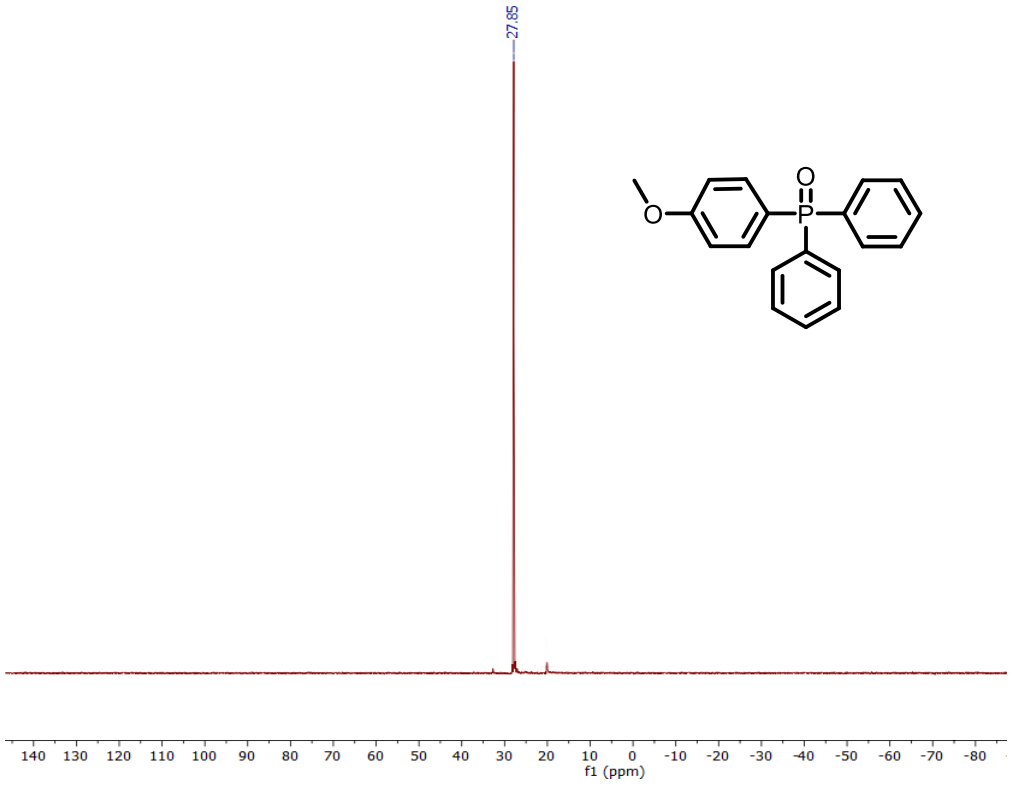
27.85
O
O
P
140 130 120 110 100 90 80 70 60 50 40 30 20 10 0 -10 -20 -30 -40 -50 -60 -70 -80
f1 (ppm)

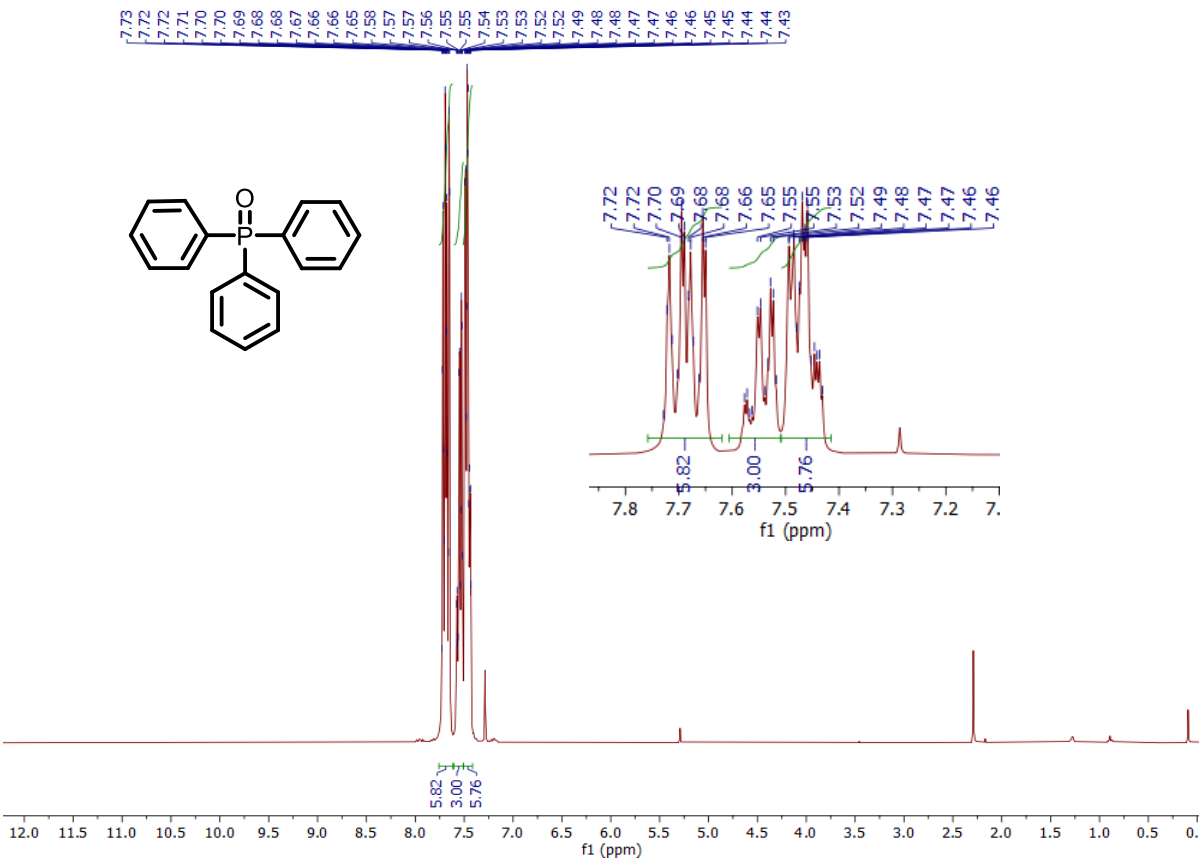
7.73 7.72 7.72 7.71 7.70 7.70 7.69 7.68 7.68 7.67 7.66 7.66 7.65 7.58 7.57 7.57 7.56 7.55 7.55 7.54 7.53 7.53 7.52 7.52 7.49 7.48 7.48 7.47 7.47 7.46 7.46 7.45 7.45 7.44 7.44 7.43
O
P
7.72 7.72 7.70 7.69 7.68 7.68 7.66 7.65 7.55 7.55 7.53 7.52 7.49 7.48 7.47 7.47 7.46 7.46
5.82 3.00 5.76
7.8 7.7 7.6 7.5 7.4 7.3 7.2 7.
f1 (ppm)
5.82 3.00 5.76
12.0 11.5 11.0 10.5 10.0 9.5 9.0 8.5 8.0 7.5 7.0 6.5 6.0 5.5 5.0 4.5 4.0 3.5 3.0 2.5 2.0 1.5 1.0 0.5 0.
f1 (ppm)

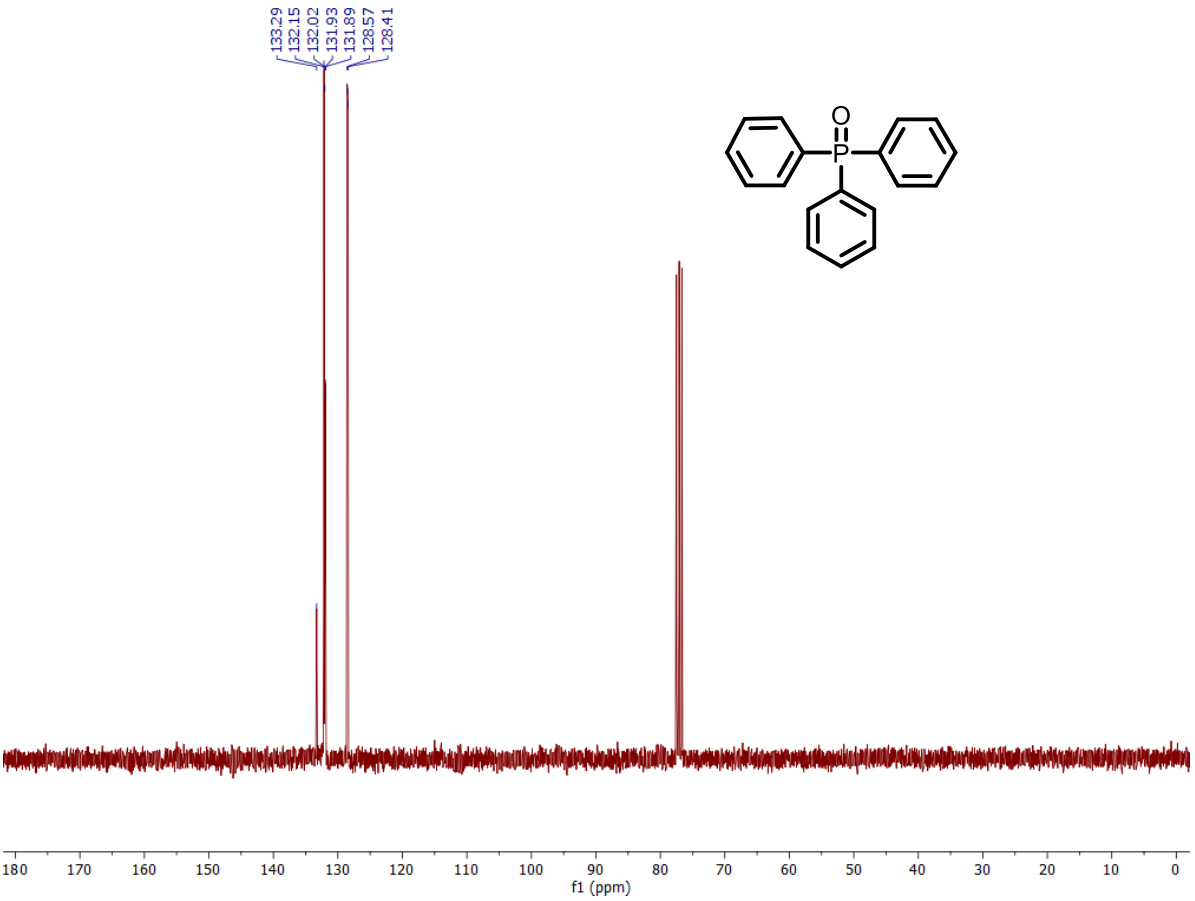
133.29 132.15 132.02 131.93 131.89 128.57 128.41
O
P
180 170 160 150 140 130 120 110 100 90 80 70 60 50 40 30 20 10 0
f1 (ppm)

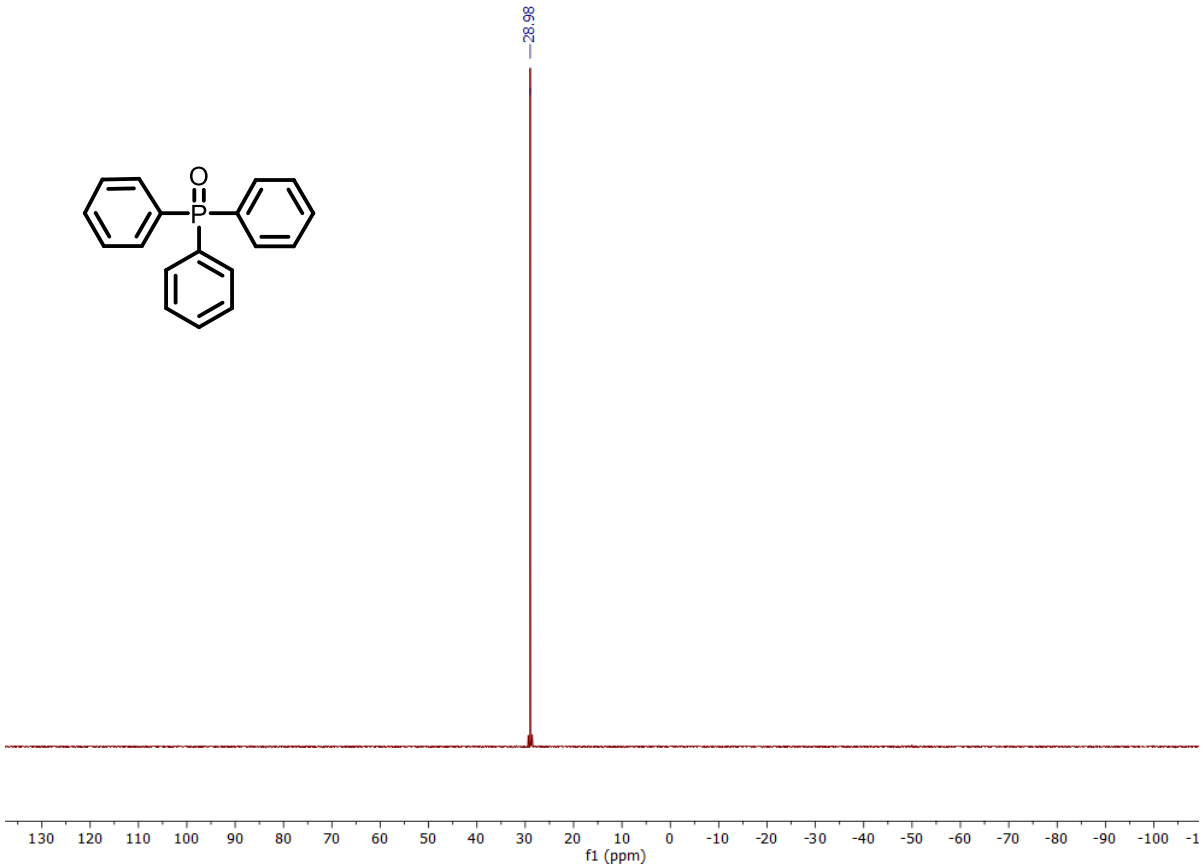
28.98
f1 (ppm)

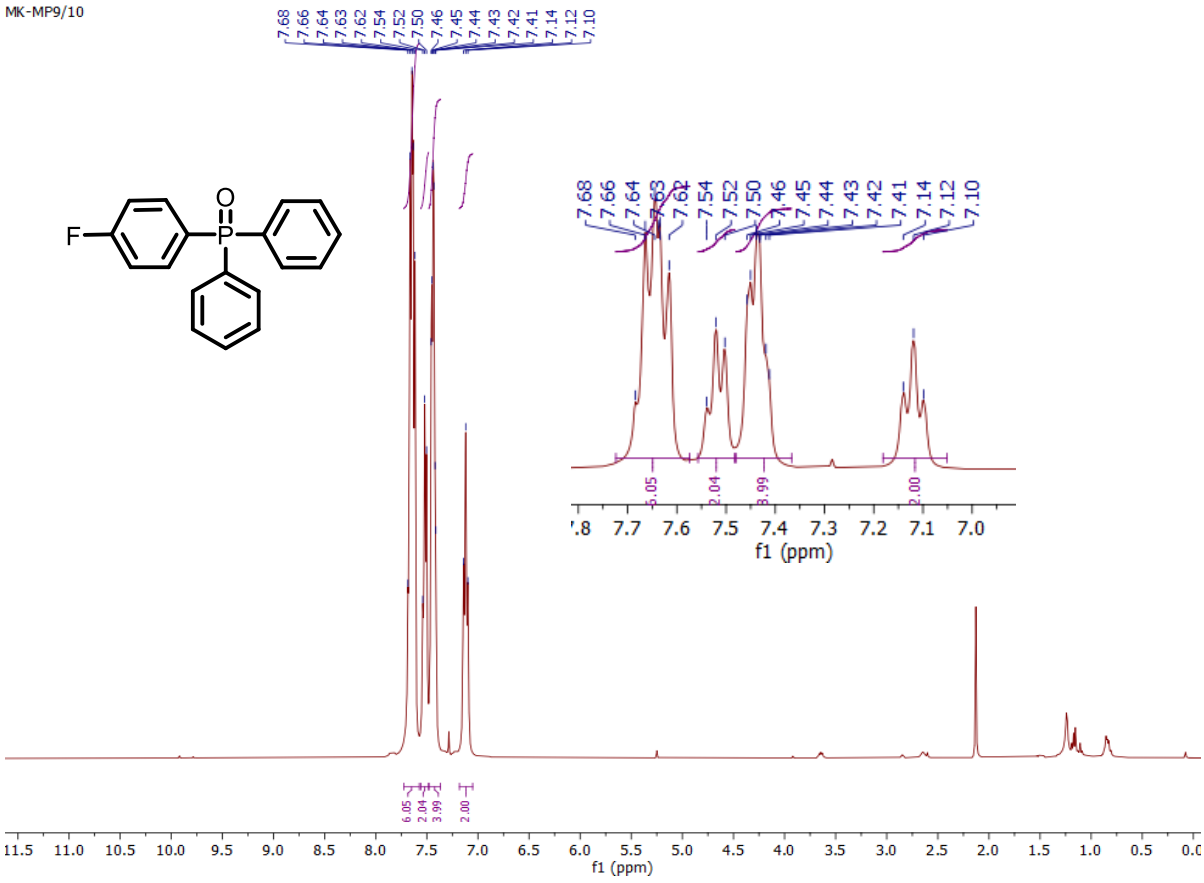
MK-MP9/10
7.68
7.66
7.64
7.63
7.62
7.54
7.52
7.50
7.46
7.45
7.44
7.43
7.42
7.41
7.14
7.12
7.10
6.05
2.04
3.99
2.00
f1 (ppm)

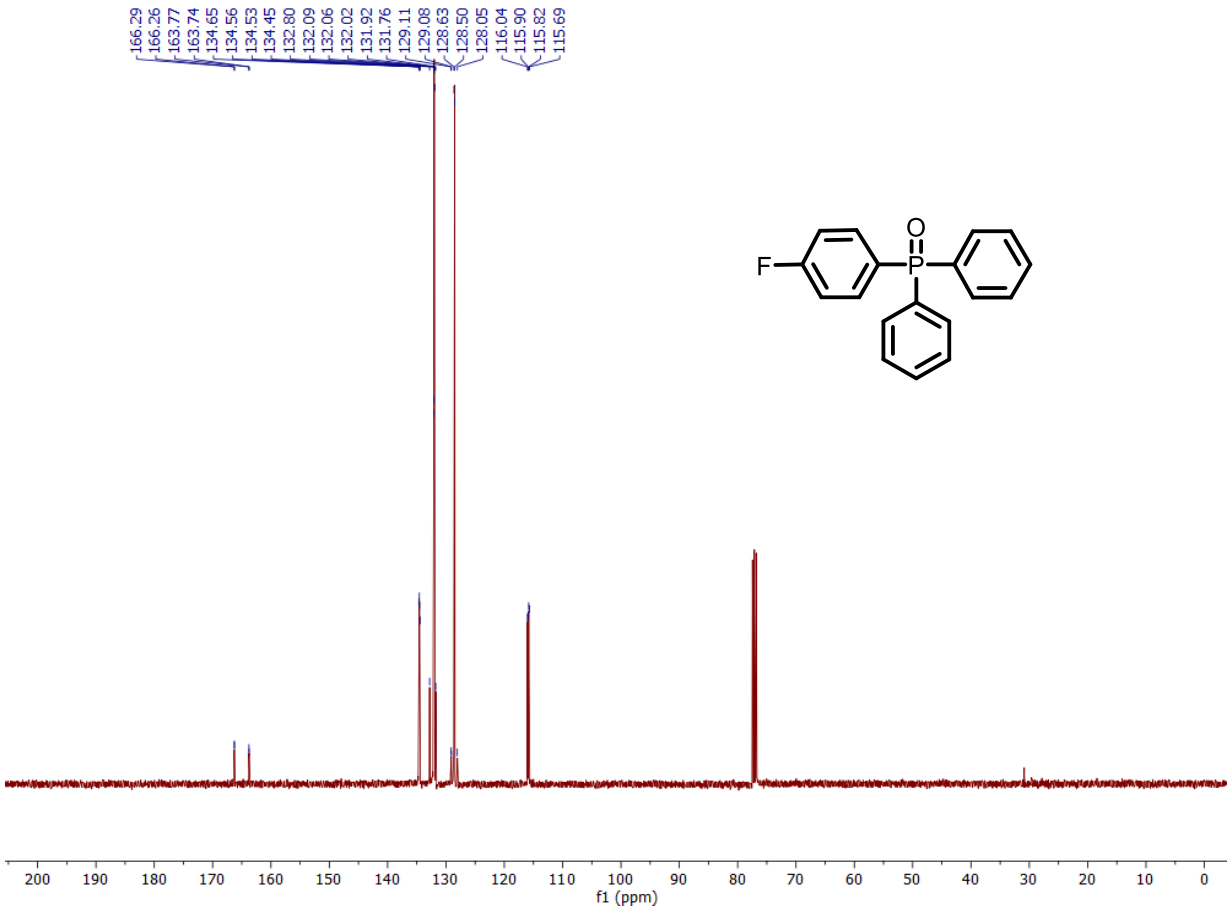
166.29
166.26
163.77
163.74
134.65
134.56
134.53
134.45
132.80
132.09
132.06
132.02
131.92
131.76
129.11
129.08
128.63
128.50
128.05
116.04
115.90
115.82
115.69
F
O
P
200 190 180 170 160 150 140 130 120 110 100 90 80 70 60 50 40 30 20 10 0
f1 (ppm)

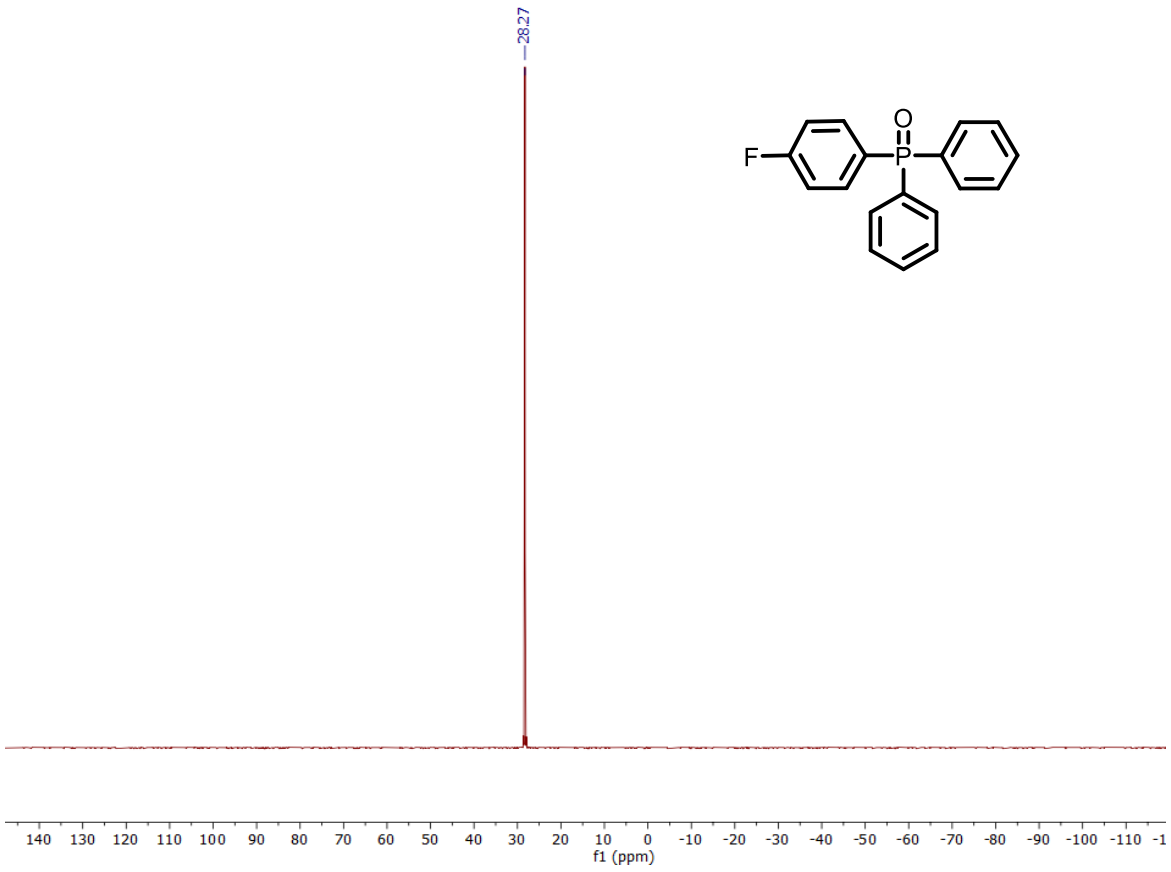
28.27
F
O
P
140 130 120 110 100 90 80 70 60 50 40 30 20 10 0 -10 -20 -30 -40 -50 -60 -70 -80 -90 -100 -110 -1
f1 (ppm)

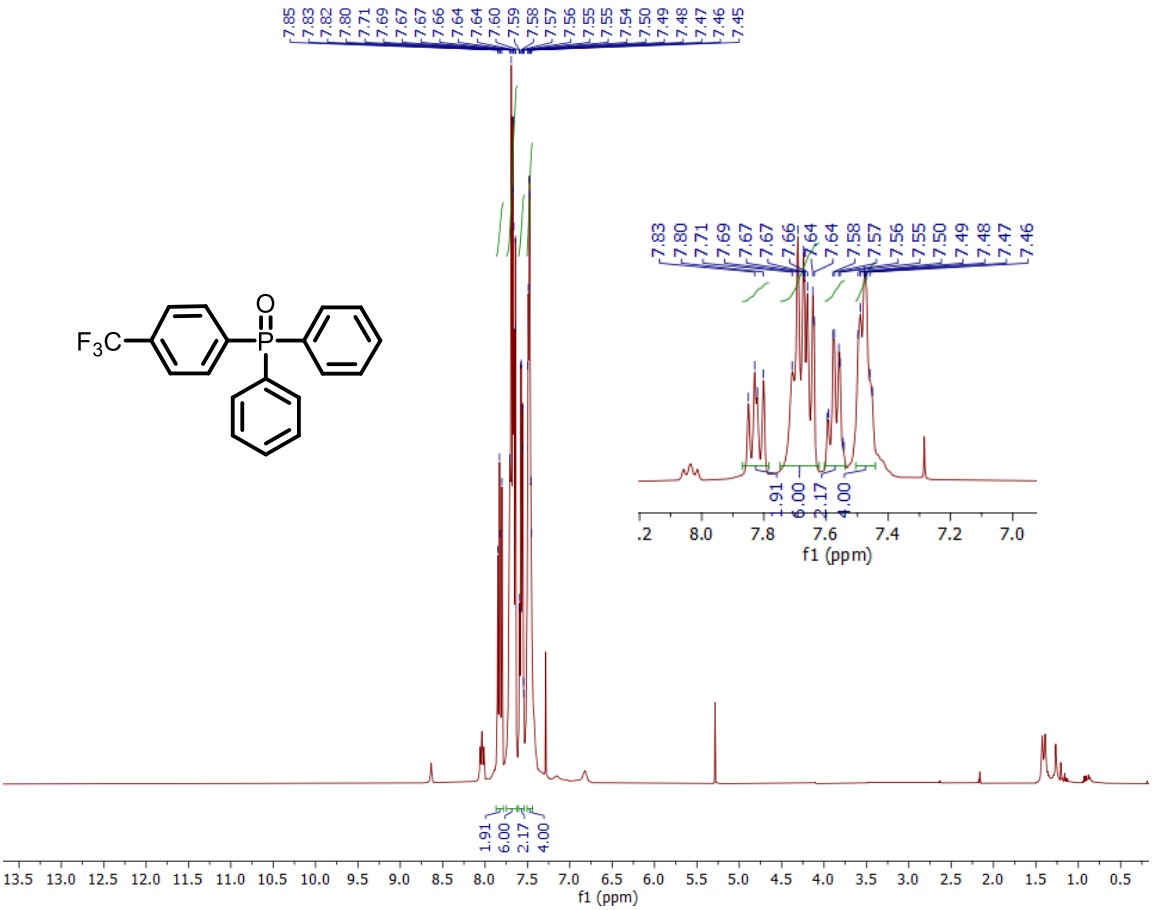
7.85
7.83
7.82
7.80
7.71
7.69
7.67
7.67
7.66
7.64
7.64
7.60
7.59
7.58
7.57
7.56
7.55
7.55
7.54
7.50
7.49
7.48
7.47
7.46
7.45
F3C
O
P
1.91
6.00
2.17
4.00
f1 (ppm)

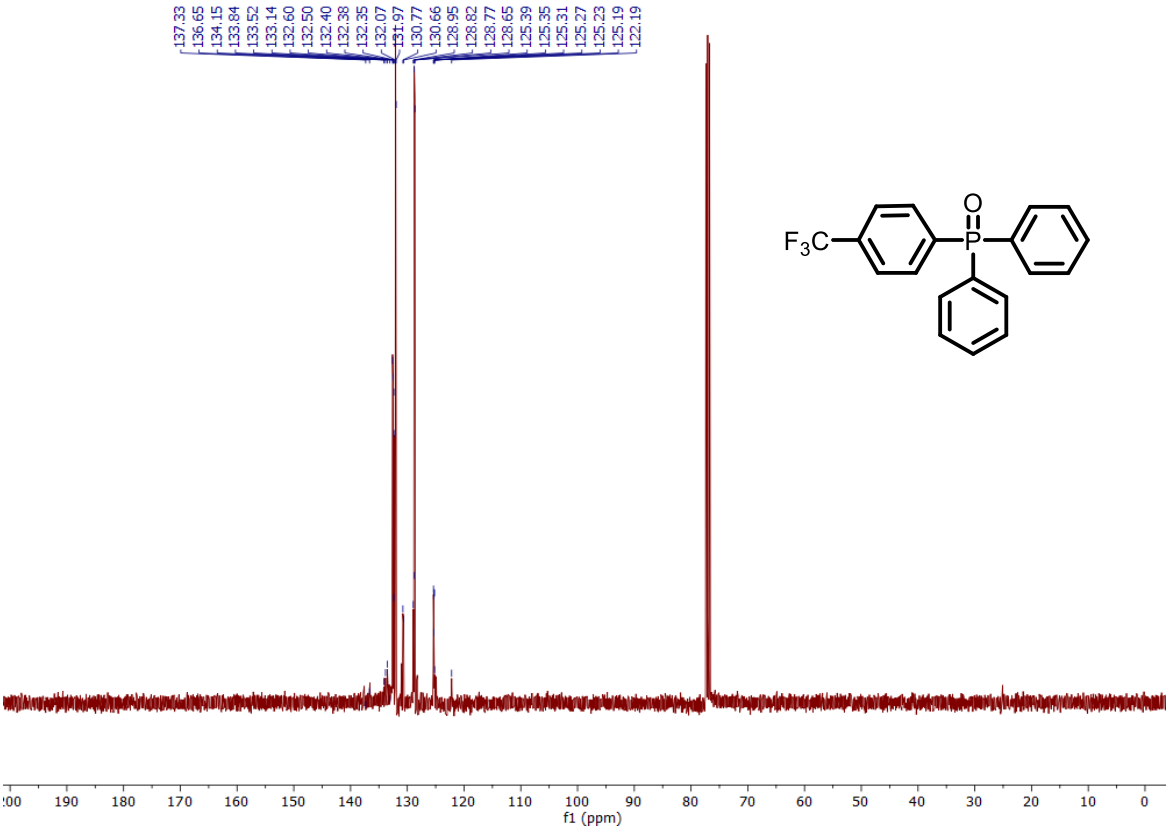
137.33
136.65
134.15
133.84
133.52
133.14
132.60
132.50
132.40
132.38
132.35
132.07
131.97
130.77
130.66
128.95
128.82
128.77
128.65
125.39
125.35
125.31
125.27
125.23
125.19
122.19
F3C
O
P
f1 (ppm)

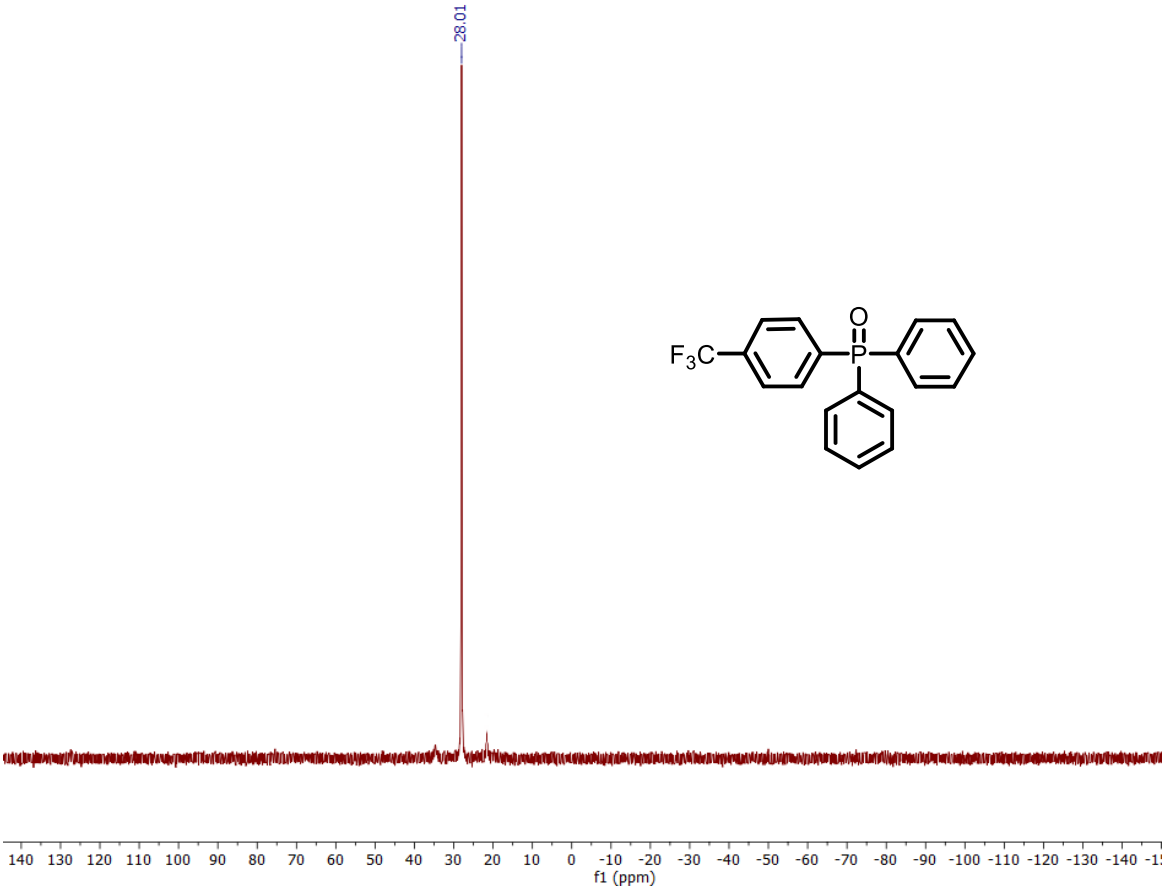
28.01
F3C
O
P
f1 (ppm)

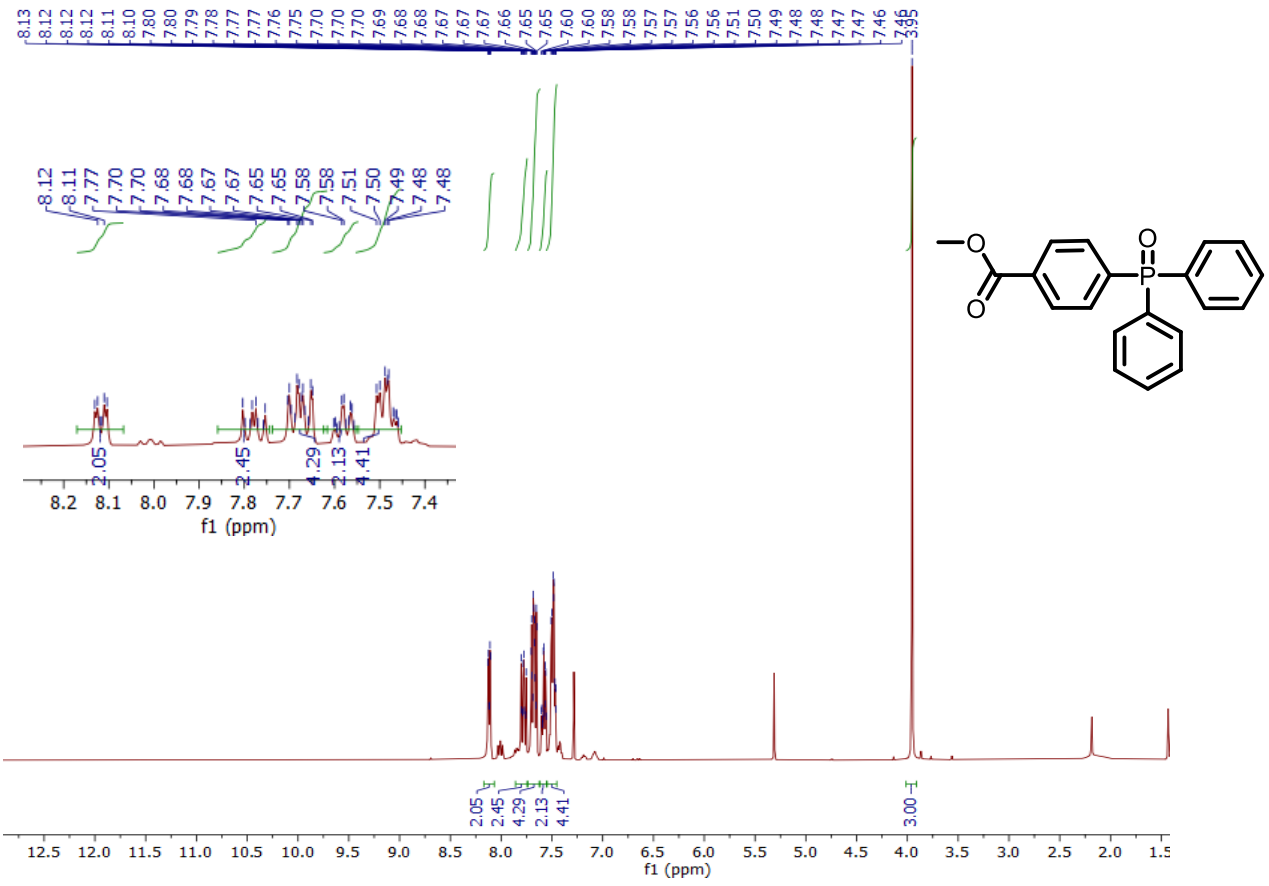
O
O
P
2.05
2.45
4.29
2.13
4.41
3.00
f1 (ppm)

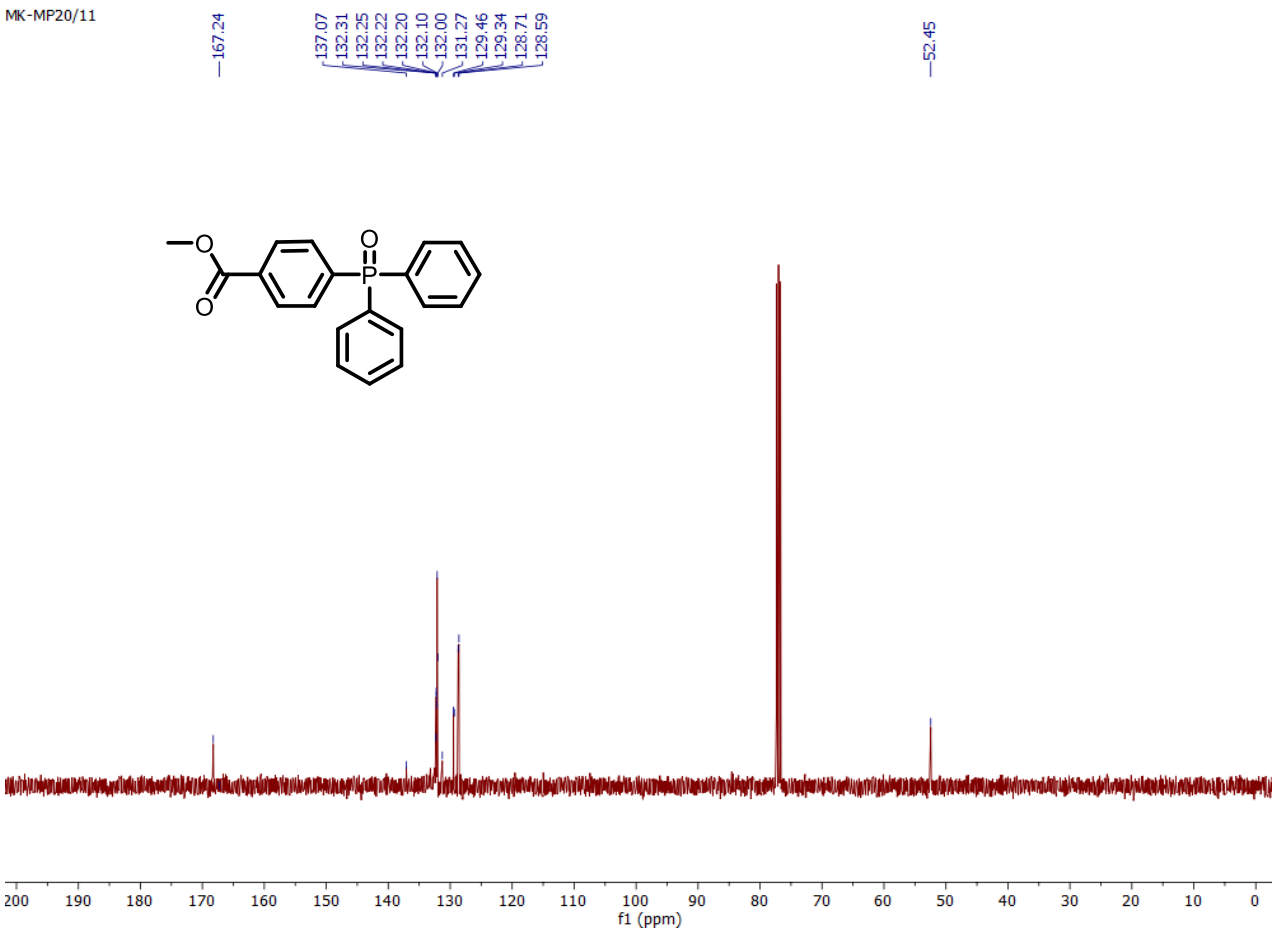
MK-MP20/11
167.24
137.07
132.31
132.25
132.22
132.20
132.10
132.00
131.27
129.46
129.34
128.71
128.59
52.45
O
O
P
O
O
200 190 180 170 160 150 140 130 120 110 100 90 80 70 60 50 40 30 20 10 0
f1 (ppm)

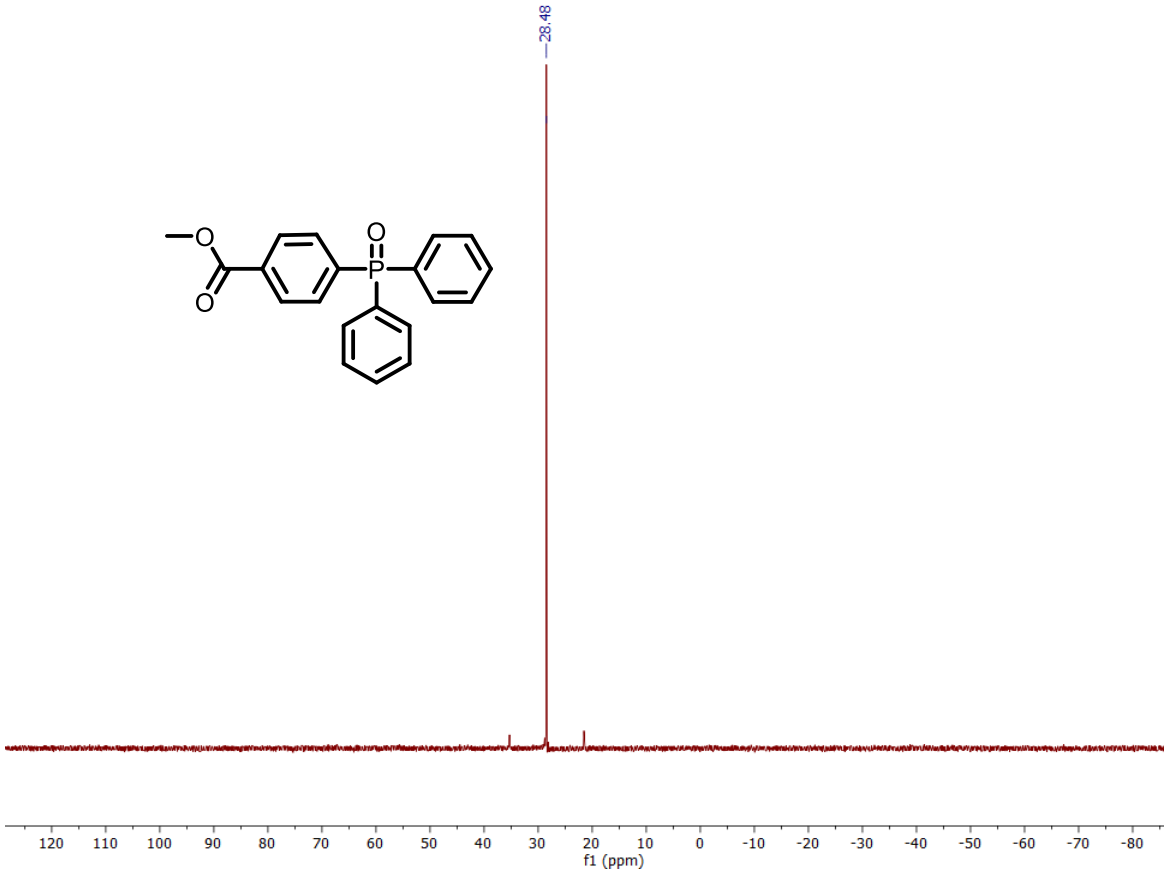
28.48
O
O
P
O
O
120 110 100 90 80 70 60 50 40 30 20 10 0 -10 -20 -30 -40 -50 -60 -70 -80
f1 (ppm)

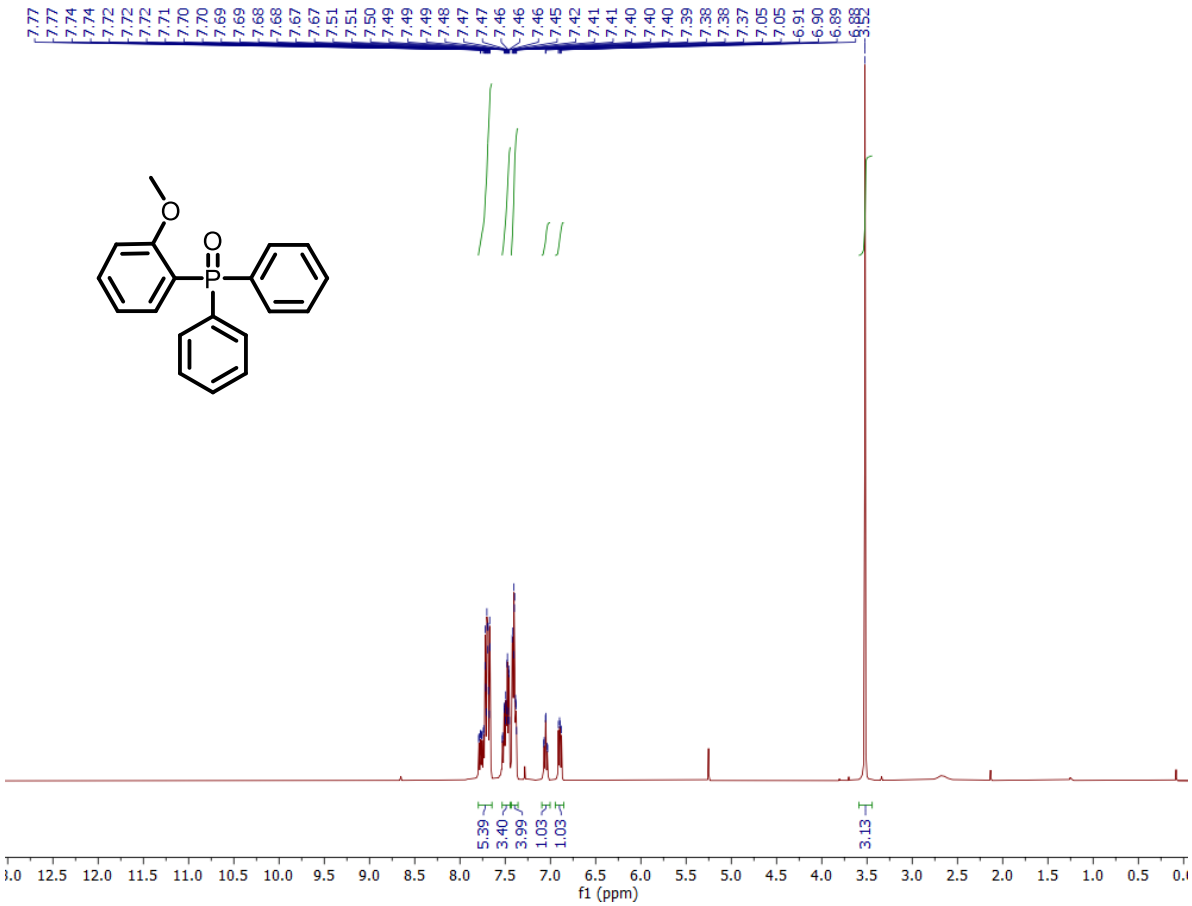
7.77
7.77
7.74
7.74
7.72
7.72
7.72
7.71
7.70
7.70
7.69
7.69
7.68
7.68
7.67
7.67
7.51
7.51
7.50
7.49
7.49
7.49
7.48
7.47
7.47
7.46
7.46
7.46
7.45
7.42
7.41
7.41
7.40
7.40
7.39
7.38
7.38
7.37
7.05
7.05
6.91
6.90
6.89
6.88
3.52
O
O
P
5.39
3.40
3.99
1.03
1.03
3.13
f1 (ppm)

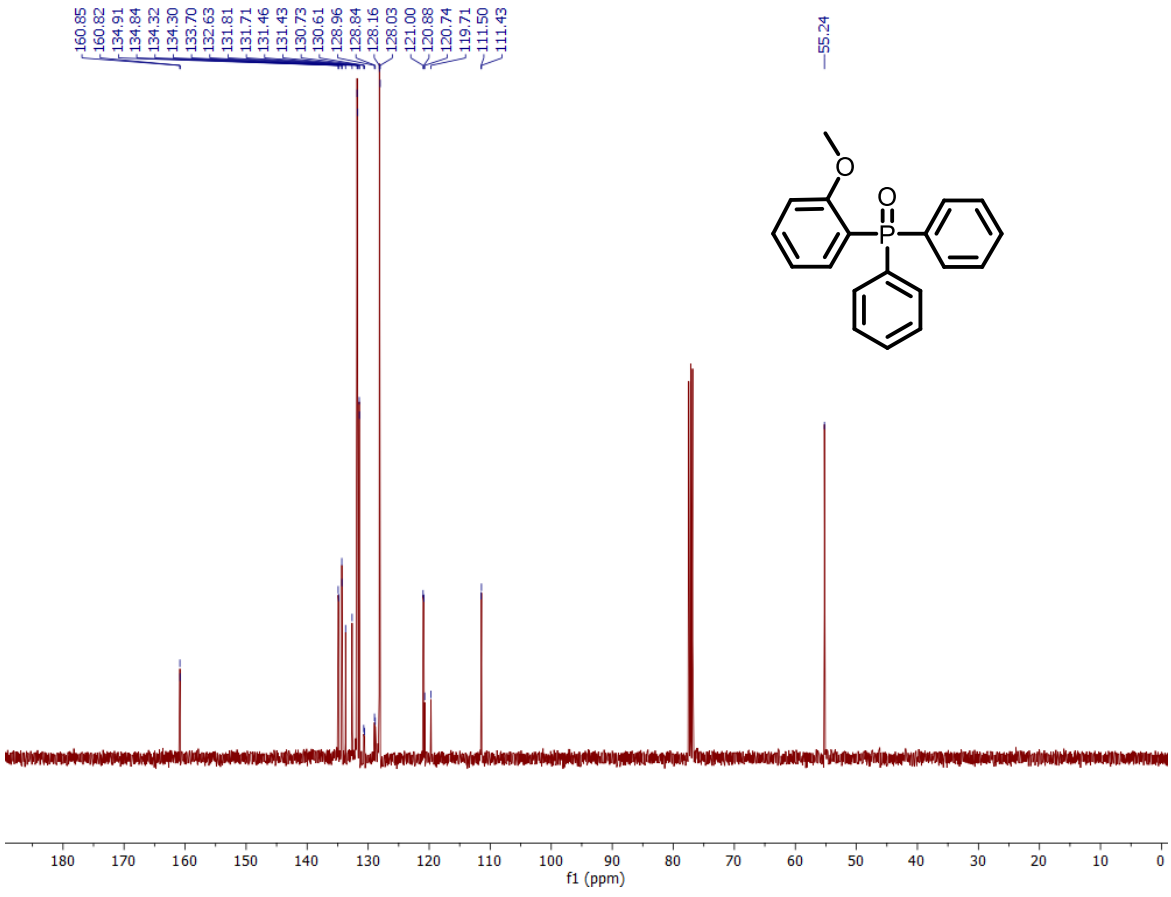
160.85
160.82
134.91
134.84
134.32
134.30
133.70
132.63
131.81
131.71
131.46
131.43
130.73
130.61
128.96
128.84
128.16
128.03
121.00
120.88
120.74
119.71
111.50
111.43
55.24
O
O
P
f1 (ppm)

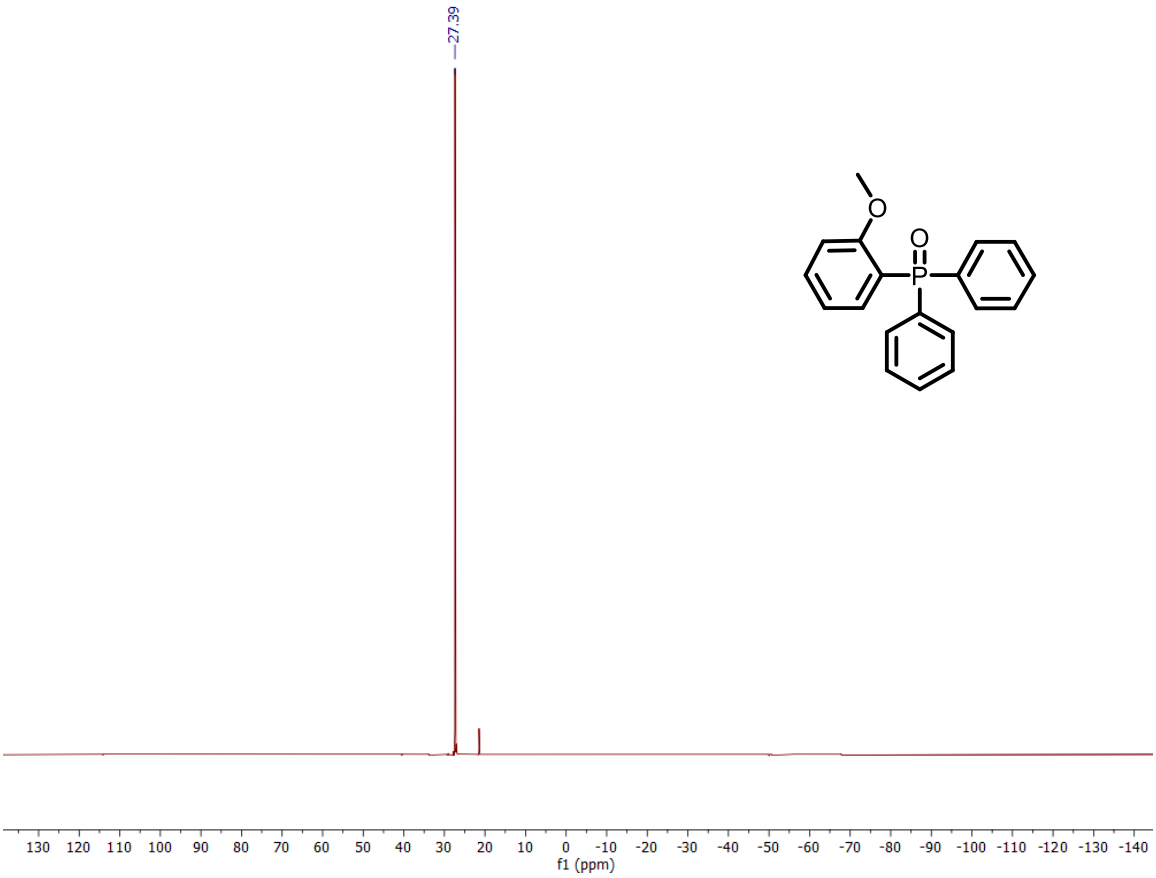
27.39
O
O
P
130 120 110 100 90 80 70 60 50 40 30 20 10 0 -10 -20 -30 -40 -50 -60 -70 -80 -90 -100 -110 -120 -130 -140
f1 (ppm)

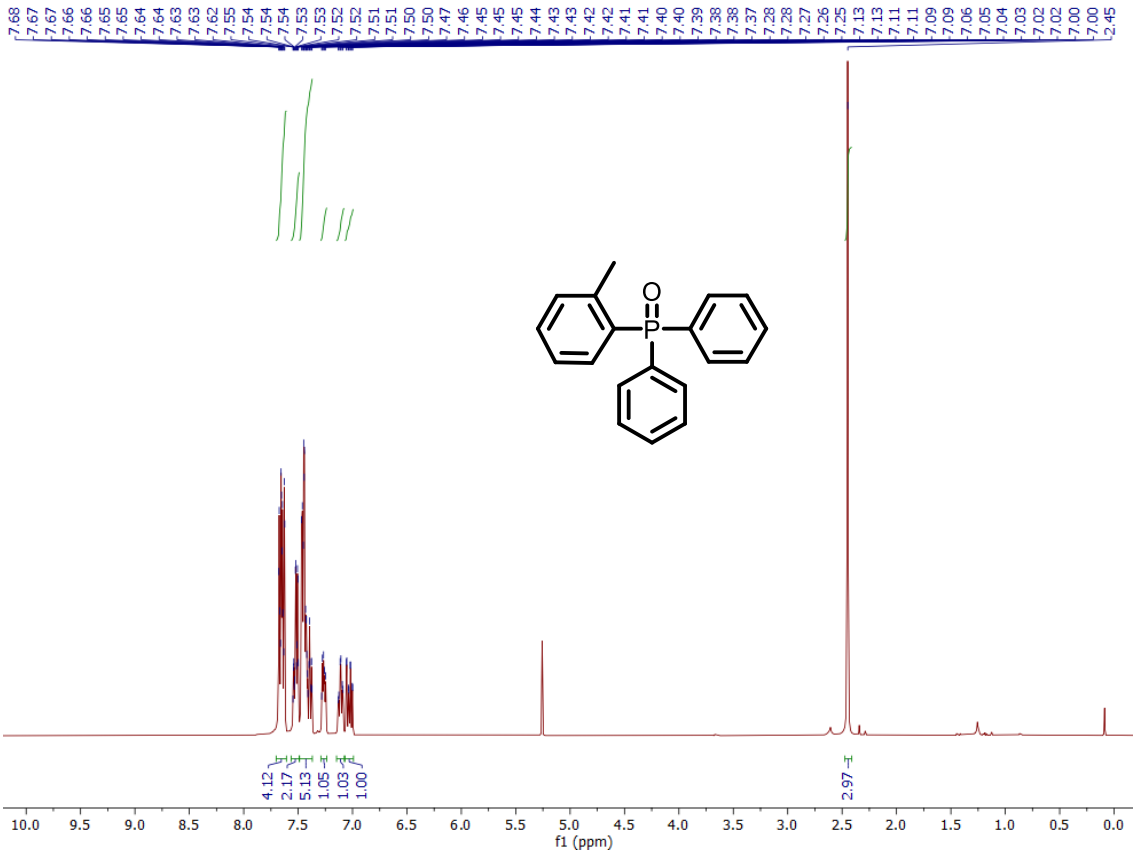
7.68 7.67 7.67 7.66 7.66 7.65 7.65 7.64 7.64 7.63 7.63 7.62 7.55 7.54 7.54 7.54 7.53 7.53 7.52 7.52 7.51 7.51 7.50 7.50 7.47 7.46 7.45 7.45 7.45 7.44 7.43 7.43 7.42 7.42 7.41 7.41 7.40 7.40 7.39 7.38 7.38 7.37 7.28 7.27 7.26 7.25 7.13 7.11 7.11 7.09 7.09 7.06 7.05 7.04 7.03 7.02 7.02 7.00 7.00 2.45
O
P
4.12 2.17 5.13 1.05 1.03 1.00
2.97
10.0 9.5 9.0 8.5 8.0 7.5 7.0 6.5 6.0 5.5 5.0 4.5 4.0 3.5 3.0 2.5 2.0 1.5 1.0 0.5 0.0
f1 (ppm)

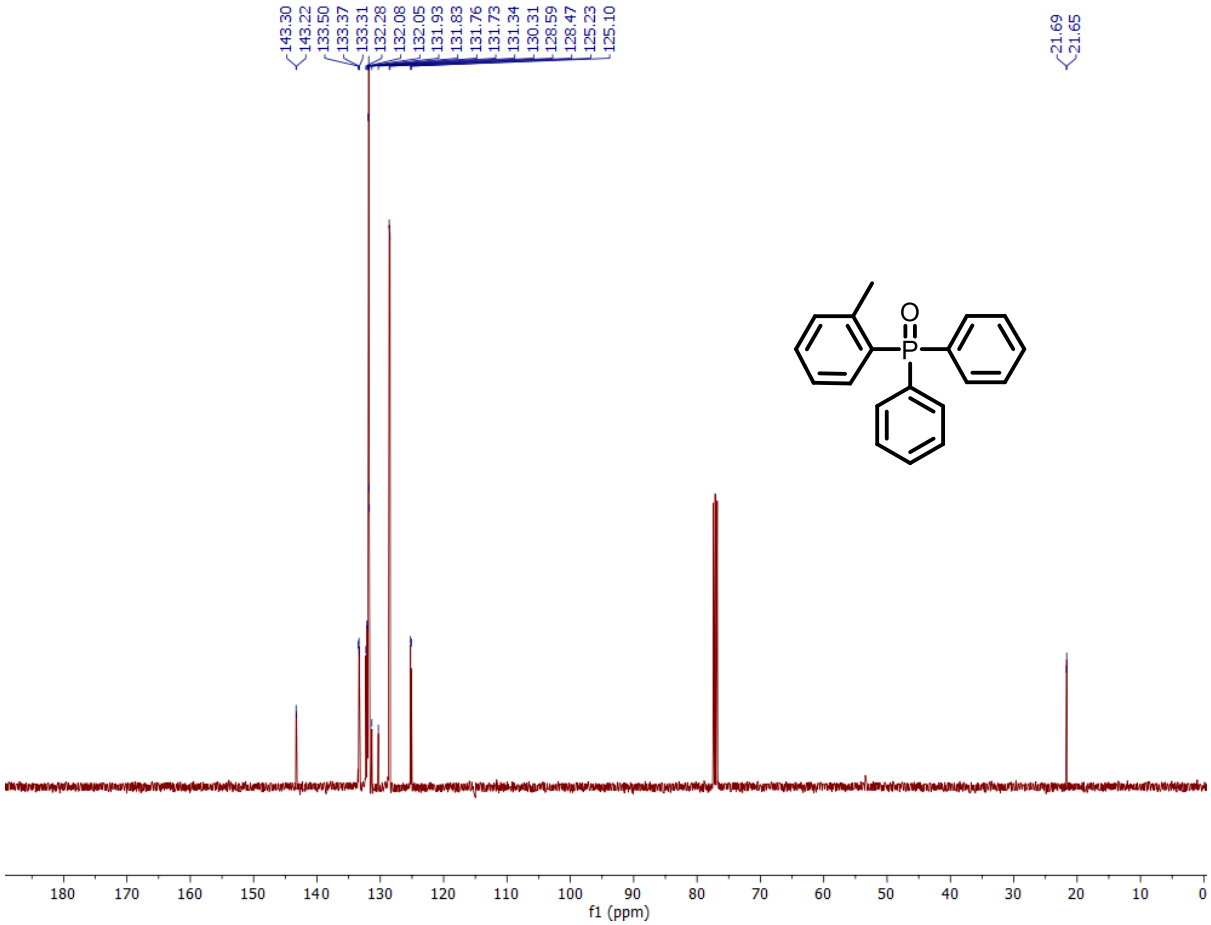
143.30
143.22
133.50
133.37
133.31
132.28
132.08
132.05
131.93
131.83
131.76
131.73
131.34
130.31
128.59
128.47
125.23
125.10
21.69
21.65
O
P
180 170 160 150 140 130 120 110 100 90 80 70 60 50 40 30 20 10 0
f1 (ppm)

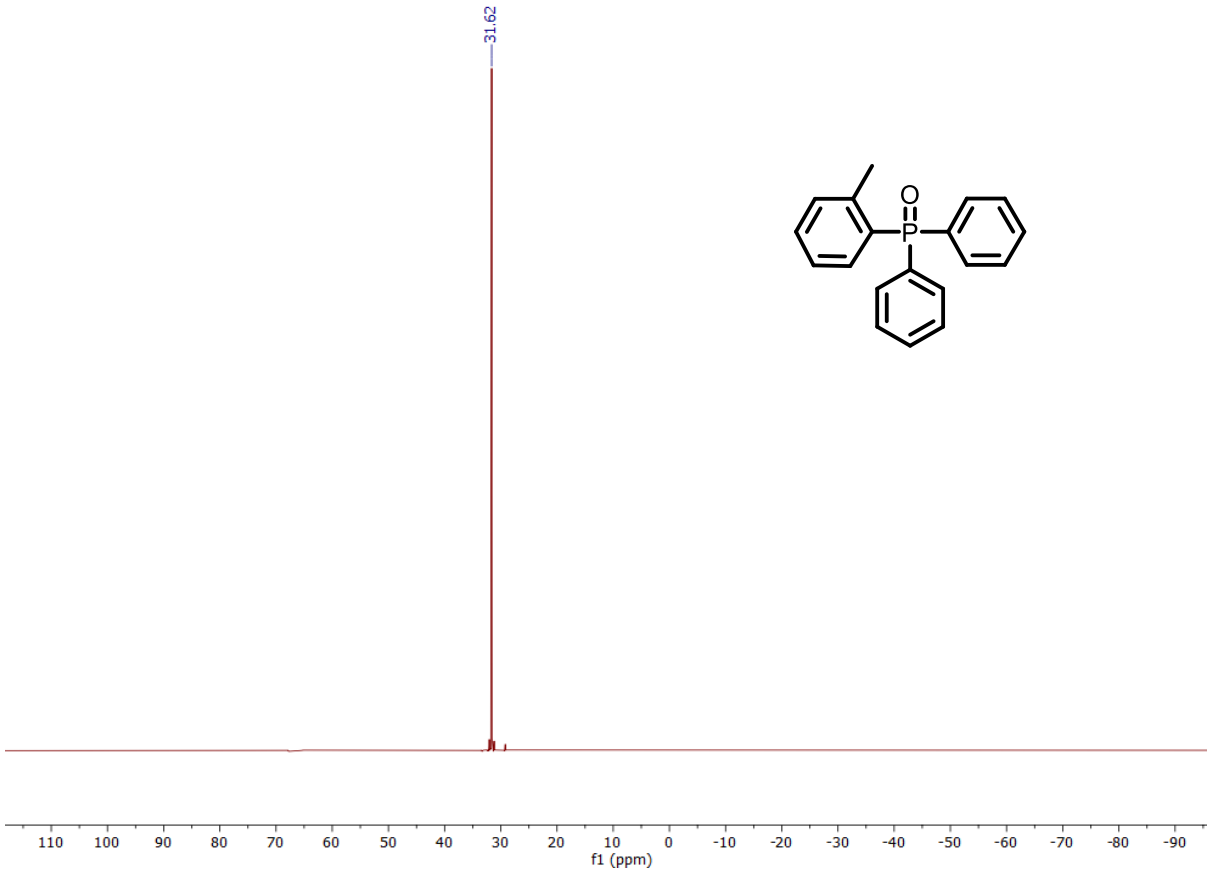
31.62
O
P
110 100 90 80 70 60 50 40 30 20 10 0 -10 -20 -30 -40 -50 -60 -70 -80 -90
f1 (ppm)

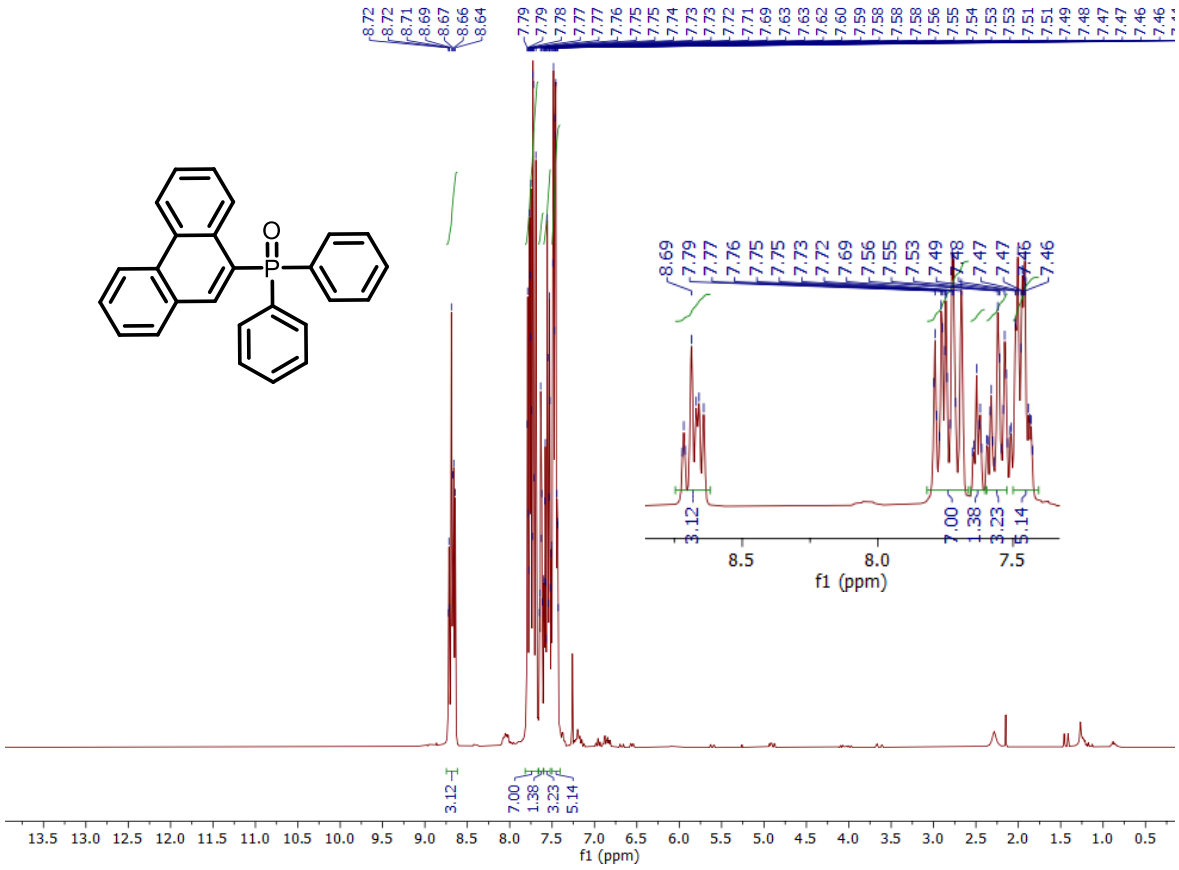
8.72 8.72 8.71 8.69 8.67 8.66 8.64
7.79 7.79 7.78 7.77 7.77 7.76 7.75 7.75 7.74 7.73 7.73 7.72 7.71 7.69 7.63 7.63 7.62 7.60 7.59 7.58 7.58 7.56 7.55 7.54 7.53 7.53 7.51 7.51 7.49 7.48 7.47 7.47 7.46 7.46
O
P
8.69 7.79 7.77 7.76 7.75 7.75 7.73 7.72 7.69 7.56 7.55 7.53 7.49 7.48 7.47 7.47 7.46 7.46
3.12 7.00 1.38 3.23 5.14
8.5 8.0 7.5
f1 (ppm)
3.12 7.00 1.38 3.23 5.14
13.5 13.0 12.5 12.0 11.5 11.0 10.5 10.0 9.5 9.0 8.5 8.0 7.5 7.0 6.5 6.0 5.5 5.0 4.5 4.0 3.5 3.0 2.5 2.0 1.5 1.0 0.5
f1 (ppm)

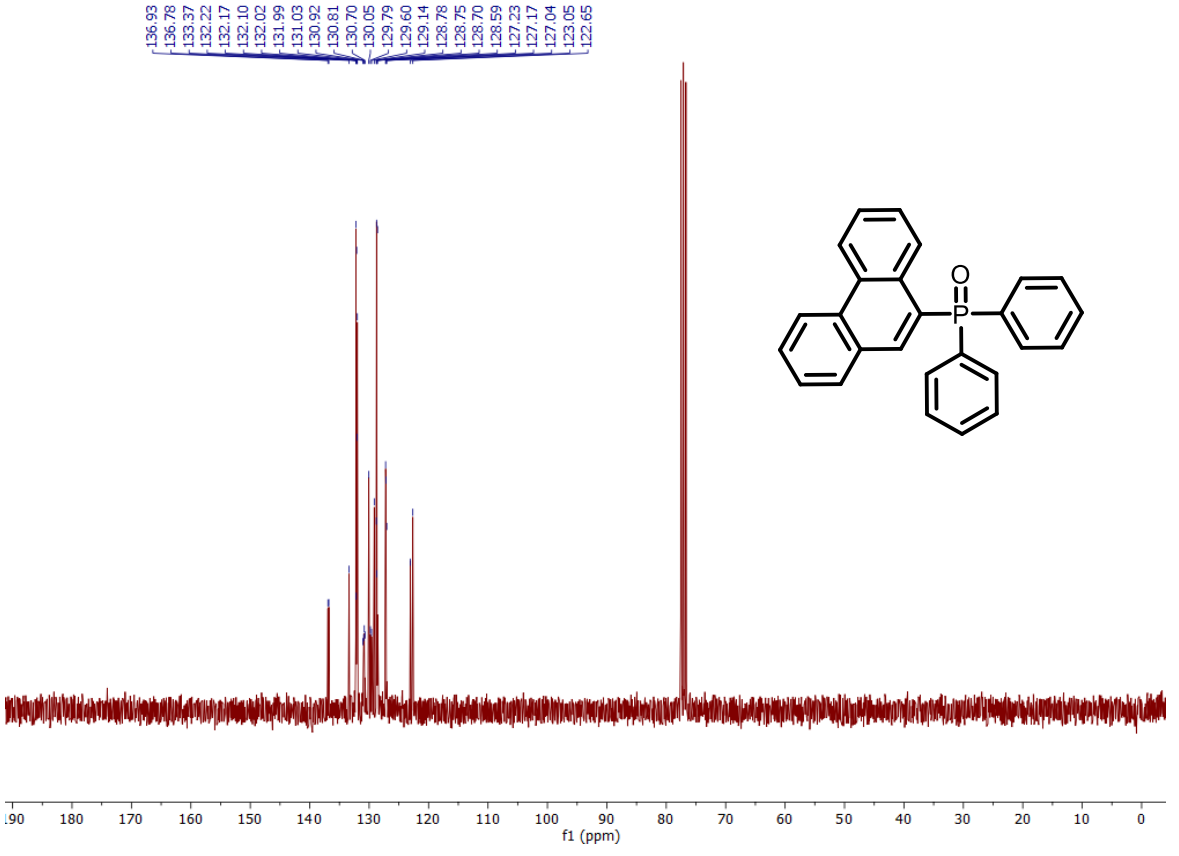
136.93 136.78 133.37 132.22 132.17 132.10 132.02 131.99 131.03 130.92 130.81 130.70 130.05 129.79 129.60 129.14 128.78 128.75 128.70 128.59 127.23 127.17 127.04 123.05 122.65
O
P
190 180 170 160 150 140 130 120 110 100 90 80 70 60 50 40 30 20 10 0
f1 (ppm)

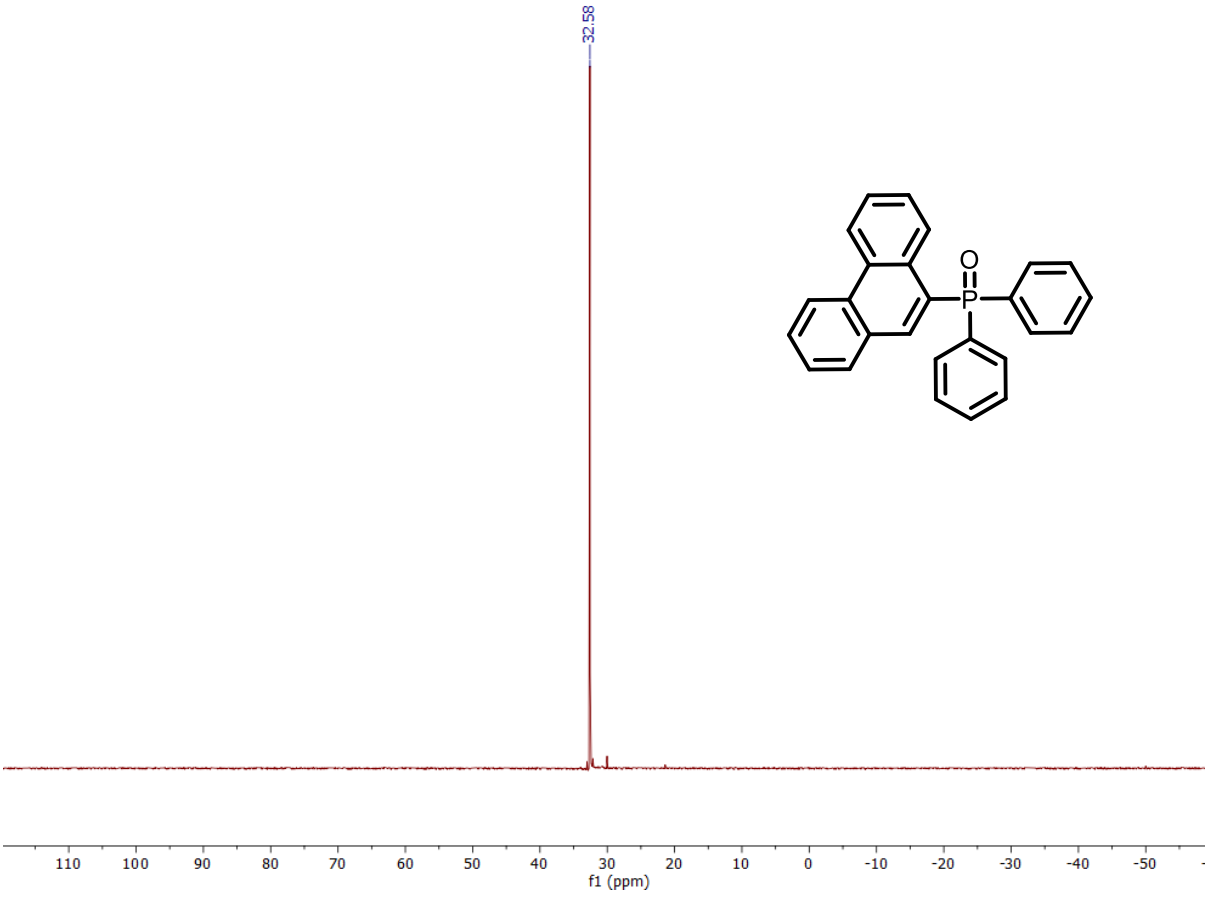
32.58
f1 (ppm)

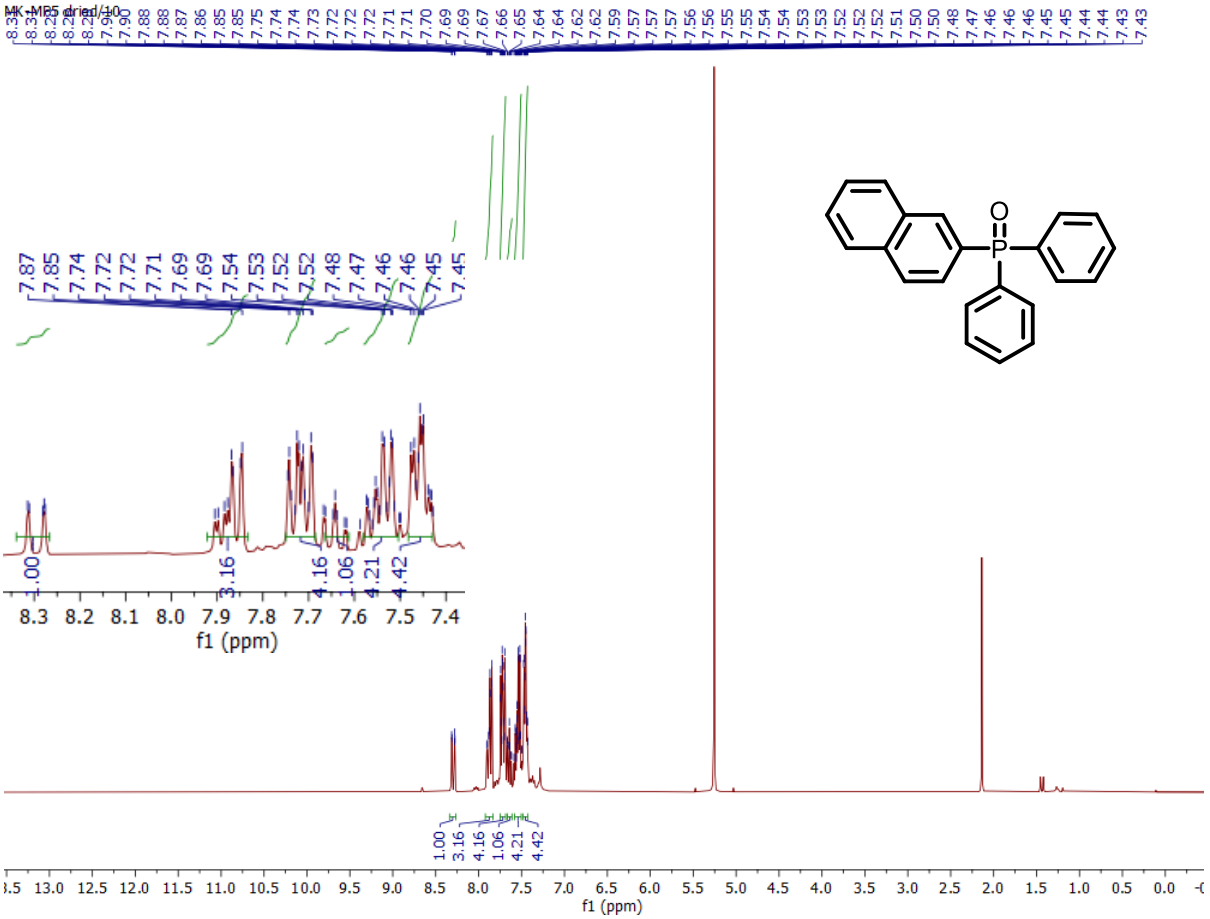
MK-MP5 dried-10
f1 (ppm)

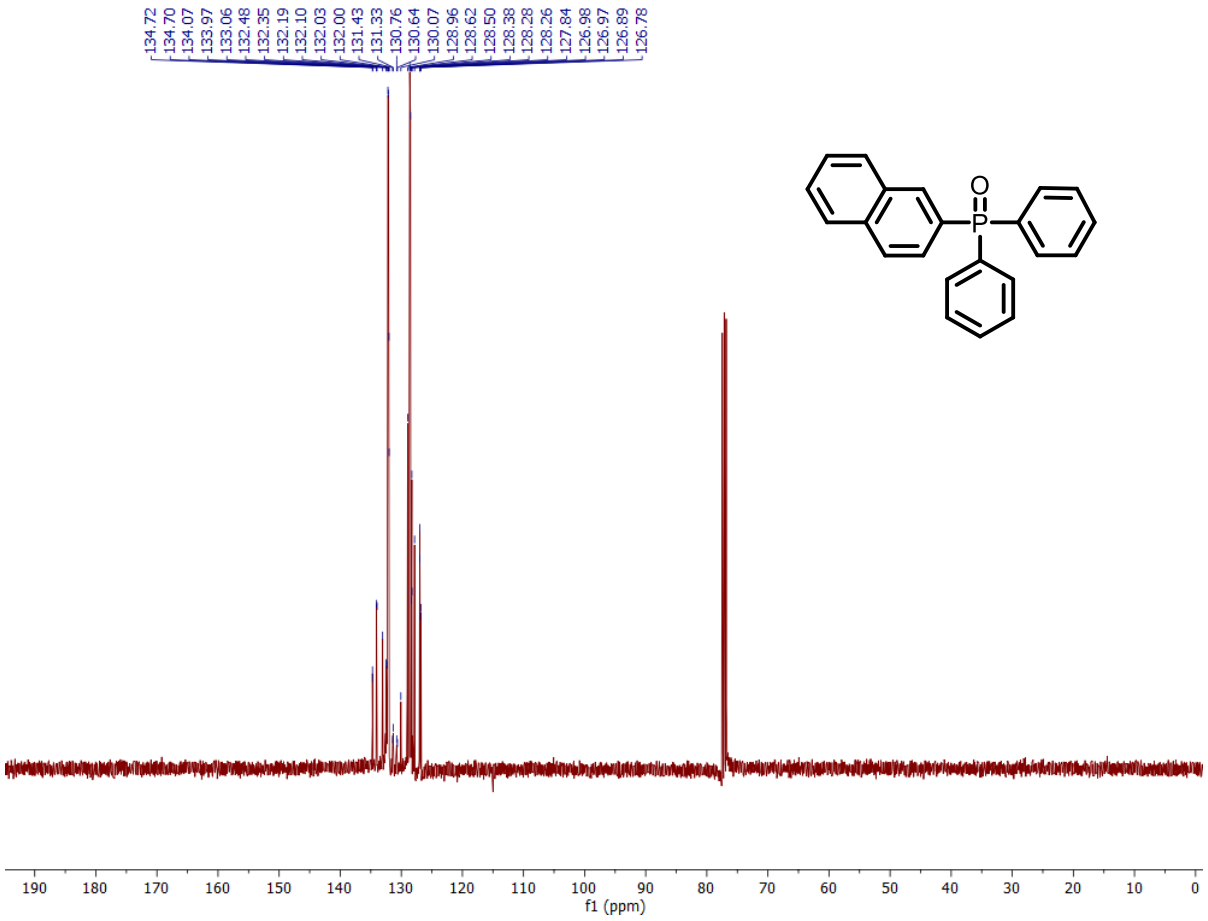
134.72
134.70
134.07
133.97
133.06
132.48
132.35
132.19
132.10
132.03
132.00
131.43
131.33
130.76
130.64
130.07
128.96
128.62
128.50
128.38
128.28
128.26
127.84
126.98
126.97
126.89
126.78
O
P
190 180 170 160 150 140 130 120 110 100 90 80 70 60 50 40 30 20 10 0
f1 (ppm)

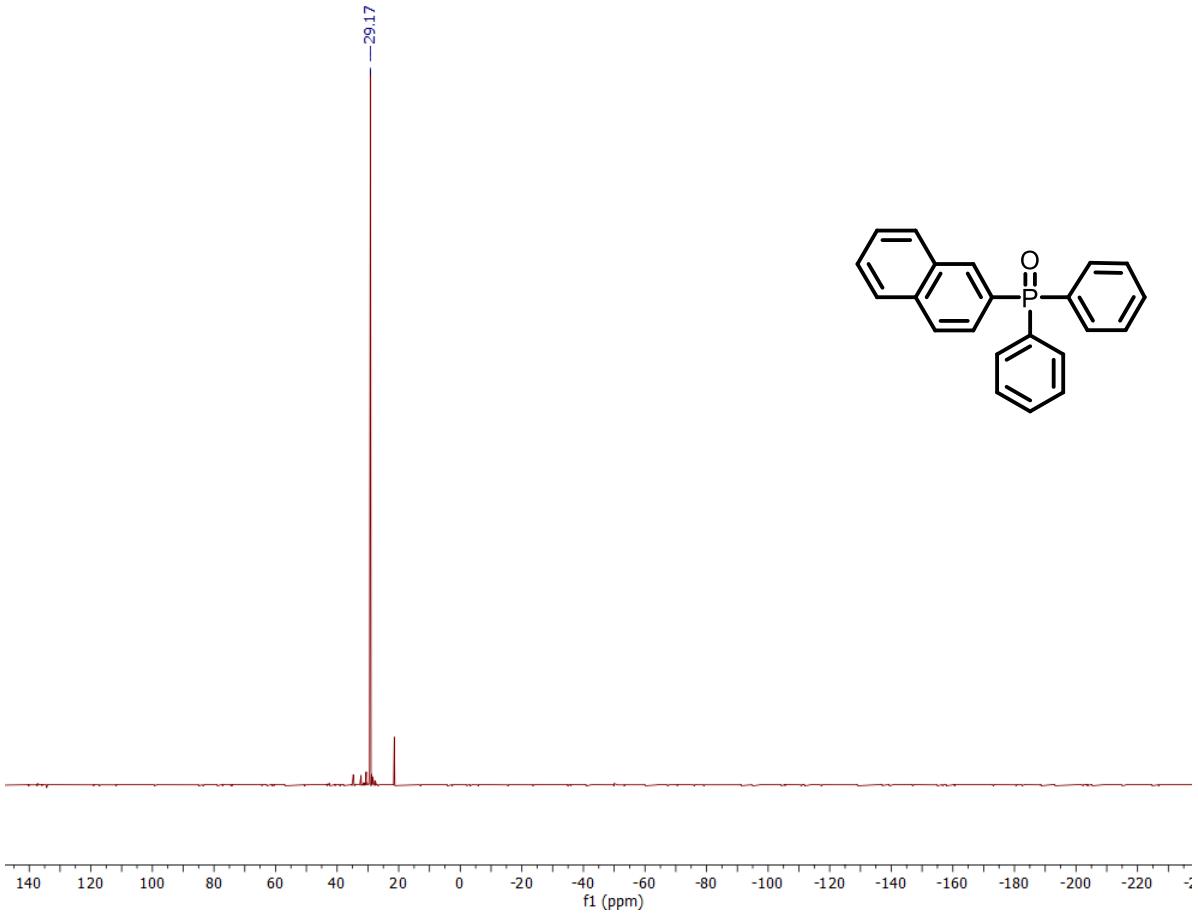
29.17
O
P
140 120 100 80 60 40 20 0 -20 -40 -60 -80 -100 -120 -140 -160 -180 -200 -220
f1 (ppm)

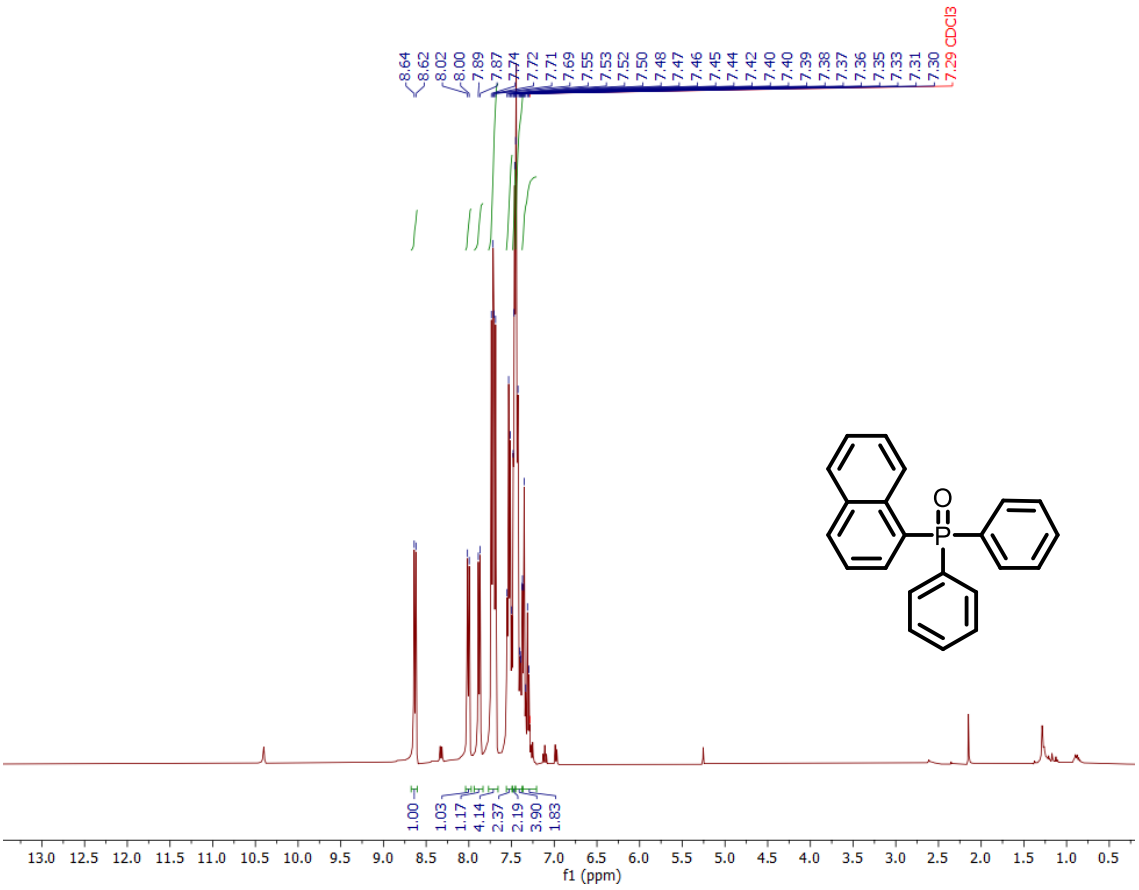
8.64
8.62
8.02
8.00
7.89
7.87
7.74
7.72
7.71
7.69
7.55
7.53
7.52
7.50
7.48
7.47
7.46
7.45
7.44
7.42
7.40
7.40
7.39
7.38
7.37
7.36
7.35
7.33
7.31
7.30
7.29 CDCl3
1.00
1.03
1.17
4.14
2.37
2.19
3.90
1.83
13.0 12.5 12.0 11.5 11.0 10.5 10.0 9.5 9.0 8.5 8.0 7.5 7.0 6.5 6.0 5.5 5.0 4.5 4.0 3.5 3.0 2.5 2.0 1.5 1.0 0.5
f1 (ppm)
O
P

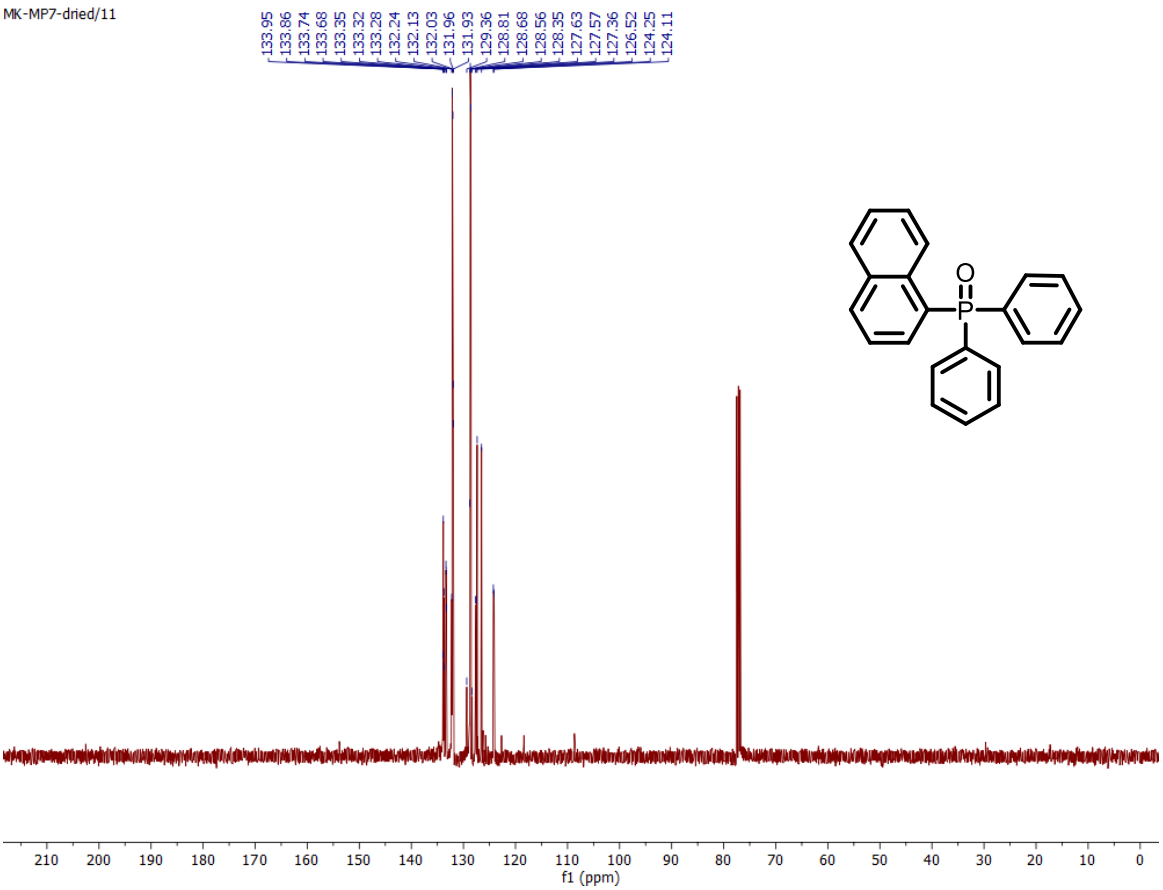
MK-MP7-dried/11
133.95
133.86
133.74
133.68
133.35
133.32
133.28
132.24
132.13
132.03
131.96
131.93
129.36
128.81
128.68
128.56
128.35
127.63
127.57
127.36
126.52
124.25
124.11
210 200 190 180 170 160 150 140 130 120 110 100 90 80 70 60 50 40 30 20 10 0
f1 (ppm)
O
P

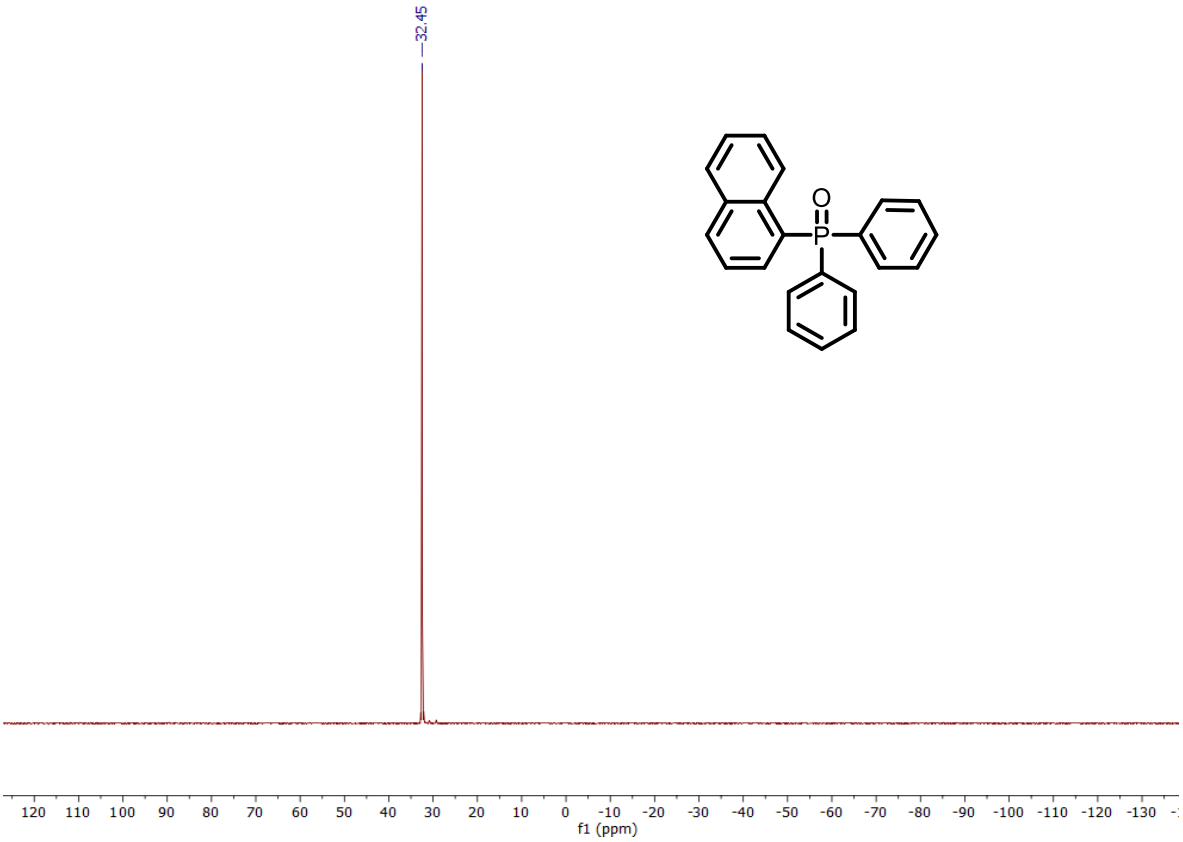
32.45
O
P
120 110 100 90 80 70 60 50 40 30 20 10 0 -10 -20 -30 -40 -50 -60 -70 -80 -90 -100 -110 -120 -130
f1 (ppm)

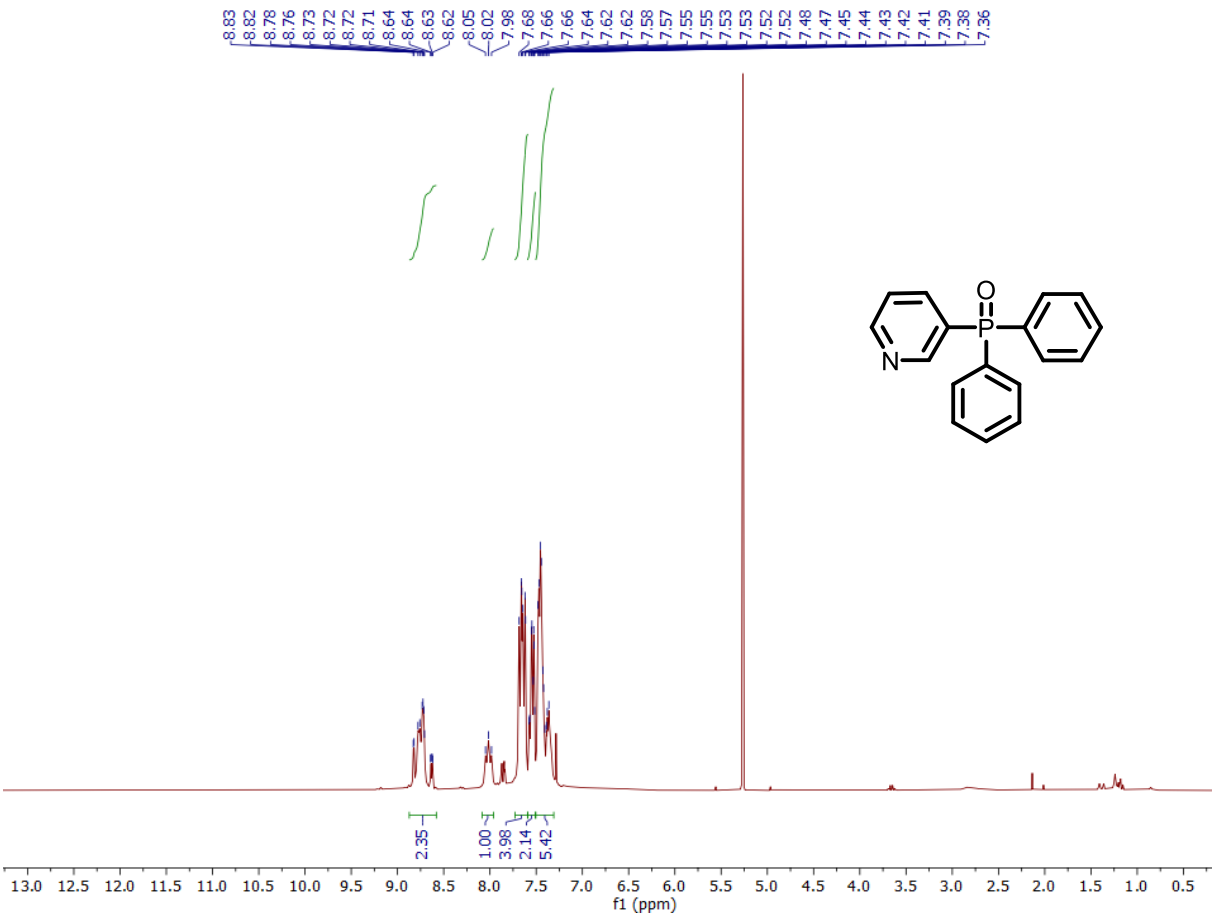
8.83 8.82 8.78 8.76 8.73 8.72 8.72 8.71 8.64 8.64 8.63 8.62 8.05 8.02 7.98 7.68 7.66 7.66 7.64 7.62 7.62 7.58 7.57 7.55 7.55 7.53 7.53 7.52 7.52 7.48 7.47 7.45 7.44 7.43 7.42 7.41 7.39 7.38 7.36
O
P
N
2.35 1.00 3.98 2.14 5.42
13.0 12.5 12.0 11.5 11.0 10.5 10.0 9.5 9.0 8.5 8.0 7.5 7.0 6.5 6.0 5.5 5.0 4.5 4.0 3.5 3.0 2.5 2.0 1.5 1.0 0.5
f1 (ppm)

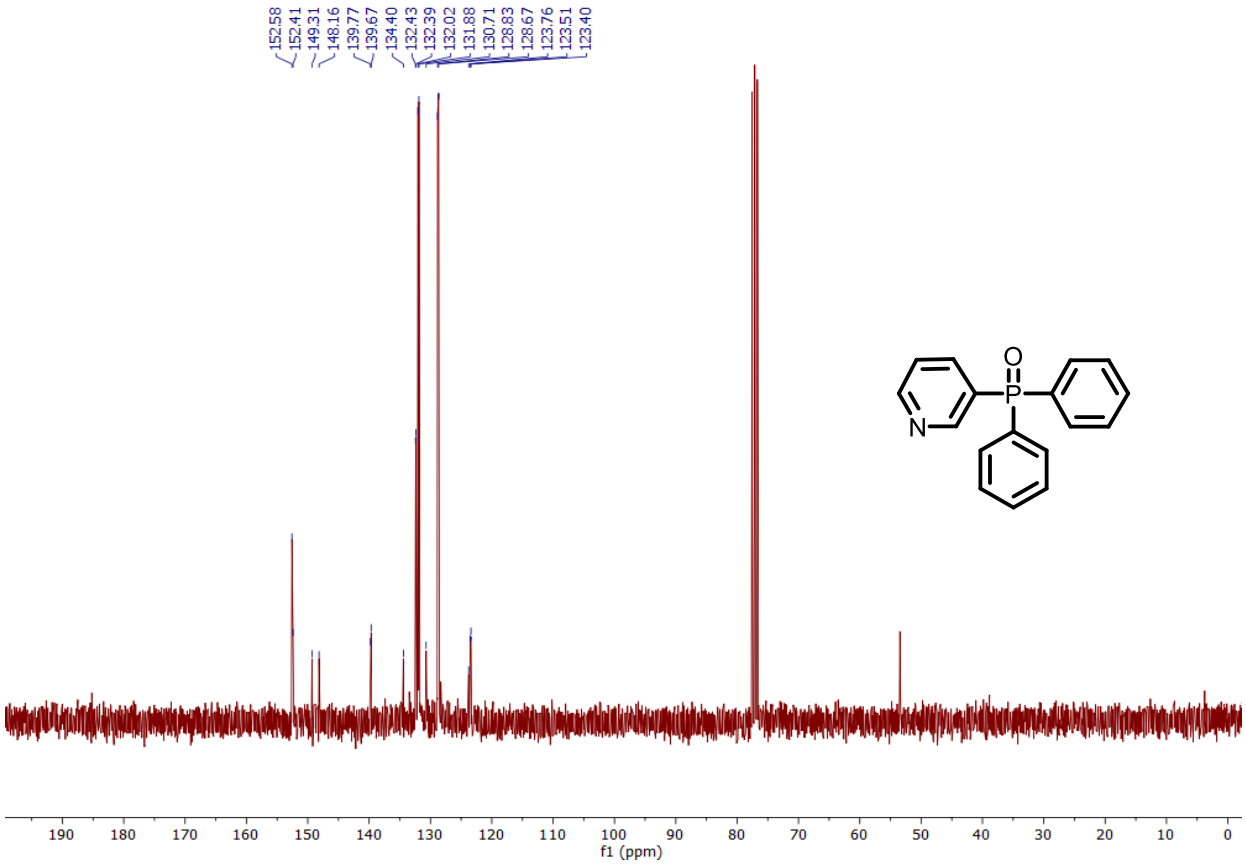
152.58
152.41
149.31
148.16
139.77
139.67
134.40
132.43
132.39
132.02
131.88
130.71
128.83
128.67
123.76
123.51
123.40
O
P
N
190 180 170 160 150 140 130 120 110 100 90 80 70 60 50 40 30 20 10 0
f1 (ppm)

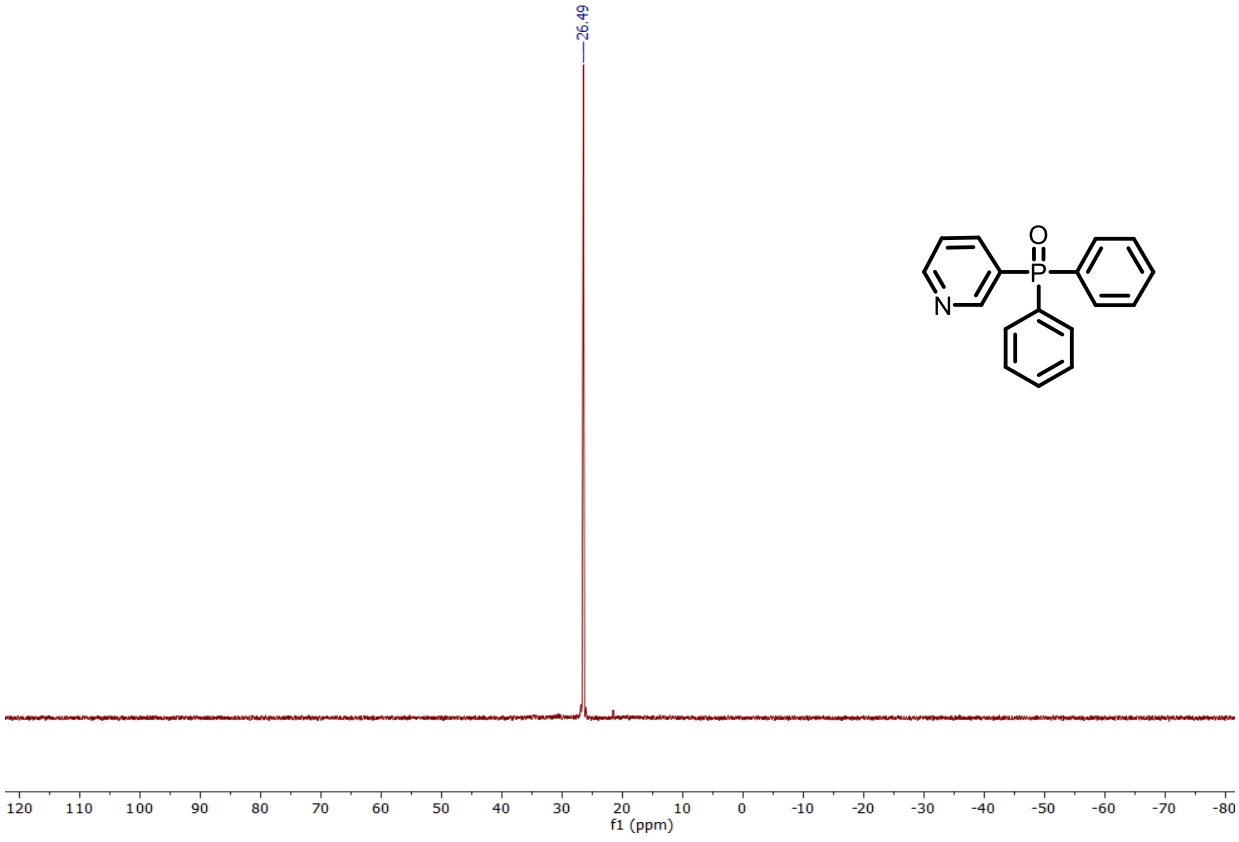
26.49
O
P
N
120 110 100 90 80 70 60 50 40 30 20 10 0 -10 -20 -30 -40 -50 -60 -70 -80
f1 (ppm)

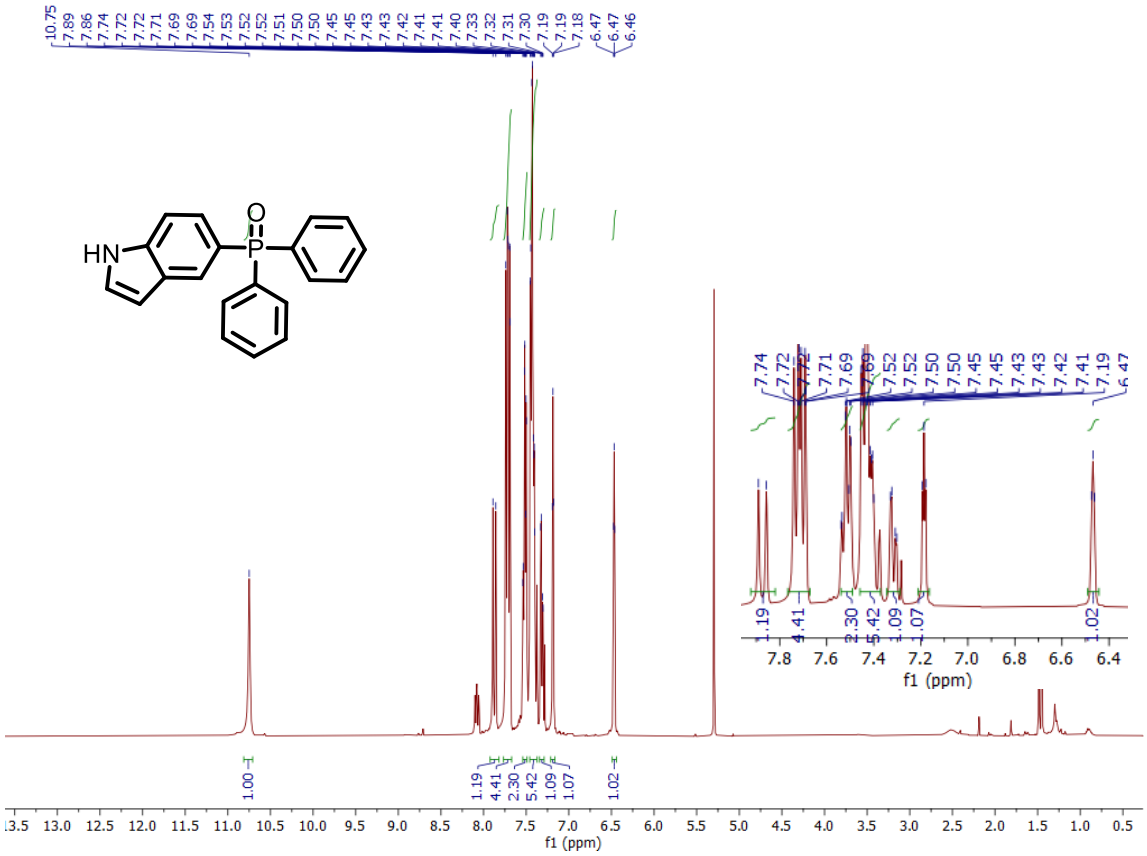
HN
O
P
f1 (ppm)

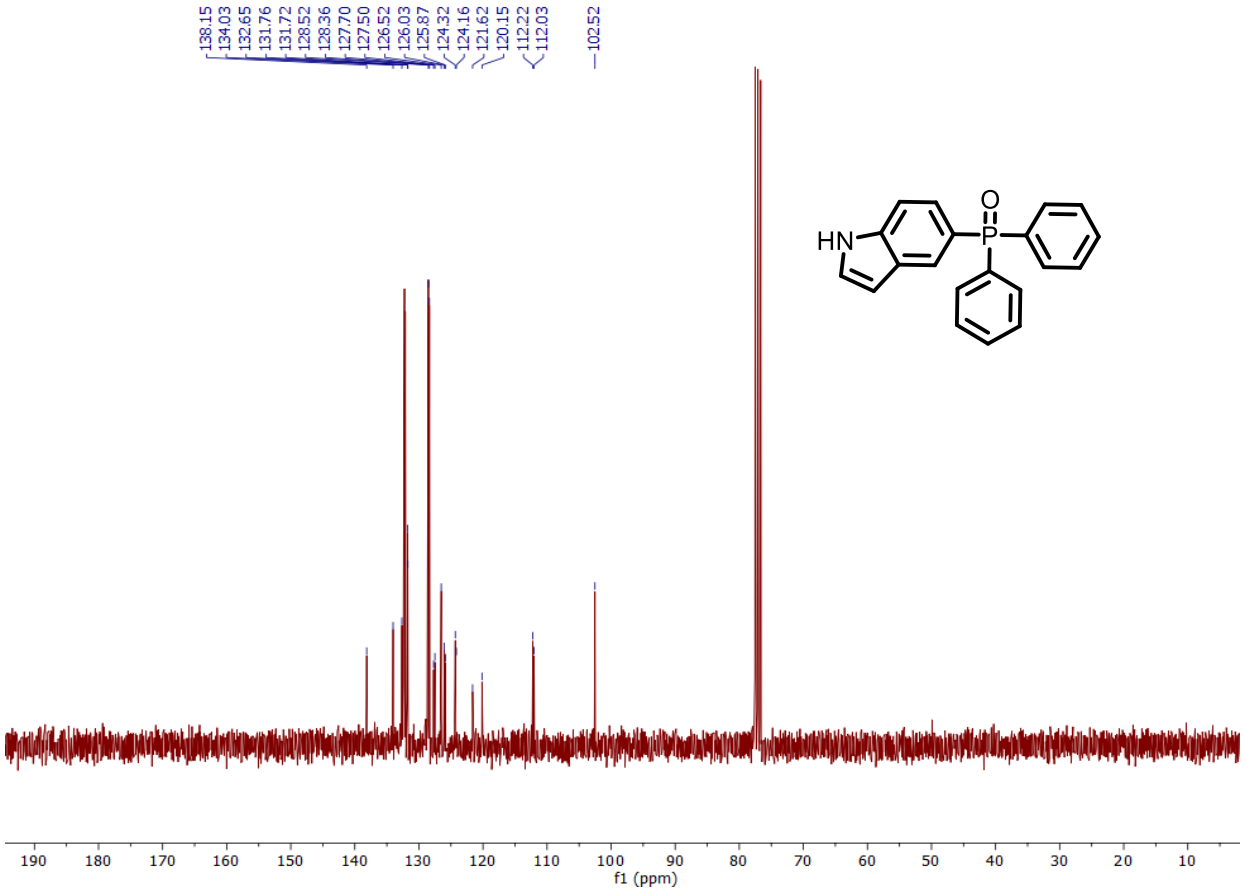
HN
O
P
f1 (ppm)

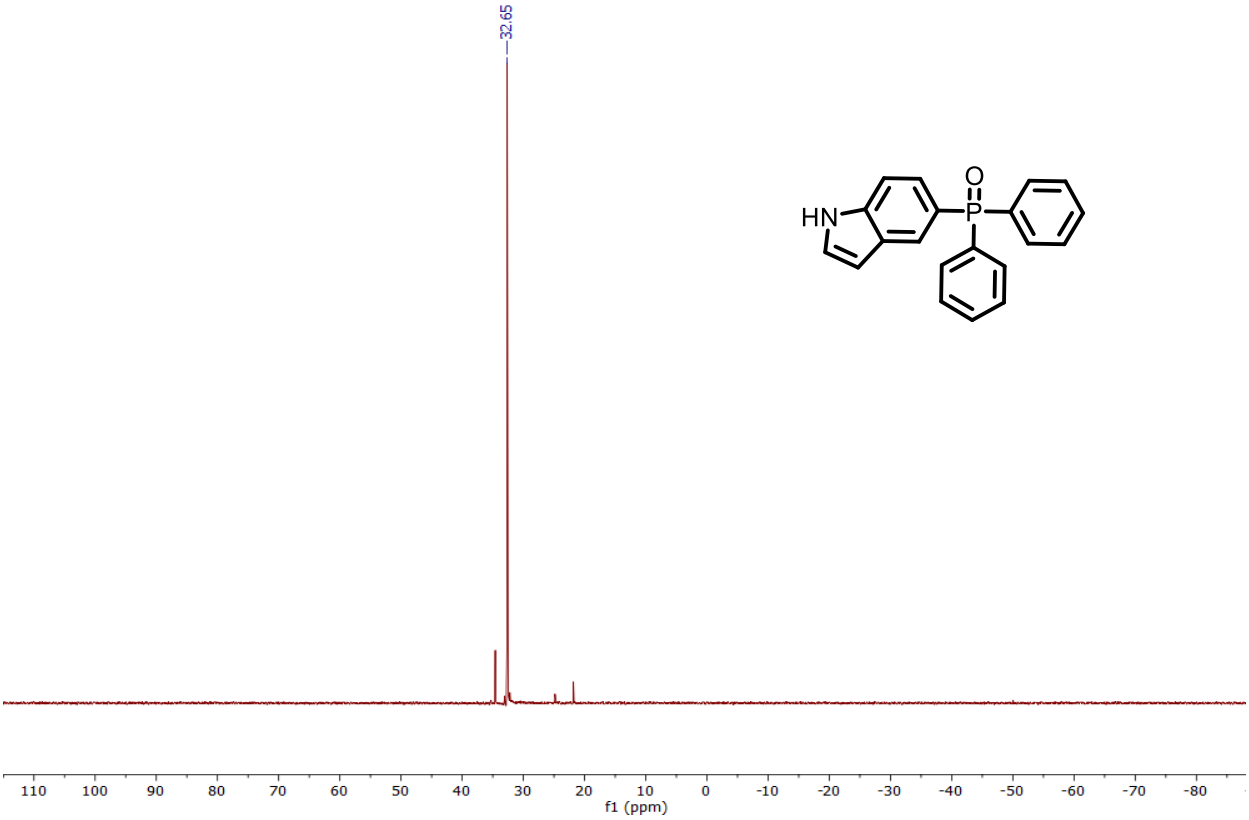
32.65
HN
O
P
110 100 90 80 70 60 50 40 30 20 10 0 -10 -20 -30 -40 -50 -60 -70 -80
f1 (ppm)

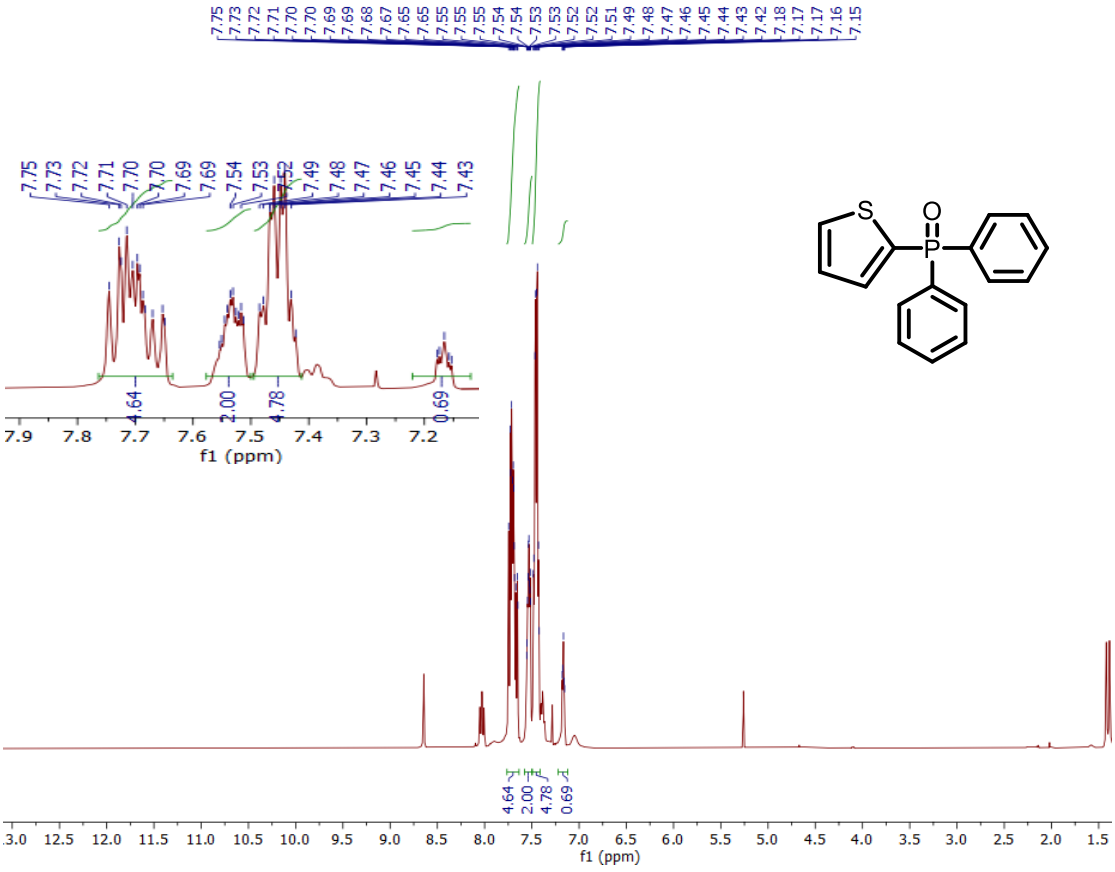
7.75 7.73 7.72 7.71 7.70 7.70 7.69 7.69 7.68 7.67 7.65 7.65 7.55 7.55 7.54 7.54 7.53 7.53 7.52 7.51 7.49 7.48 7.47 7.46 7.45 7.44 7.43 7.42 7.18 7.17 7.16 7.15
S
O
P
4.64 2.00 4.78 0.69
7.9 7.8 7.7 7.6 7.5 7.4 7.3 7.2
f1 (ppm)
3.0 12.5 12.0 11.5 11.0 10.5 10.0 9.5 9.0 8.5 8.0 7.5 7.0 6.5 6.0 5.5 5.0 4.5 4.0 3.5 3.0 2.5 2.0 1.5
f1 (ppm)

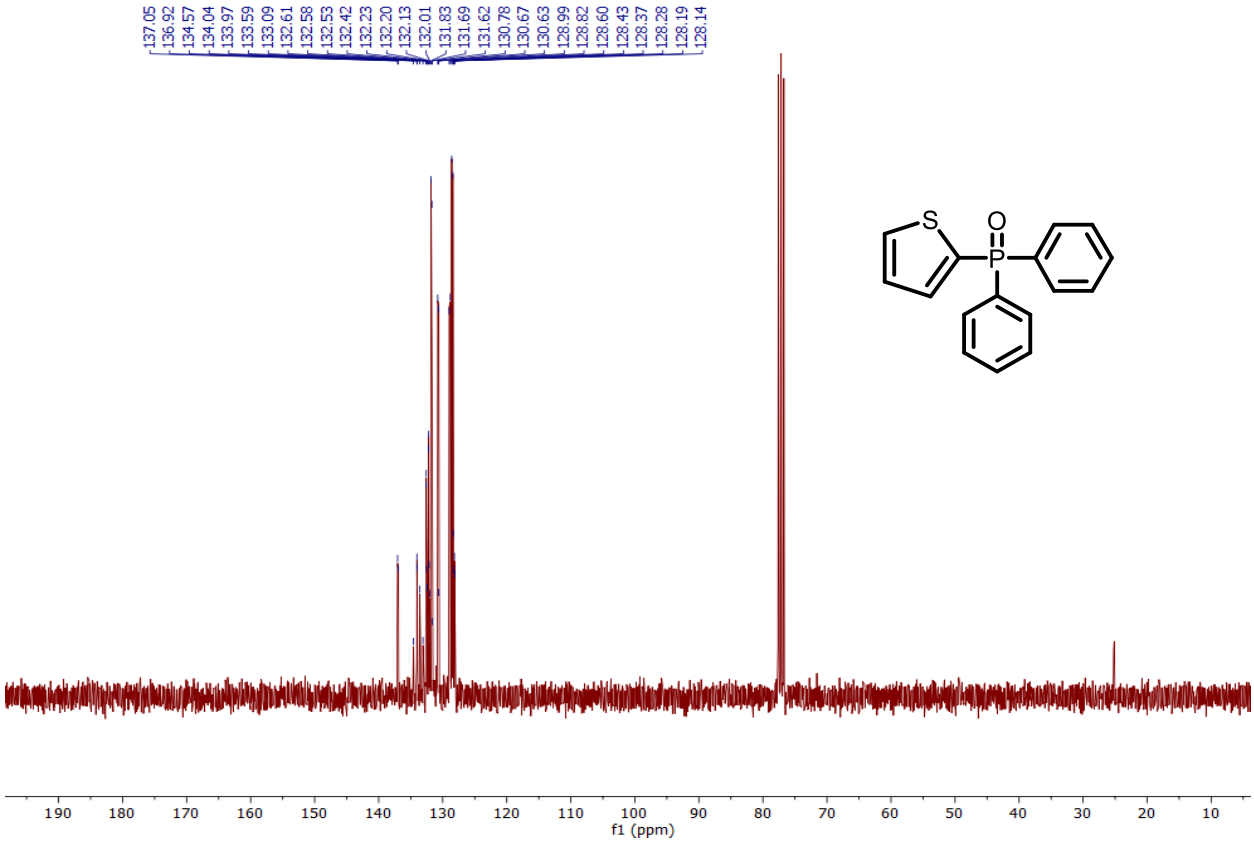
137.05
136.92
134.57
134.04
133.97
133.59
133.09
132.61
132.58
132.53
132.42
132.23
132.20
132.13
132.01
131.83
131.69
131.62
130.78
130.67
130.63
128.99
128.82
128.60
128.43
128.37
128.28
128.19
128.14
S
O
P
190 180 170 160 150 140 130 120 110 100 90 80 70 60 50 40 30 20 10
f1 (ppm)

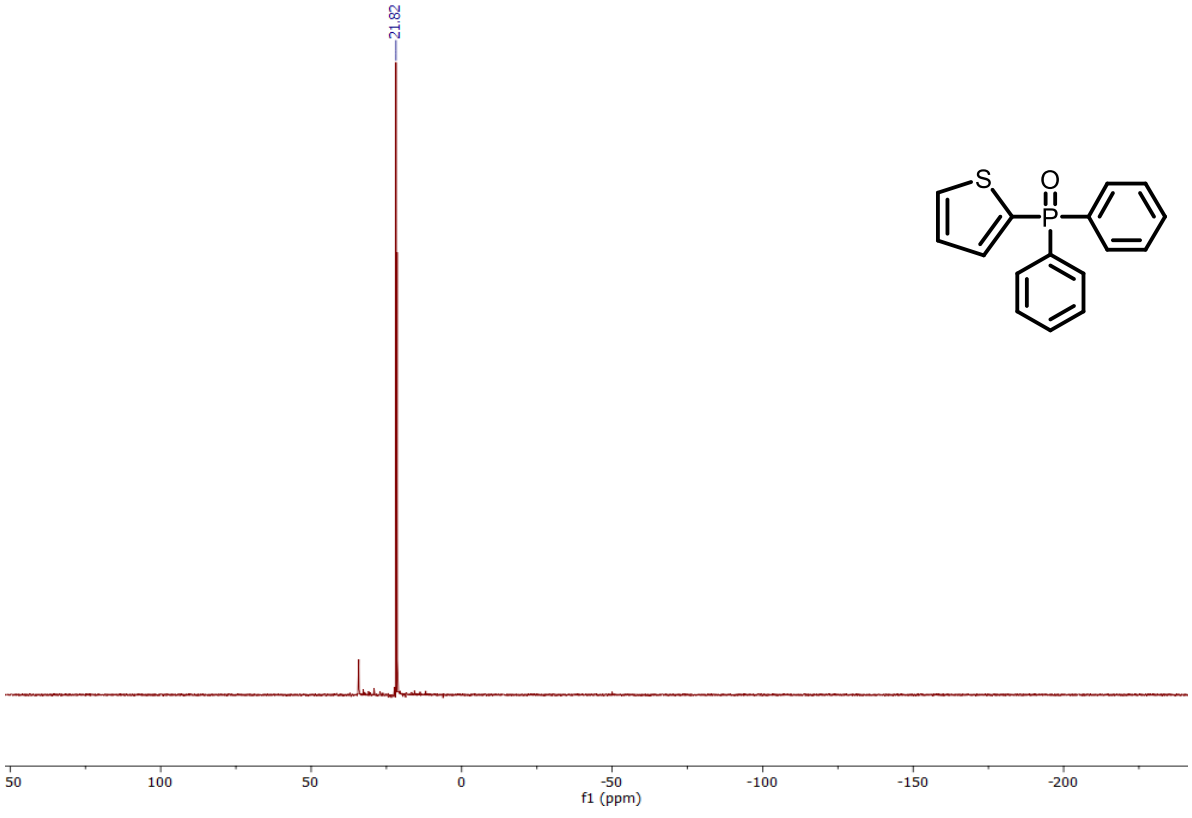
21.82
S
O
P
50 100 50 0 -50 -100 -150 -200
f1 (ppm)

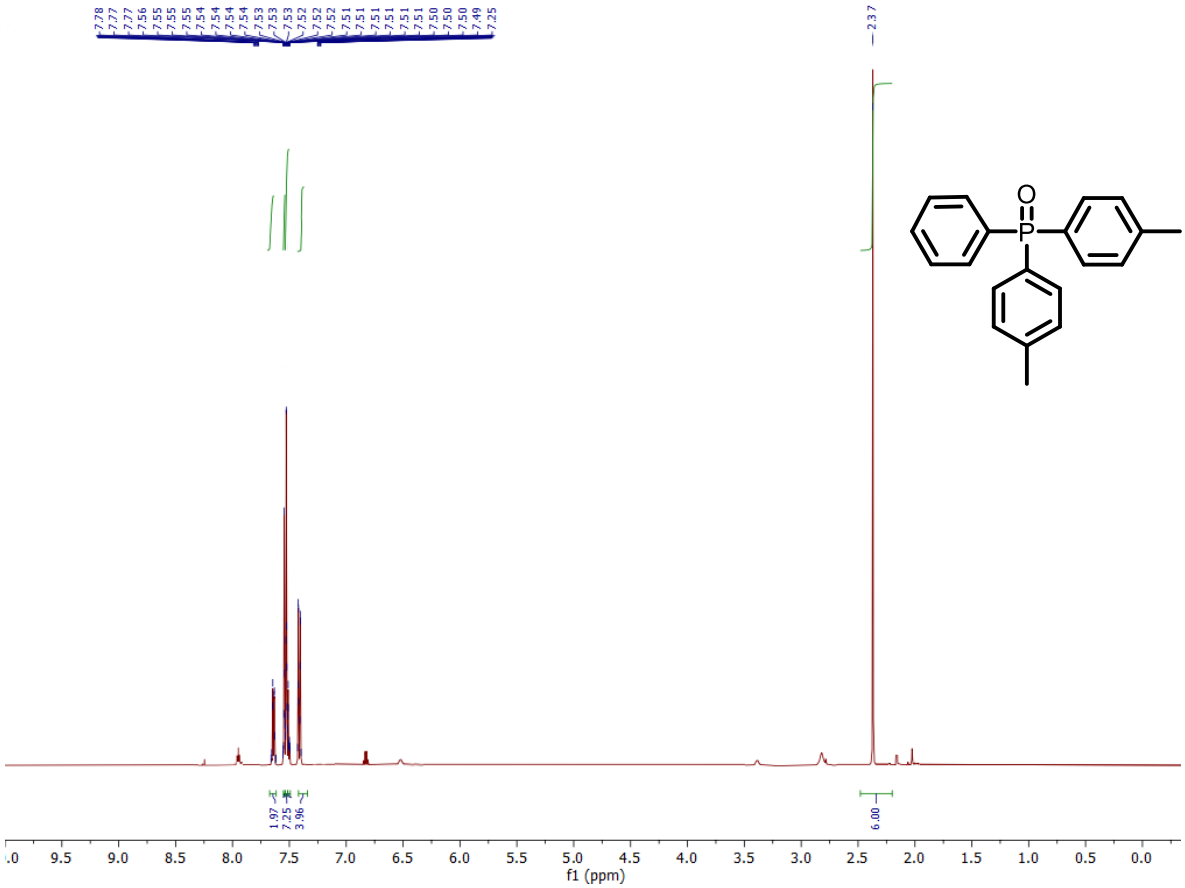
7.78
7.77
7.77
7.77
7.56
7.55
7.55
7.55
7.54
7.54
7.54
7.54
7.53
7.53
7.53
7.52
7.52
7.52
7.51
7.51
7.51
7.51
7.51
7.51
7.50
7.50
7.50
7.49
7.25
2.37
1.97
7.25
3.96
6.00
f1 (ppm)

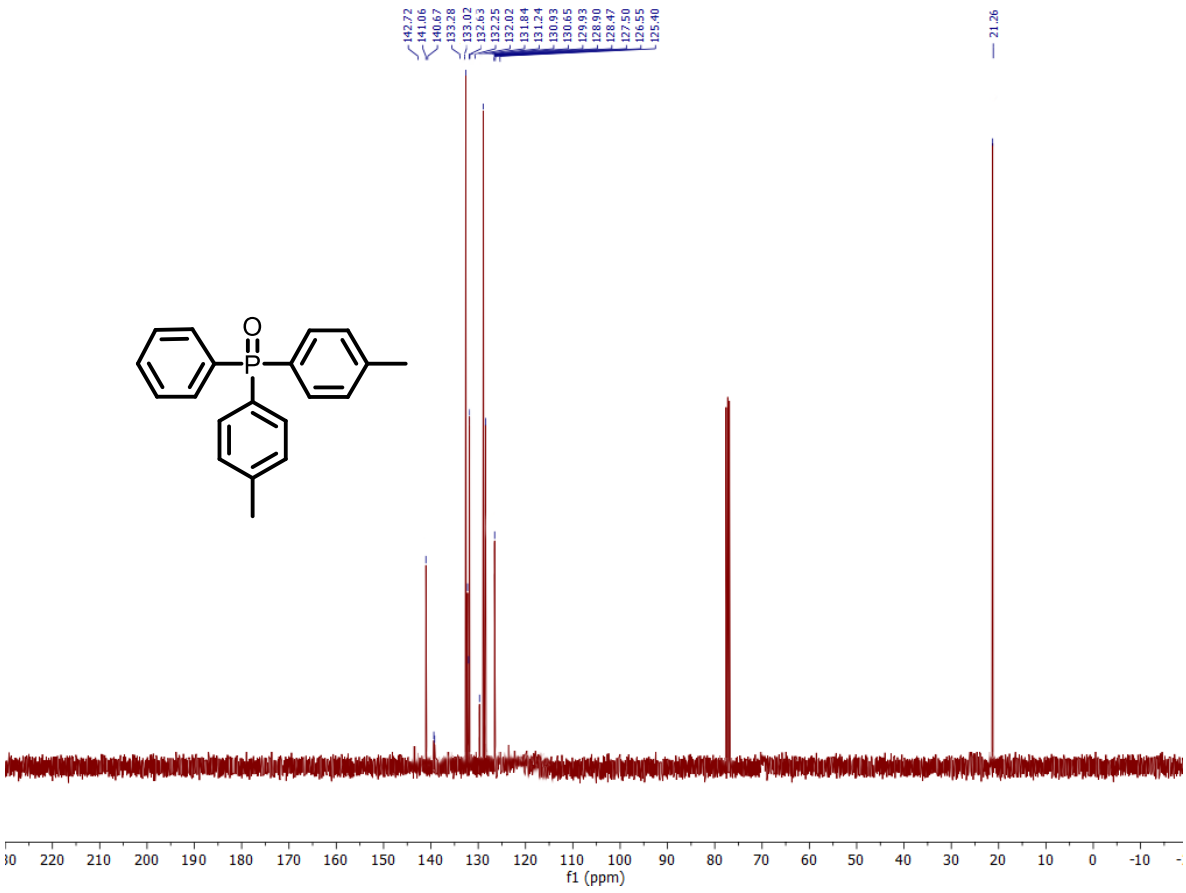
142.72
141.06
140.67
133.28
133.02
132.63
132.25
132.02
131.84
131.24
130.93
130.65
129.93
128.90
128.47
127.50
126.55
125.40
21.26
f1 (ppm)

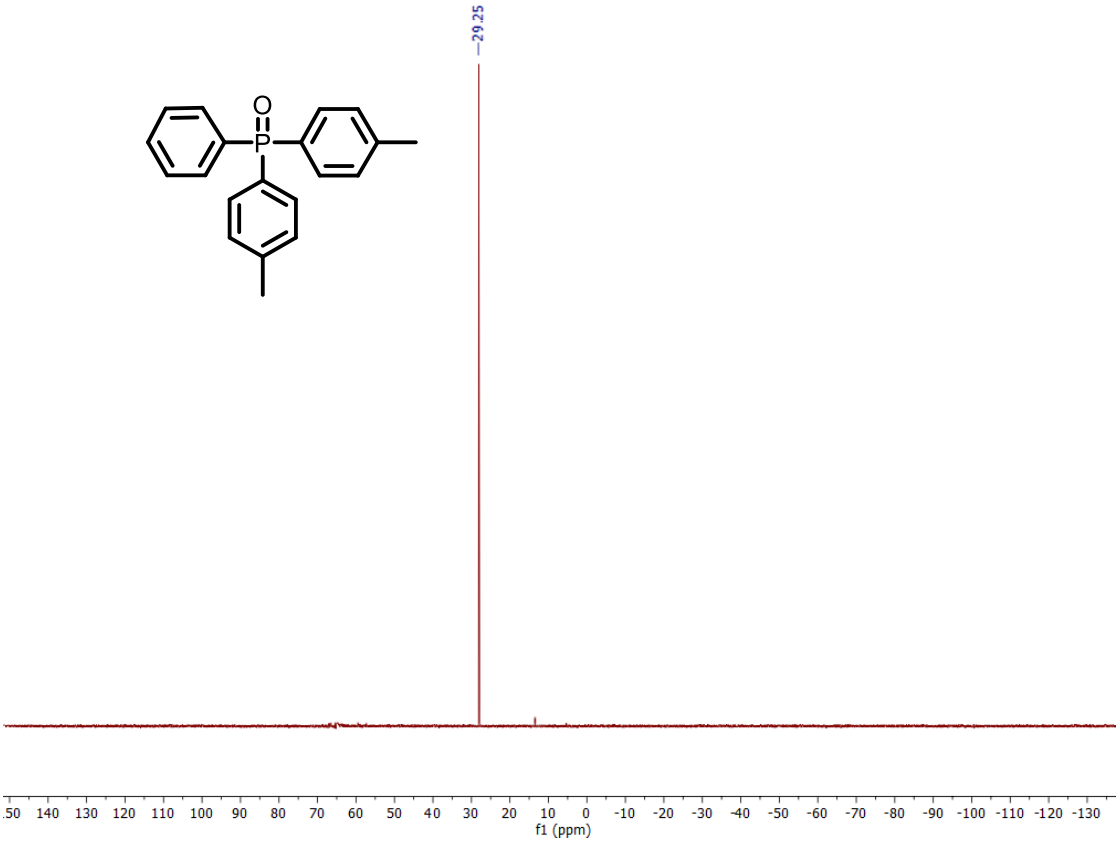
29.25
f1 (ppm)

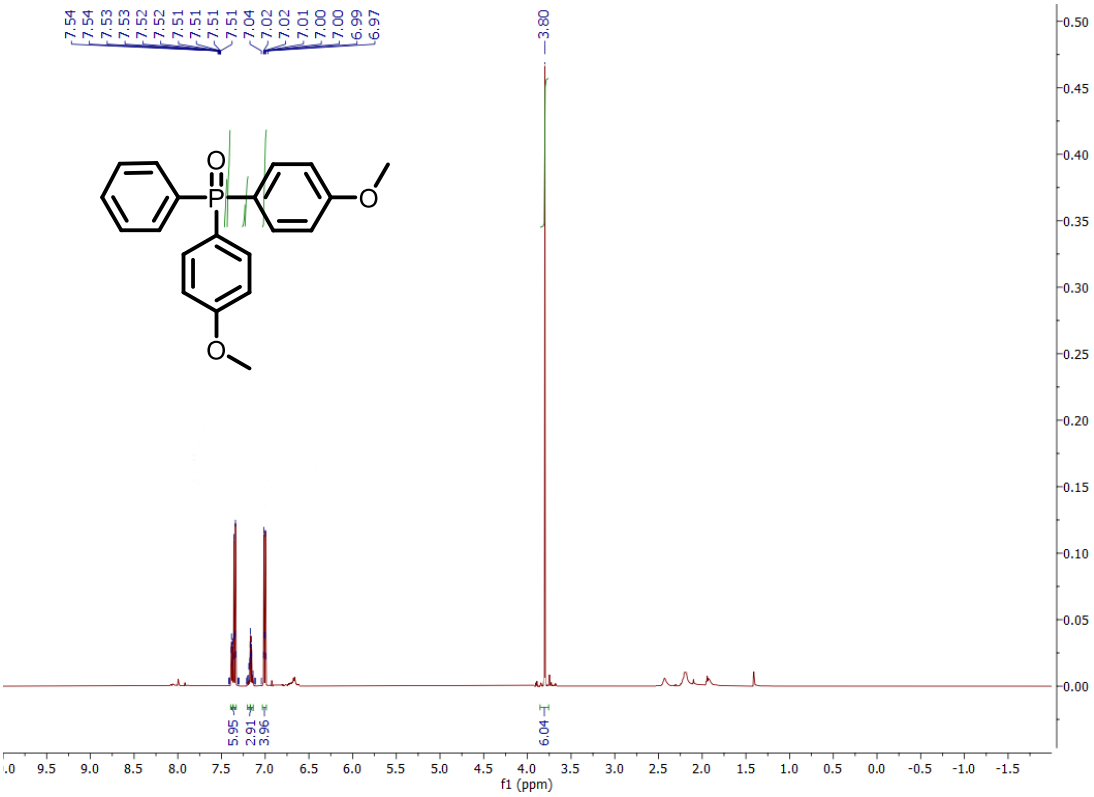
7.54
7.54
7.53
7.53
7.52
7.52
7.51
7.51
7.51
7.51
7.04
7.02
7.02
7.01
7.00
7.00
6.99
6.97
3.80
5.95
2.91
3.96
6.04
f1 (ppm)

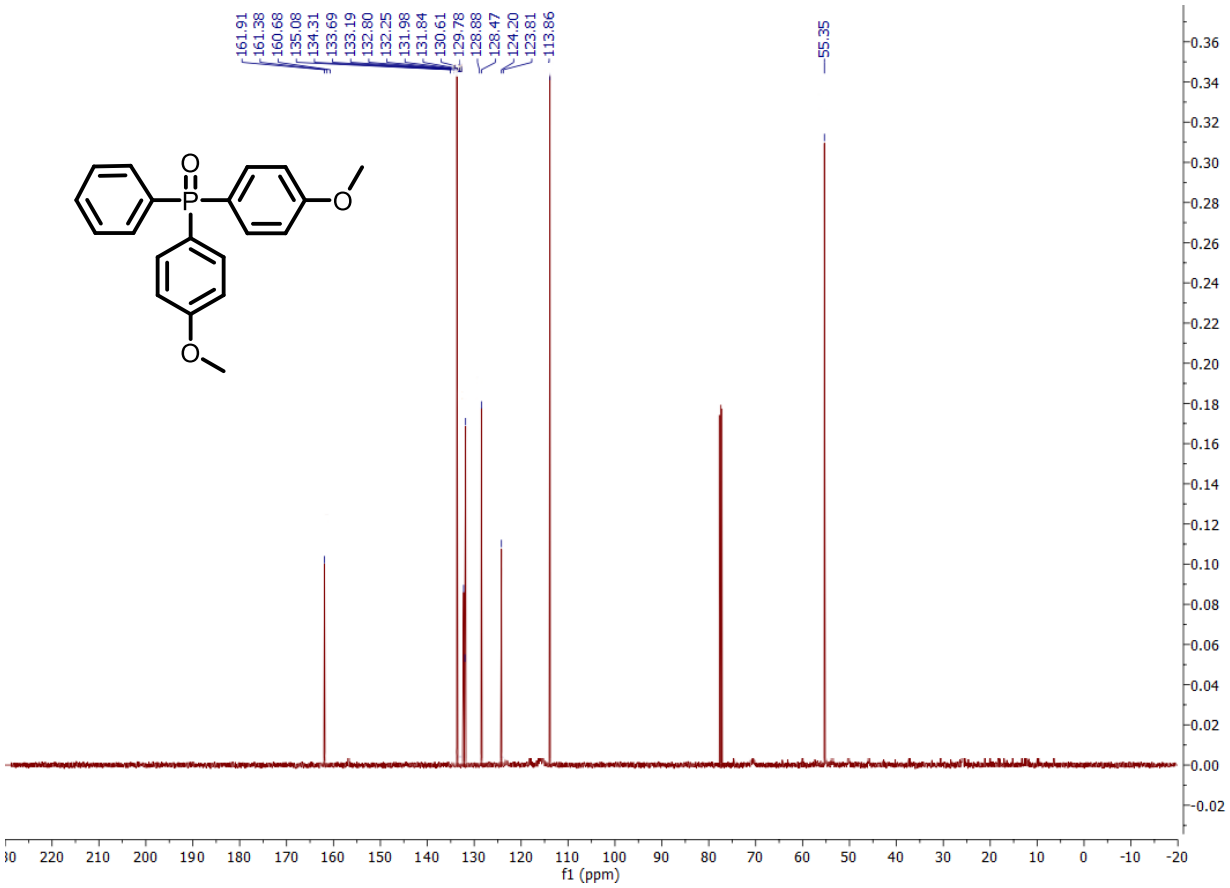
161.91
161.38
160.68
135.08
134.31
133.69
133.19
132.80
132.25
131.98
131.84
130.61
129.78
128.88
128.47
124.20
123.81
113.86
55.35
O
P
O
O
f1 (ppm)

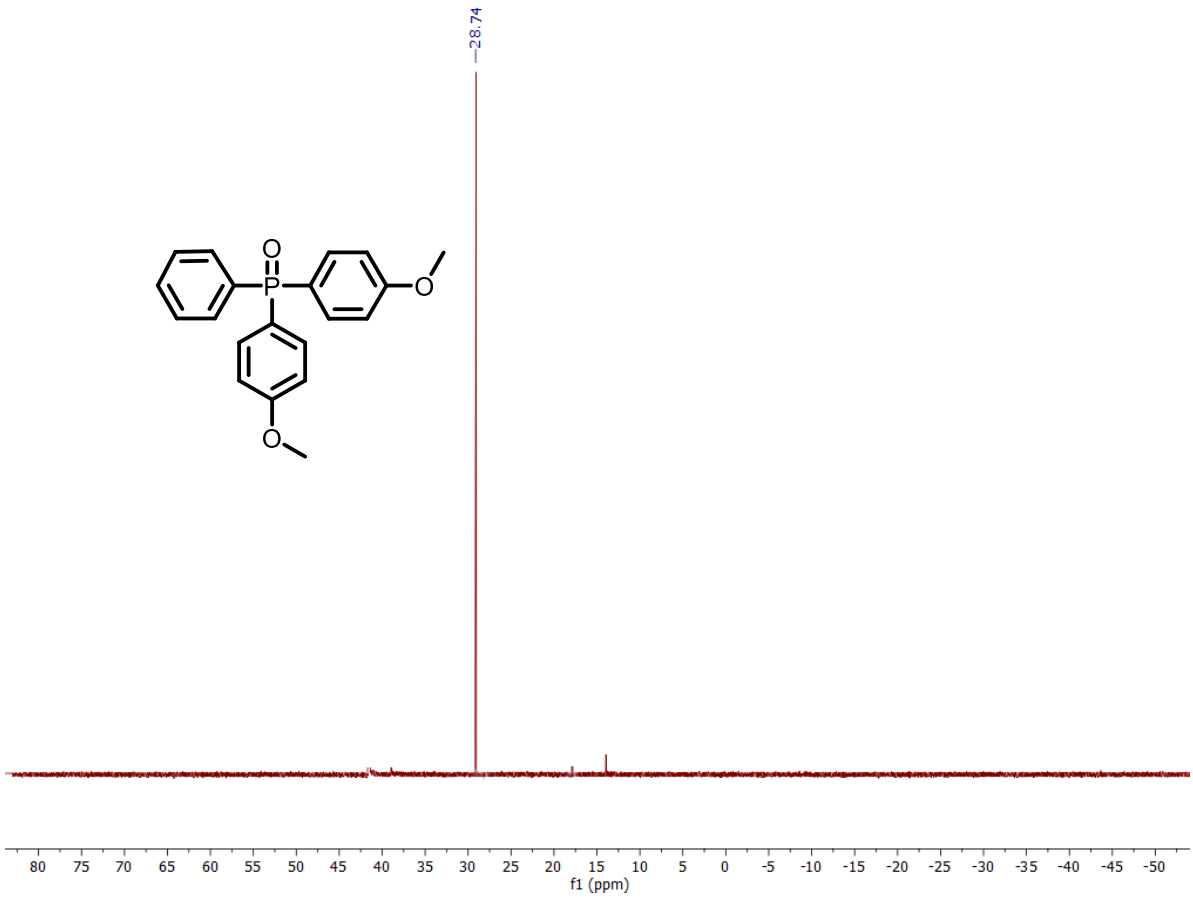
28.74
O
P
O
O
f1 (ppm)

7. References

1 H. Tan, Z. Zhao, M. Niu, C. Mao, D. Cao, D. Cheng, P. Feng and Z. Sun, *Nanoscale*, 2014, **6**, 10216.

2(a) M. Hosseini-Sarvari, Z. Hosseinpour and M. Koohgard, *New Journal of Chemistry*, 2018, **42**, 19237; (b) M. Hosseini-Sarvari, F. Jafari, A. Mohajeri and N. Hassani, *Catalysis Science & Technology*, 2018, **8**, 4044.

3(a) M. Wang, D.-j. Guo and H.-l. Li, *J. Solid State Chem.*, 2005, **178**, 1996; (b) V. Jovic, W.-T. Chen, D. Sun-Waterhouse, M. G. Blackford, H. Idriss and G. I. N. Waterhouse, *J. Catal.*, 2013, **305**, 307.

4 A. Fuerte, M. D. Hernández-Alonso, A. J. Maira, A. Martínez-Arias, M. Fernández-García, J. C. Conesa, J. Soria and G. Munuera, *Journal of Catalysis*, 2002, **212**, 1.

5(a) A. S. Hassanien and A. A. Akl, *Superlattices and Microstructures*, 2016, **89**, 153; (b) S. A. Ansari and M. H. Cho, *Scientific reports*, 2016, **6**, 25405.

6(a) R. López and R. Gómez, *Journal of sol-gel science and technology*, 2012, **61**, 1; (b) J. Tauc, R. Grigorovici and A. Vancu, *physica status solidi (b)*, 1966, **15**, 627.

7 M. Butler, *Journal of Applied Physics*, 1977, **48**, 1914.

8(a) S. Kashiwaya, C. Olivier, J. Majimel, A. Klein, W. Jaegermann and T. Toupance, *ACS Applied Nano Materials*, 2019, **2**, 4793; (b) Y.-H. Tseng and B.-K. Huang, *International Journal of Photoenergy*, 2012, **2012**, 832180.

9(a) Z. Jiao, Z. Zhai, X. Guo and X.-Y. Guo, *The Journal of Physical Chemistry C*, 2015, **119**, 3238; (b) D. Dvoranová, Z. Barbieriková and V. Brezová, *Molecules*, 2014, **19**, 17279.

10(a) W. Deng, H. Zhao, F. Pan, X. Feng, B. Jung, A. Abdel-Wahab, B. Batchelor and Y. Li, *Environmental science & technology*, 2017, **51**, 13372; (b) H. L. Tan, X. Wen, R. Amal and Y. H. Ng, *The journal of physical chemistry letters*, 2016, **7**, 1400.

11 X. Zhang, H. Liu, X. Hu, G. Tang, J. Zhu and Y. Zhao, *Organic letters*, 2011, **13**, 3478.

12 J. Xu, P. Zhang, Y. Gao, Y. Chen, G. Tang and Y. Zhao, *The Journal of organic chemistry*, 2013, **78**, 8176.

13 J. Yang, J. Xiao, T. Chen, S.-F. Yin and L.-B. Han, *Chemical Communications*, 2016, **52**, 12233.

14 T. Fu, H. Qiao, Z. Peng, G. Hu, X. Wu, Y. Gao and Y. Zhao, *Organic & biomolecular chemistry*, 2014, **12**, 2895.

15 H.-Y. Zhang, M. Sun, Y.-N. Ma, Q.-P. Tian and S.-D. Yang, *Organic & biomolecular chemistry*, 2012, **10**, 9627.

16 J. Xuan, T.-T. Zeng, J.-R. Chen, L.-Q. Lu and W.-J. Xiao, *Chemistry – A European Journal*, 2015, **21**, 4962.